CONTENTS

	PAGE	
SUMMARY	1	1/A9
INTRODUCTION	5	1/A11
Study Background	5	1/A11
Dual Fuel Concept	6	1/A12
Study Approach	8	1/A14
SYMBOLS	3	1/A2
TECHNOLOGY PROJECTIONS - STEP 1	9	1/B1
PARAMETRIC TRADE STUDIES - STEP 2	10	1/B2
Performance Analysis	13	1/B5
Propulsion Analysis	22	1/C1
Configuration Analysis	26	1/C5
Weights Analysis	33	1/C12
Cost Analysis	40	1/D5
VEHICLE DESIGN AND PERFORMANCE POTENTIAL - STEP 3	49	1/D14
Vehicle Design, Layout and Structural Analysis	49	1/D14
Ground Accelerator	56	1/E7
Propulsion Design	60	1/E11
Subsystems Installation	60	1/E11
Environment	64	1/F1
Weights	72	1/F9
Flight Performance	76	1/F13
Aerodynamics	78	1/G1
Vehicle Weights Assessment	81	1/G4
TECHNOLOGY EVALUATION - STEP 4	84	1/G7
CONCLUSIONS AND RECOMMENDATIONS	85	1/G8
Study Results	85	1/G8
Conclusions	86	1/G9
Study Recommendations	86	1/G9
REFERENCES	88	1/G11

SYMBOLS

A. C.	Aerodynamic Center
ALRS	Advanced Launch and Recovery System
APU	Auxiliary Power Unit
BL	Buttock Line
C_D	Drag Coefficient
C.G.	Center of Gravity
C_L	Lift Coefficient
DDT&E	Design, Development Test and Evaluation
F_{ty}	Tensile Yield Strength
G&N	Guidance and Navigation
GH_2	Gaseous Hydrogen
GLOW	Gross Lift-Off Weight
GSE	Ground Support Equipment
h	Altitude
H/C	Honeycomb
He	Helium
HTO	Horizontal Take-Off
Isp	Specific Impulse - Seconds
kW	Kilowatts
LCC	Life Cycle Cost
LH_2	Liquid Hydrogen
LO_2	Liquid Oxygen
M	Mach Number

NASA	National Aeronautics And Space Administration
O/F	Oxidizer/Fuel Ratio
OMS	Orbit Maneuvering System
P_C	Chamber Pressure
P/L	Payload
PSR	Propellant Split Ratio = $\frac{\text{Weight of } LO_2/RP}{\text{Weight } LO_2/RP + \text{Weight } LO_2/LH_2}$
RCS	Reaction Control System
RI/SD	Rockwell International/Space Division
SSME	Space Shuttle Main Engine
SSTO	Single-Stage-to-Orbit
S_W	Wing Reference Area
t/c	Thickness/Chord Ratio
Ti	Titanium
T/W	Thrust/Weight Ratio
TVC	Thrust Vector Control
VTO	Vertical Take-Off
W_{inj}	Injected Weight
W_P	Propellant Weight
α	Angle of Attack
ϵ	Nozzle Expansion Ratio
ΔV	Velocity Change
β	Angle of Yaw
ϕ	Bank Angle

Jesn 930-H-14 NASI.26:3037

NASA Contractor Report 3037

JUL 20 1978

COMPLETED

ORIGINAL

Technology Requirements for Advanced Earth Orbital Transportation Systems

Volume 3: Summary Report - Dual Mode Propulsion

A. K. Hepler and E. L. Bangsund

CONTRACT NAS1-13944
JULY 1978

NASA

95

Peter 830-H-14 NAS1.26:3037

NASA Contractor Report 3037

Technology Requirements for Advanced Earth Orbital Transportation Systems

Volume 3: Summary Report - Dual Mode Propulsion

A. K. Hepler and E. L. Bangsund
Boeing Aerospace Company
Seattle, Washington

Prepared for
Langley Research Center
under Contract NAS1-13944

NASA
National Aeronautics
and Space Administration

Scientific and Technical
Information Office

1978

BLANK PAGE

FOREWORD

This report presents the detailed results of an investigation conducted as an addendum to a study of Technology Requirements for Advanced Earth Orbital Transportation Systems by The Boeing Company under Contract NAS1-13944 from June 1976 through January 1977. The primary objective of the added task was to determine the impact of dual mode propulsion technology on the cost effective technology requirements for a horizontal take-off and landing Advanced Earth Orbital Transportation System.

The work was performed by the Advanced High Speed Transportation group of the Space Systems Division, Boeing Aerospace Company, at its Kent Space Center.

Study manager was Mr. E. L. Bangsund under the administration of Mr. A. K. Hepler. A listing of the Boeing personnel who contributed directly in the studies and preparation of the report is as follows:

M. J. Baker	Propulsion
B. E. Clingan	Loads
V. Deriugin	Aerothermal Analysis
H. N. Johnson	Configuration
G. A. Dishman	Structural Design
R. T. Savage	Aerothermal Analysis
A. R. Swegle	Stress
W. H. Walker	Subsystems/Ground Accelerator
H. Zeck	Aerodynamics and Performance

Contract documentation is provided as follows:

Document	Boeing No.	NASA No.
Executive Summary	D180-19168-3	CR-2878 Vol. 1
Summary Report	D180-19168-4	CR-2879 Vol. 2
Summary Report - Dual Mode Propulsion	D180-19168-5	CR-3037 Vol. 3

BLANK PAGE

SUMMARY

The basic technology requirements study reported upon in Volumes 1 and 2 was expanded by including an additional task which had the primary objective of determining the impact of dual-mode propulsion on the cost-effective technology requirements for Advanced Earth-Orbital Transportation Systems. Additional objectives were the comparison of series burn (two propulsion systems operating sequentially) and parallel burn (two different propulsion system operating together or overlapping) dual mode propulsion concepts and the determination of advantages of the best dual mode concept relative to the LO_2/LH_2 concept of the basic study.

In fulfillment of this objective, normal technology requirements applicable to horizontal takeoff and landing Single Stage to Orbit (SSTO) systems utilizing dual mode propulsion were projected to the 1985 time period. These technology projections consisted of the same type of projections as made in the basic study for the all LO_2/LH_2 vehicle (i.e. Rene'41 honeycomb, aluminum brazed titanium panel, metal matrix composites, advanced landing gear, hydraulics and avionics) and the addition of a high pressure LO_2/hydrocarbon engine and a high pressure engine capable of burning LO_2/hydrocarbon and LO_2/LH_2 sequentially (dual fuel). These technology projections were then incorporated in a vehicle parametric design analysis for two different operational concepts of a dual mode propulsion system. The operational concepts included series and parallel burn. The resultant performance, weights and costs of each concept were then compared and a series burn dual fuel concept with a propellant split of 61% LO_2/RP-1 and 39% LO_2/LH_2 was selected for detailed design study. This entailed evaluation to confirm the parametric trending/scaling of weights and to optimize the configuration based on figure of merit. The final configuration GLOW is

projected to be between 1,374,840 kg (3.031,000 lb) and 1,568,000 kg (3,450,000 lb) to deliver a 29545 kg (65,000 lb) payload to orbit using an easterly launch from Cape Kennedy. The lower GLOW value is based on the assumption that through continued configuration development (1) significant improvement may be achieved in overall vehicle balance, (2) wing bending moments and torsion will be reduced and (3) weights resulting from heating generated by the LO_2 - RP plume radiation and plume induced flow separation will be reduced.

Liftoff speed, entry planform loading and RP-1 tank thermal isolation are major constraints to an uninsulated all-metallic horizontal takeoff design. Comparisons of life cycle costs between the dual fuel and all LO_2/LH_2 vehicle considering these constraints show development, production and operations costs to be lower with the single fuel system.

In summary, the dual fuel system configurations, as constrained by the requirements of this study, show neither lower program costs nor improved operational characteristics relative to the single fuel (LO_2/LH_2) system. Therefore, based on cost/operation figure of merit, no recommendations are made for technology developments unique to the dual-fueled horizontal takeoff/horizontal landing Single Stage to Orbit systems.

INTRODUCTION

The Space Shuttle Program is currently in the final development stages and hardware is being fabricated. It is anticipated that this vehicle system, together with the planned space tug, will provide the space transportation capability for most of the requirements to transport men and material between earth and earth orbit at least until the 1990 time frame and, more probably, for several years to follow. This program has provided a significant technology base (and will continue to do so throughout its lifetime) upon which to build for future aerospace transportation systems. For long range planning purposes, consideration of the lead times associated with major vehicle system programs and the assumption of a nominal fifteen year operational lifetime for the Space Shuttle gives a clue to the possible schedule for the development of more advanced systems. The lead time from an "Authority to Proceed" to an operational system is of the order of eight to ten years, based on both Apollo and Space Shuttle experience.

For study purposes, the assumption was made that a follow-on system to be available in the 1995 time frame based on a nominal schedule would require that the planning for and development of the necessary technology base must be accomplished within the next ten years. A fundamental assumption underlies any consideration of these more advanced systems; any new system must offer clear and significant cost/performance advantages over current systems.

Study Background

Three operational concepts (horizontal takeoff, vertical takeoff and aerial launch or refuel, Reference 1) of a Single Stage to Orbit system using advanced hydrogen fueled rocket engines for the main propulsion system were previously examined under the basic contract. A detailed examination of these systems in light of both normal technology growth anticipated for the time frame of interest and focused growth in selected areas have provided clues as to which technology areas should and must be pursued on a cost/performance basis for a single fuel system.

The fundamental objective was to identify those areas of technology associated with future earth orbit transportation systems which are either critical to the development of such systems or which offer a significant cost and performance advantage as a result of their development. Secondary objectives were to determine the most efficient operational mode and to define performance potential as a function of technology growth.

Another class of advanced propulsion schemes is that of dual mode (or dual fuel) propulsion. This is based on NASA in-house studies and other published reports showing benefits in vehicle sizing (such as Reference 1). The purpose of this additional task (Task 5) was to add dual mode propulsion to the features that were evaluated under the objectives of the basic study.

Additional objectives were to determine the most efficient propulsion mode for these systems by the comparison of series burn and parallel burn dual mode concepts and to determine the advantages of the best dual mode concept relative to the LO_2/LH_2 concept of the basic study.

Dual Fuel Concept

The types of rocket propulsion schemes considered under the basic study accomplished previously (Tasks 1-4) were restricted to high chamber pressure engines utilizing LO_2/LH_2 propellants similar to the Space Shuttle Main Engine presently under development. The dual mode propulsion concept, as shown in Figure 1, indicates by definition that there are two approaches to dual fuel propulsion system design. The first (series burn) dual fuel engine concept employs a single engine to burn a high density hydrocarbon and LO_2 during the first burn and then transition to hydrogen and LO_2 in the same engine for the second burn. The other concept (parallel burn) uses separate engines, a hydrocarbon/LO_2 engine and a LO_2/LH_2 engine, which are operated together or in parallel at lift-off. Transition from the first burn to the second burn can be varied dependent upon nozzle options and desired propellant split ratios for both dual mode concepts.

The principle behind dual fuel is shown by the lower illustration on Figure 1. To achieve an ideal ΔV required for a Single Stage to Orbit vehicle, both high specific impulse and high mass ratio are necessary. With a high

mass ratio, the gain from specific impulse is not constant but increases significantly with propellant consumption. This is one of the reasons the SII and SIVB stages of the Saturn V vehicle are run on PMR (Program Mixture Ratio), initially a high MR (low Isp, high thrust) and then at lower MR (higher Isp, lower thrust). The left hand figure shows ideal Δ V plotted versus propellant consumption for a typical LO_2/LH_2 single stage vehicle.

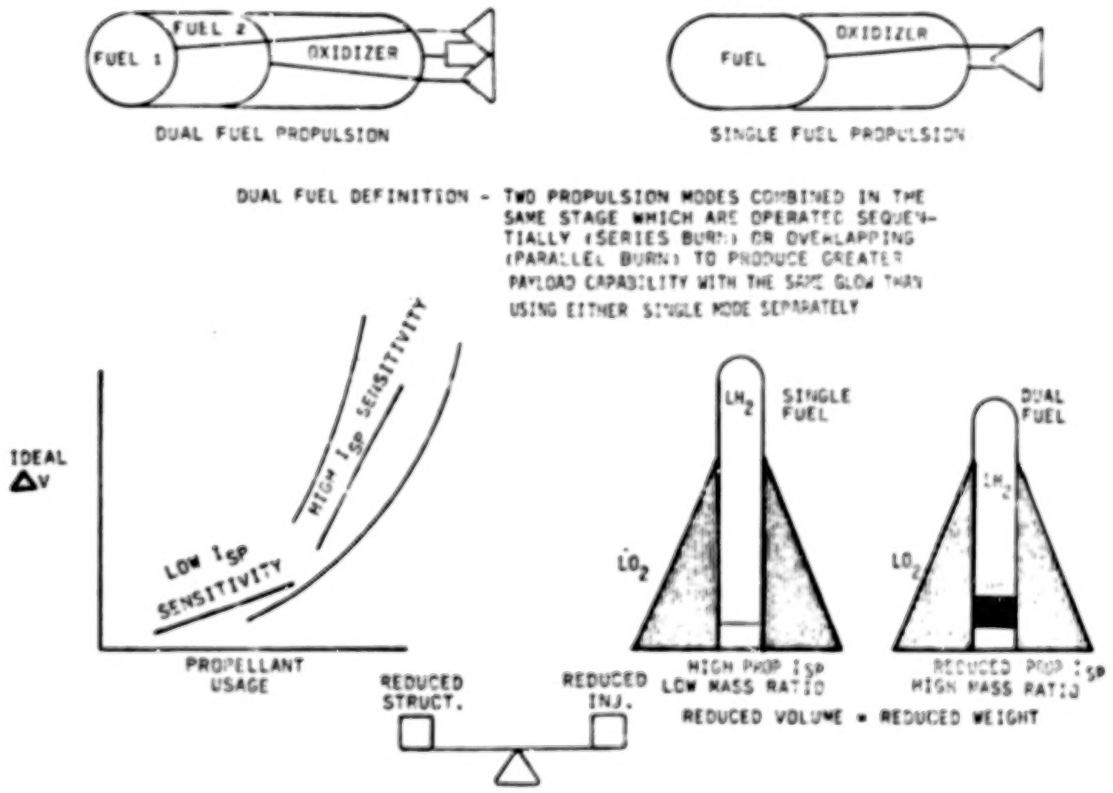

FIGURE 1 DUAL FUEL THEORY

The propellant consumption is significantly greater at the lower portion of the total ideal ΔV than at the higher ΔV. The effect of a given change in Isp upon ΔV when the last propellants are used is over 4-6 times that which is obtained when the first propellants are burned. Thus, one can say, at the lower ΔV's the curve tends to be less sensitive to Isp than later in the burn. This fact leads to a system using high density-low impulse propellants at low flight velocities and then, where the slopes of the performance curves are nearly equal, switching to a high impulse-low density propellant at the higher velocities. The system uses a common oxidizer so that only the fuel is changed.

There are three primary factors to consider in dual mode propulsion. Two positive factors and one negative or detrimental factor. It is the trade-off of these factors that determines if dual fuel/dual mode propulsion is an attractive technology option to pursue. The factors are (1) propellant bulk density (2) projected rocket engine mass, and (3) ascent flight trajectory performance or mass ratio requirements. Large increases in overall propellant bulk density will enable size reductions in propellant tankage. Rocket engines utilizing a hydrocarbon fuel are projected to have the potential for higher T/W than engines using LH_2 as fuel; therefore, engine system mass reductions could be possible. However, LO_2/Hydrocarbon engines have lower specific impulse characteristics than LO_2/LH_2 engines, therefore some overall reduction in the effective specific impulse will occur. The effect of this loss in performance can be minimized by using some form of sequential burn mode (as described previously) and selecting the proper staging parameters. The overall impact of dual mode propulsion is a trade-off of these various factors which requires a detailed and careful analysis.

Study Approach

Figure 2 depicts the various tasks required to accomplish the objectives stated in the study background. Technology assessments for current and normal growth were first projected to the 1985 time frame. The data were then used in the parametric performance and configuration analysis for a constant GLOW vehicle of 997,900 kg (2,200,000 lb). Inert weight trending (structures, subsystems and fluids) as a function of propellant split (ratio of mode 1 propellant to total propellant) was then determined. The vehicle was then scaled up to provide a constant 29,483 kg (65,000 lb) payload capability. Cost estimating relationships were formulated and life cycle costs developed for the vehicle systems. A selection was then made of the most promising dual fuel concept (series or parallel burn) and optimum propellant split ratio. A detailed point design of the selected configuration was then conducted to verify the parametric weight and performance. The dual fuel concept was then compared with the all LO_2/LH_2 vehicle to determine future technology requirements and recommendations.

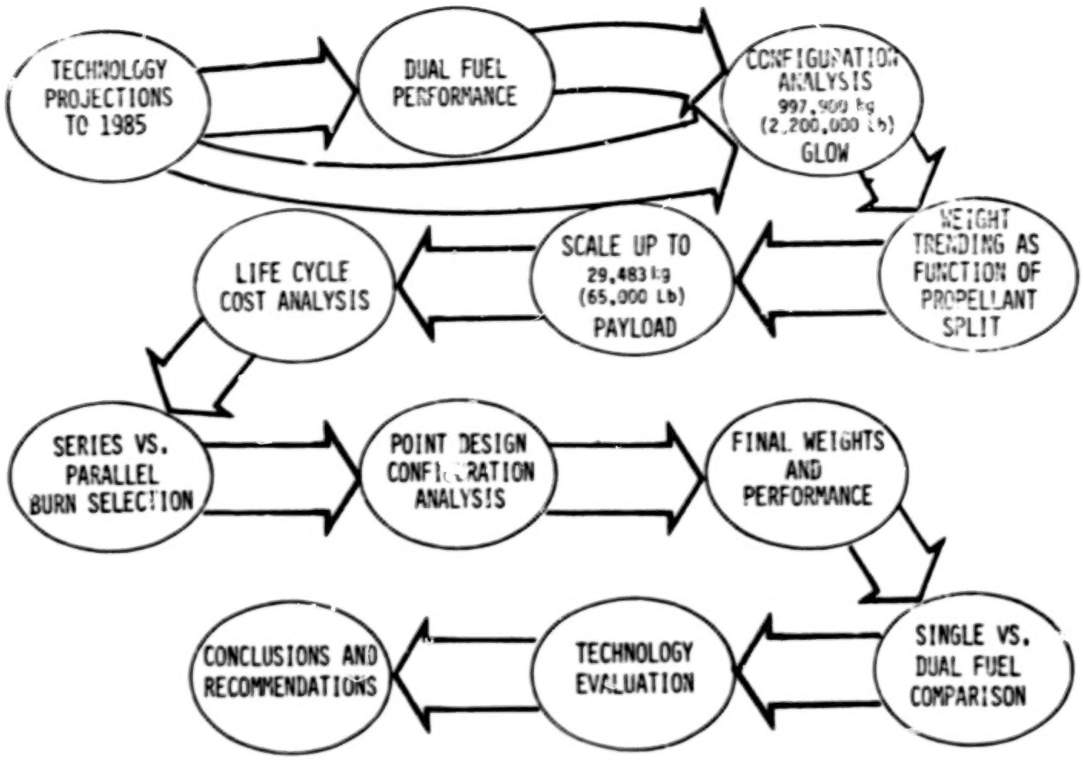
TECHNOLOGY PROJECTIONS TO 1985
DUAL FUEL PERFORMANCE
CONFIGURATION ANALYSIS
997,900 kg (2,200,000 Lb) GLOW
WEIGHT TRENDING AS FUNCTION OF PROPELLANT SPLIT
SCALE UP TO 29,483 kg (65,000 Lb) PAYLOAD
LIFE CYCLE COST ANALYSIS
SERIES VS. PARALLEL BURN SELECTION
POINT DESIGN CONFIGURATION ANALYSIS
FINAL WEIGHTS AND PERFORMANCE
SINGLE VS. DUAL FUEL COMPARISON
TECHNOLOGY EVALUATION
CONCLUSIONS AND RECOMMENDATIONS

FIGURE 2 STUDY ACTIVITIES SUMMARY

TECHNOLOGY PROJECTIONS - STEP 1

This task consists of providing assessments of current technology and normal growth to 1986 in key system and subsystem technology areas as applied to advanced earth-orbital transportation systems with dual mode propulsion systems. Data for this effort were obtained from recent literature, subcontractors, government and industry sources and in-house field specialists. For this purpose it was first necessary to define the required systems together with their operational environments and performance requirements generated in the course of the configuration development activities.

As a result of the work on the previous study (Reference 1) and early

configuration development activities on a dual fuel vehicle, the following items were projected as examples of 1985 technology projections:

Structures - Rene'41 Honeycomb Panel
- Aluminum Brazed Titanium Panel
- Metal Matrix Composites
- Refractory/Superalloy Materials

Systems - 2.8% x Vehicle Weight Landing Gear
- 34.5 M Pa (5,000 psi) Hydraulics and Controls
- Composite Materials
- LSI Circuitry, Laser Radar, Micro-Processors
- Bubble Memories, Solid State Display
- Solid State Power and Switching

Propulsion - Dual Fuel Engine
- LO_2/RP Engine
- Two-Position Nozzle

The majority of projections are similar to those proposed during the course of the previous study. Technology projections associated with the dual fuel aspects include development of a dual fuel engine and a high pressure hydrocarbon engine. Rationale for this technology is based primarily on Aerojet-General's NASA/Lewis study results (Reference 2).

A description of dual mode propulsion and technology is presented in the performance analysis paragraphs of the parametric trade studies section. The performance projections for the dual fuel and LO_2/RP engines should be considered as accelerated growth technology as the SSTO application is the only major driving factor for this development category.

PARAMETRIC TRADE STUDIES - STEP 2

This step consisted of defining alternate dual fuel horizontal take-off configurations, defining subsystem performance requirements and environments, selecting subsystem concepts, analyzing and sizing subsystems and determining

parametric weights. In addition, guidelines were established which provided a consistent set of groundrules to permit a valid comparison of the vehicle system concepts developed in the study. Table 1 summarizes the top level mission requirements. Both NASA directed and Boeing proposed requirements are included.

- **Lifetime:** 500 missions (low cost refurbishment and maintenance as design goal)
- **Mission duration:** 12 hours of self-sustaining lifetime from lift-off to landing
- **Eastern launch from KSC @ 28.5° inclination** (Reference energy orbit 93 x 185 km (50 x 100 nmi)
- **Payload:** 29,484 kg (65,000 lb) (Payload volume 18.29 m (60 ft) long; 4.57 m (15 ft) diameter)
- **Orbital maneuvering system:** ΔV = 198 m/s (650 fps)
- **Reaction control system:** ΔV = 30.5 m/s (100 fps)
- **TPS design mission (reentry):** Entry from due east 28.5° inclination
  371 km (200 nmi) altitude orbit
  Return payload 29,484 kg (65,000 lb)
  2,038 km (1,100 nmi) cross range capability
- **Fuel:** LO_2/LH_2 and LO_2/RP-1: Main Engine: High pressure bell (SSME type) High pressure LO_2/RP-1 (new development) and $LO_2/RP\text{-}1/LH_2$ dual fuel engine (new development)
- **Load:** n_x = 3g ascent; n_z = 2.2g entry; n_z = 2.5g subsonic maneuver
- **Aerodynamic heating:** Boundary layer transition onset = RI/SD correlation
- **Subsonic aerodynamics:** Minimum landing speed = 84.8 m/s @ = 15°
  Minimum static margin = 2% $\bar{C}$ (non CCV design)
  Static directional stability $\geq$.002 (non CCV design)
- **Hypersonic aerodynamics:** Trimmable α range = 20° min to 40° or greater
  Trimmable through entry with control surfaces and RCS

TABLE 1 VEHICLE REQUIREMENTS SUMMARY

Several different dual fuel system concepts were analyzed during Step 2. These vehicles would have a first operational flight in 1995. A generic structural configuration was used by all concepts. Design differences between concepts reflect consistent design approaches, philosophy and technology levels. Due to this approach it was possible to avoid repetition in the analysis of the various configurations and to apply analysis results to more than one configuration.

Figure 3 illustrates the task flow associated with developing the parametric weights. Performance analysis was conducted for the parallel and series burn configurations and results supplied to the configuration analysis. The configuration effort utilized a .5 propellant split ratio to investigate six series burn and two parallel burn configurations. The configurations differed in body/wing shape, engine installation and RP tank location. Thermal and load profiles, subsystem operation profiles, structures sizing and weights and aerodynamic characteristics were developed for each configuration. The most promising configuration of each dual mode propulsion concept was then selected based on

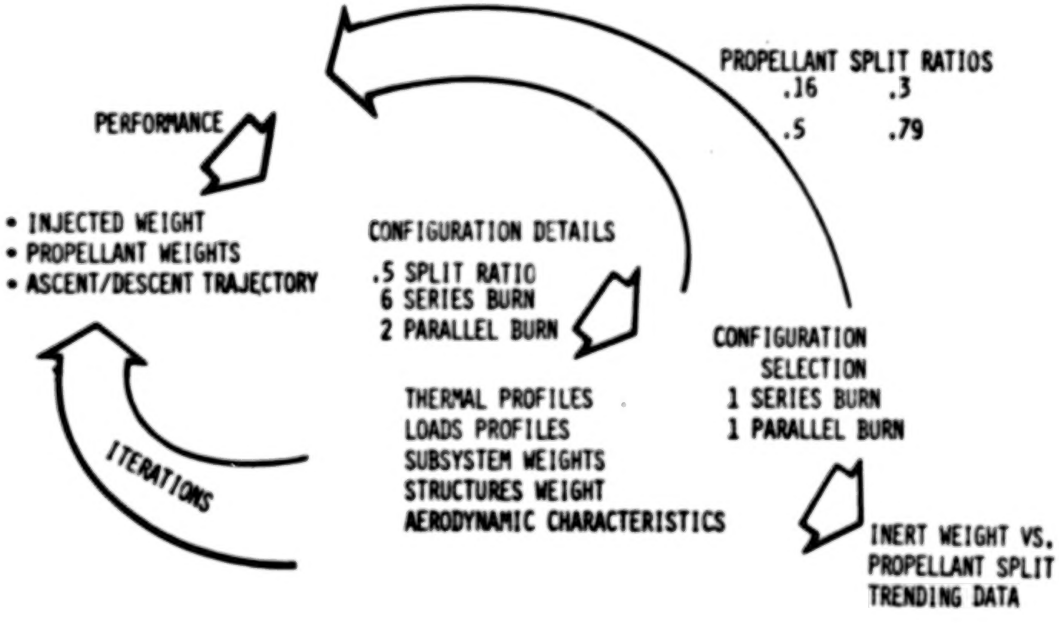

FIGURE 3 CONFIGURATION PARAMETERS SUMMARY

this preliminary analysis. These concepts were then iterated to optimize performance in terms of payload for propellant split ratios of .16, .3, .5 and .79. Inert weight trends were then developed for these vehicles as a function of propellant split ratio at a constant 997,900 kg (2,200,000 lb) GLOW.

Performance Analysis

As discussed previously, the dual mode propulsion theory projects that the structural and engine weight savings realized from packaging a higher density fuel will more than offset the performance loss from utilizing a propellant combination with a lower overall effective Isp.

In addition to the reduction in overall effective Isp, there are some other performance constraints that are attributed to dual fuel design. For the series burn configuration there is a small performance penalty resulting from a drop in thrust level associated with the switch over of burn one to burn two which is applicable to both HTO and VTO configurations. Another constraint which is applicable to both take-off modes but more constraining to the horizontal take-off design is the engine configuration and its relationship to base drag. The horizontal take-off vehicle is sensitive to aerodynamic drag. Dual fuel propulsion enables the designer to reduce the fuel tank size which results in smaller diameter bodies with less structures weight. However, performance gains do not directly relate to this size reduction as the base area is dictated by the engine size.

Injected Weight Trade - Series Burn. The overriding performance parameter for determining orbital payload is the weight injected into orbit. This is determined from a trajectory analysis which utilizes aerodynamic, propulsion and system weights as basic inputs. For the dual fuel studies, the propellant split ratio (LO_2/RP-1/total propellant ratio) is the most significant performance variable, as shown in Figure 4. These results apply to series burn dual fuel propulsion systems and horizontal take-off at a speed of 182.9 m/s (600 fps). The effect of take-off thrust to weight ratio varying from 0.78 to 0.94 is also presented in Figure 4. The number of engines was fixed to three and "rubberized" to satisfy the sea level thrust to GLOW ratio, T_{SL}/GLOW. The shape of these plots (i.e. injected weight versus split) are stronbly influenced by

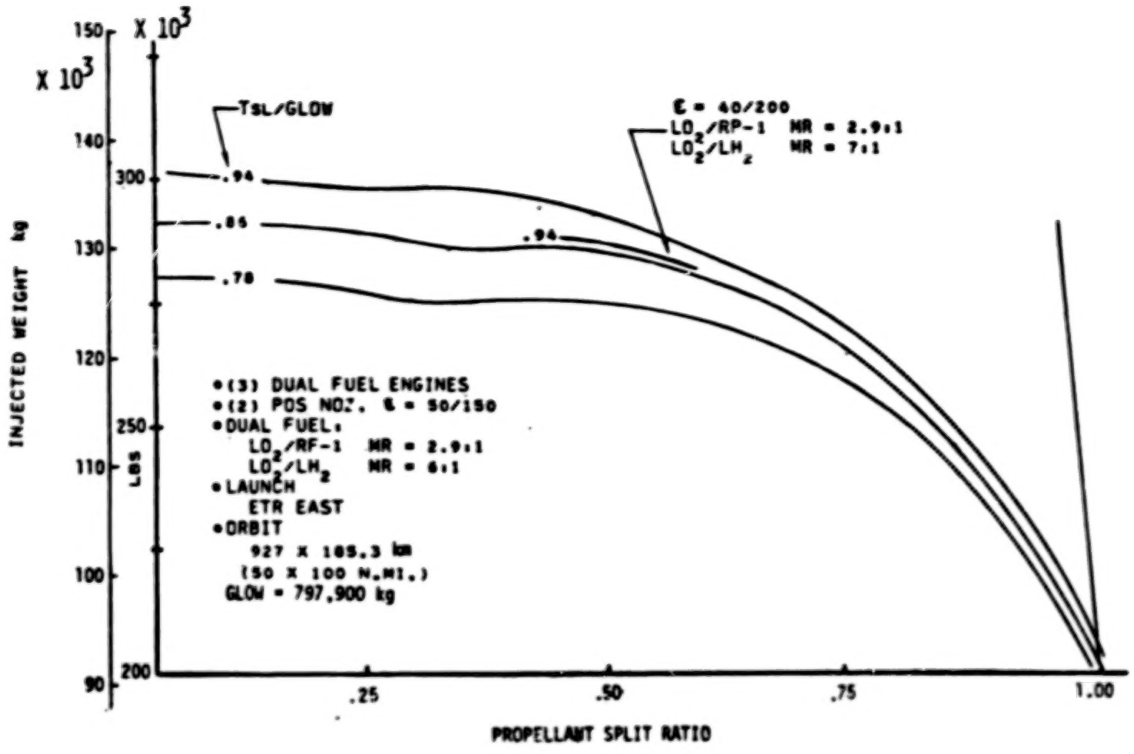

FIGURE 4 SERIES BURN INJECTED WEIGHT TRADE

the sharp drop in thrust when the dual fuel engine is shifted from using RP-1 to LH_2. The thrust is reduced about 20 percent due to the engine pump power requrements. (See following section on velocity losses for effect on tangential load factor). These early preliminary results were updated for the final results.

Dual Fuel Propellant Split Trade. The data presented in Figure 5 include the effects of aerodynamic drag relevant to the configurations for various propellant splits, as well as propulsion refinements on mixture ratio and thrust vector control allowances for both series and parallel burn propulsion systems. A discontinuity in the shape of the curve for the series burn occurs at a zero percent split due to the conditions of constant thrust to weight at lift-off of 0.78 and the dual fuel thrust ratio previously mentioned. For propellant split ratios less than 0.50 a parallel burn propulsion system results in higher injected weights over series burn systems. GLOW was fixed at 997,900 kg (2,200,000 lb) and lift-off thrust to weight at 0.78. All nozzles

were extended at an altitude of 13.72 km (45,000 ft) to increase thrust performance. The propulsion system design selected for the study was that with the staged combusion cycle since preliminary analysis indicated only small differences in overall vehicle performance.

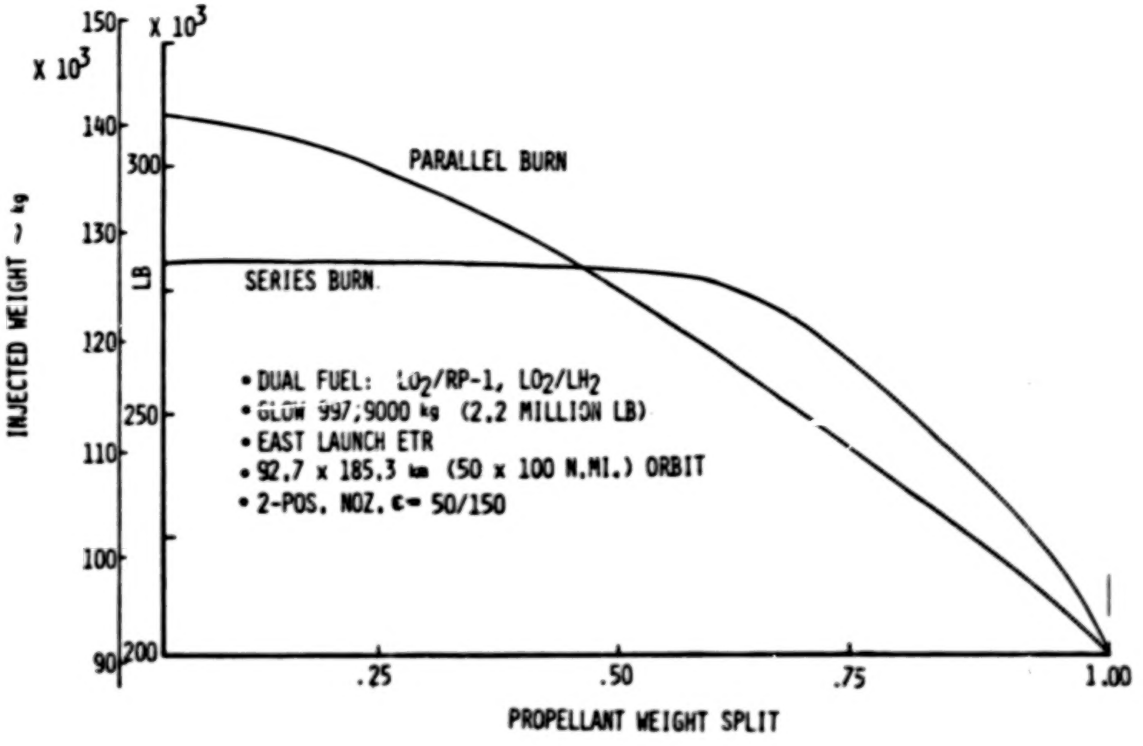

FIGURE 5 DUAL FUEL PROPELLANT SPLIT TRADE

For the parallel burn, the resultant plot was obtained by optimizing the thrust split ratio and staging velocity (for propellant fuel changeover from combined RP-1 and LH_2 to LH_2 only) at each propellant split ratio. For example, at a propellant split ratio of 0.57 the best thrust split ratio (i.e. thrust LO_2/RP-1 to total vacuum) is 0.657 and the staging or changeover velocity is 4267 m/s (14,000 ft/sec). Thus the parallel burn curve is the optimum envelope of the combination of these parameters.

Dual Fuel Performance Parameters. The following analysis makes use of effective specific impulse and velocity losses to determine injected weight and to explain the trends with propellant split. The basic relationships are presented as follows:

Required ideal velocity = orbital inertial injection velocity - initial velocity - earth rotational velocity + sum velocity losses

$$\Delta V_{IDEAL} = V_{INJ} - V_{INIT} - V_{ROT} + \Delta V_{LOSS}$$

for 93 x 185 km orbit and east launch from ETR

$$\Delta V \text{ (m/s)} = 7891 - 183 - 415 + V_{LOSS}$$

$$\Delta V_{IDEAL} = 7294 + \Delta V_{LOSS}$$

Also, from ideal rocket equation

$$\Delta V_{IDEAL} = g I_{EFF} \ln \left(\frac{W_{INIT}}{W_{FINAL}} \right)$$

Where, I_{EFF} = effective specific impulse

W_{INIT} = GLOW

W_{FINAL} = weight injected = W_{INJ}

or,

$$\Delta V_{IDEAL} = g\, I_{EFF} \ln \left(\frac{GLOW}{W_{INJ}} \right)$$

thus,

$$g\, I_{EFF} \ln \left(\frac{GLOW}{W_{INJ}} \right) = 7294 + \Delta V_{LOSS}$$

$$\left(\frac{GLOW}{W_{INJ}} \right) = e^{\left(\frac{2794 + \Delta V_{LOSS}}{g\, I_{EFF}} \right)}$$

$$W_{INJ} = GLOW\, e^{\left[\frac{7394 + \Delta V_{LOSS}}{g\, I_{EFF}} \right]}$$

For GLOW fixed, the injected weight is only a function of velocity loss and effective specific impulse, and a carpet plot of these performance parameters was obtained. The carpet plot shown on Figure 6 is for a GLOW = 997,900 kg (2,200,000 lb). The ΔV_{LOSS} and I_{sp} effective were obtained from Figure 7 for various propellant split ratios. The injected weight variations are the same as those shown in Figure 5.

Velocity Loss and Effective Specific Impulse. As the propellant split ratio was varied from zero to 1 the vehicle performance characteristics in terms of velocity losses (ΔV_{LOSS}) and effective specific impulse (I_{EFF}) was changed as shown in Figure 7 for both series and parallel burn dual fuel vehicles. The ΔV_{LOSS} trend with propellant split is most closely associated with the total burn time or average tangential load factor, see Figure 8. For parallel burn the ΔV_{LOSS} is almost constant around a value of about 1,524 m/s (5000 fps). For series burn the ΔV_{LOSS} is relatively high at 2,012 m/s (6600 ft/sec) near zero decreasing to slightly less than the 1,524 m/s (5000 ft/sec) at high propellant split ratios. This trend for series burn as shown on Figures 6 and 7 is mainly caused by the approximately 20 percent drop in engine thrust as the dual fuel engine is switched over from RP-1 to LH_2 fuel during the ascent trajectory.

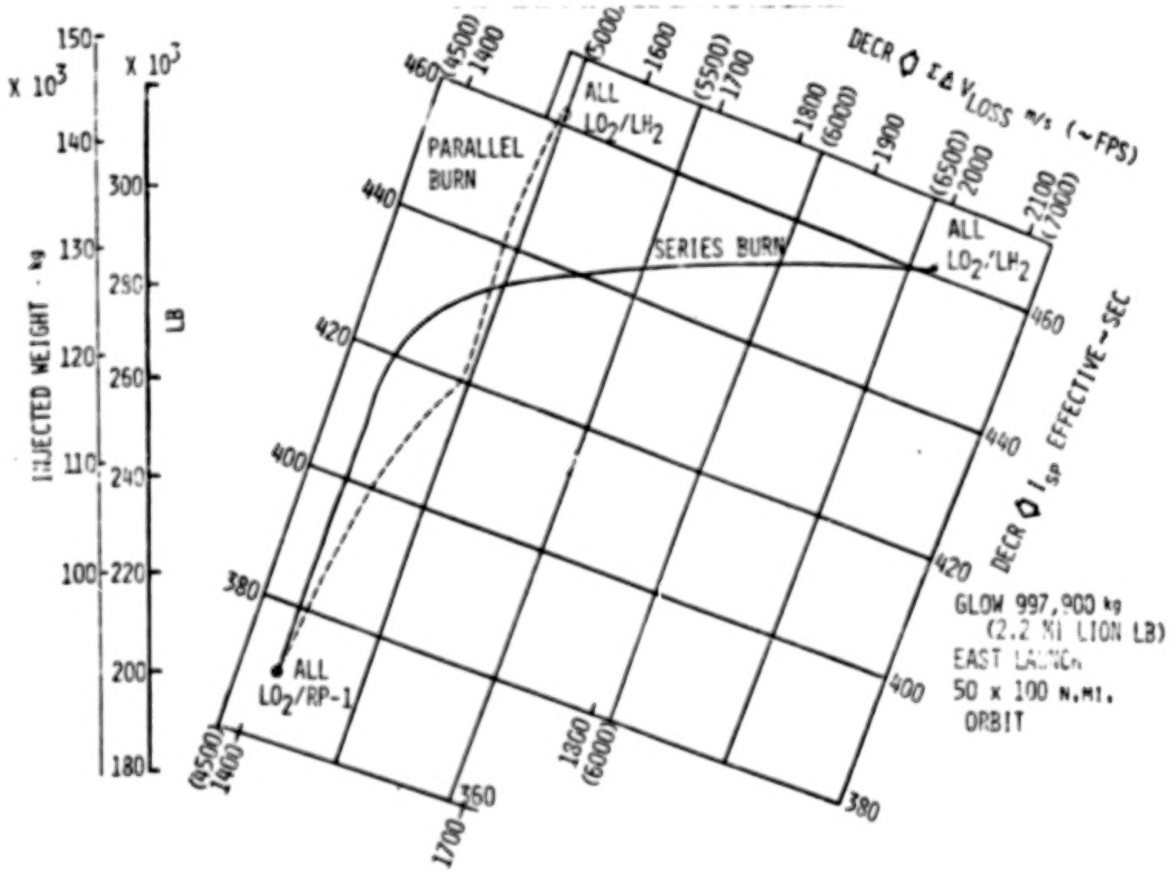

FIGURE 6 DUAL FUEL PERFORMANCE PARAMETERS

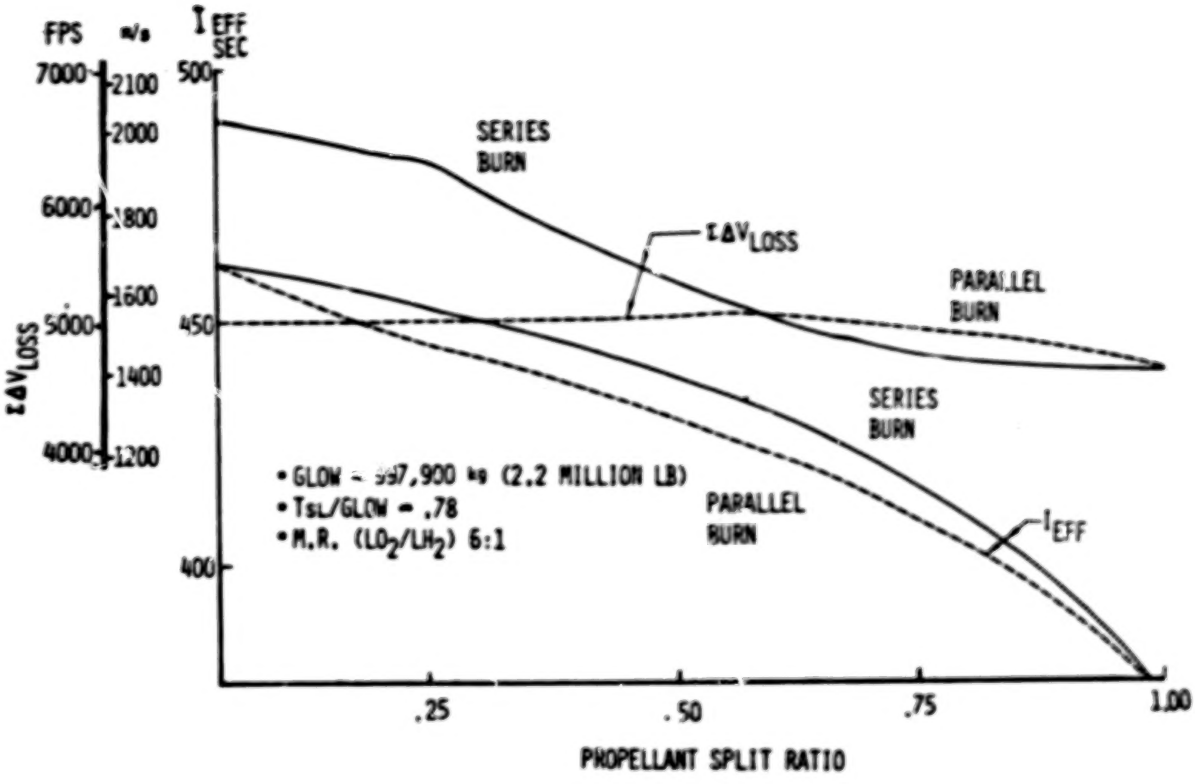

FIGURE 7 VELOCITY LOSS AND EFFECTIVE IMPULSE

The effective specific impulse varied with propellant split ratio (zero) from a value of 465 seconds for all LO_2/LH_2 propellant to 375 seconds for all LO_2/RP-1 propellant (1.0). Values for parallel burn are somewhat higher than those obtained from series burn at any given propellant split ratio. The non-linear shape of the effective specific impulse curve is explained in the following discussion and analysis of this performance parameter.

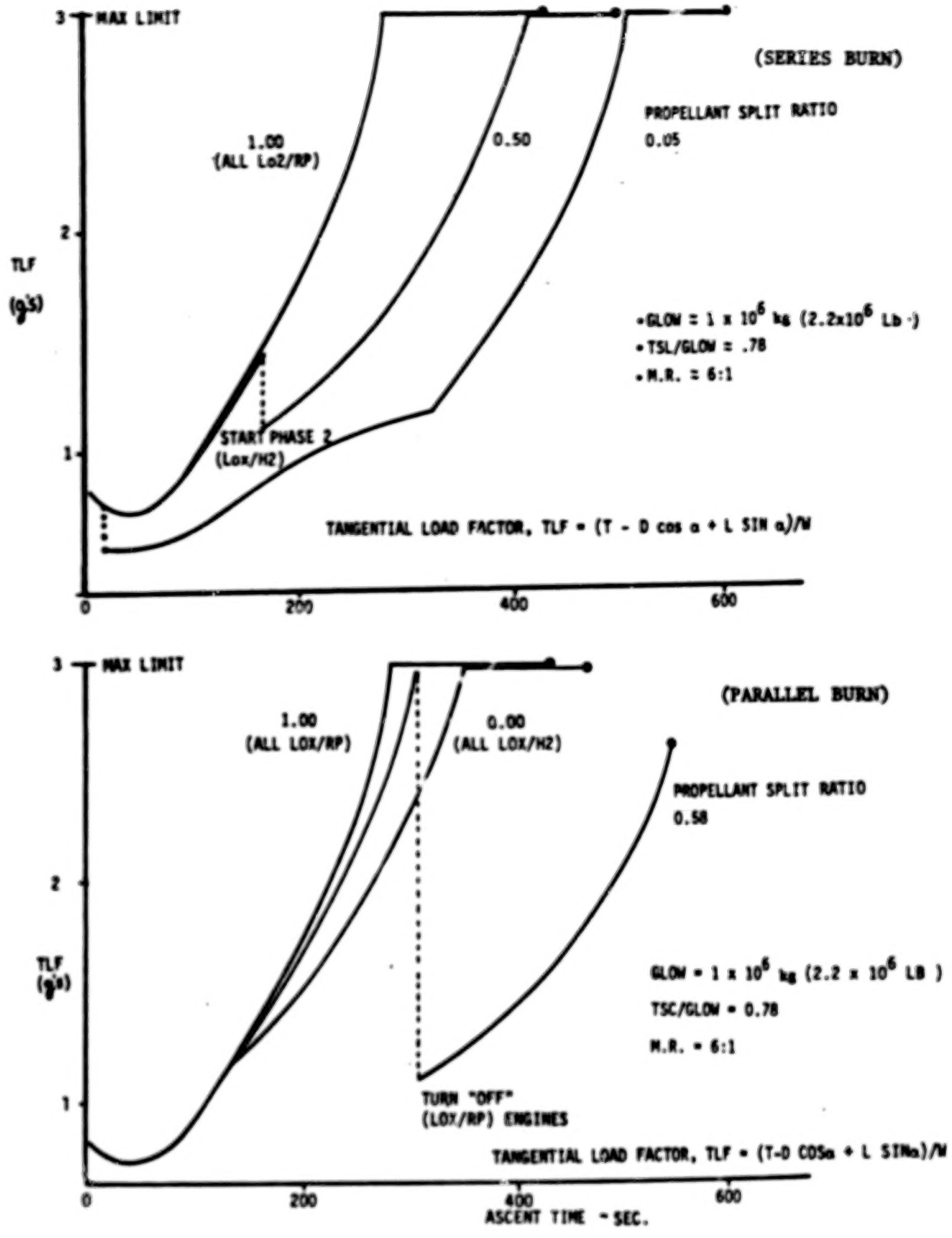

FIGURE 8 COMPARISON DUAL FUEL ENGINES TANGENTIAL ACCELERATION

Effective Specific Impulse Determination. An analysis for determining the specific impulse with a propellant split ratio of .47 and series burn is presented in Figure 9. Even at this propellant split ratio the dominance of the last term (i.e. all LO_2/LH_2) in terms of ΔV or propellant loading explains the non-linear nature of the plot of effective specific impulse

(1) STAGE $$\Delta V = gI \ln\left(\frac{GLOW}{GLOW - WT_{PROP}}\right) = g\,I \ln \frac{1}{1-\zeta}$$

WHERE, $\zeta = WT_{PROP}/GLOW$ = PROPELLANT LOADING, OR

$$\zeta_1 = \frac{W_1}{GLOW}\ ;\ \zeta_2 = \frac{W_2}{GLOW - W_1}\ ;\ \zeta_3 = \frac{W_3}{GLOW - [W_1 + W_2]}\ ;\ \zeta_{TOT} = \frac{W_{TOT}}{GLOW}$$

WHERE W_1 = PROPELLANT BURN (1) PHASE

W_2 = PROPELLANT BURN (2) PHASE

W_3 = PROPELLANT BURN (3) PHASE

W_{TOT} = PROPELLANT BURN - TOTAL

MULTI-STAGE (OR PHASES)

$$\Delta V = \Delta V_1 + \Delta V_2 + \Delta V_3$$

$$gI_{EFF} \ln\left(\frac{1}{1-\zeta_{TOT}}\right) = \underbrace{gI_1 \ln\left(\frac{1}{1-\zeta_1}\right) + gI_2 \ln\left(\frac{1}{1-\zeta_2}\right)}_{\text{1st POS}} + \underbrace{gI_3 \ln\left(\frac{1}{1-\zeta_3}\right)}_{\text{2nd POS}}$$

$\text{1st POS}: LO_2/RP\text{-}1$; $\text{2nd POS}: LO_2/LH_2$

$\zeta_{TOT} = .874$ $\quad I_1 = 355$ $\quad I_2 = 372$ $\quad I_3 = 465$

$\zeta_1 = .251$ $\quad \zeta_2 = .211$ $\quad \zeta_3 = .788$

$$I_{EFF}(.207) = 355(.289) + 372(.237) + 465(1.55)$$
$$= 103 + 88 + 720$$

I_{EFF} = 439.1 SEC FOR: SERIES BURN (.47 SPLIT RATIO)

	WT
$LO_2/RP\text{-}1$	= 408,231 kg (900,000 LB)
GLOW	= 997,900 kg (2.2 MILLION LB)

FIGURE 9 EFFECTIVE SPECIFIC IMPULSE DETERMINATION - SERIES BURN

and propellant split. To further illustrate the effect of propellant split ratio these relations can be processed to result in the following expressions:

$$I_{EFF}_{OVERALL} = \left[I_{EFF}_{LO_2/RP-1} \left(\ell n \frac{1}{1 - (PSR)\,\zeta_{TOT}} \right) + I_3 \ell n \left(\frac{1}{1 - \frac{(1-PSR)\,\zeta_{TOT}}{1-PSR\ \zeta_{TOT}}} \right) \right] \Bigg/ \ell n \frac{1}{1 - \zeta_{TOT}}$$

where, For Series Burn

$$PSR, \text{ Propellant Split Ratio} = \frac{WT_{LO_2/RP-1}}{WT_{LO_2/RP-1} + WT_{LO_2/LH_2}}$$

Note: The two terms for the $LO_2/RP-1$ phases have been combined into a single term by use of an intermediate effective specific impulse for only the $LO_2/RP-1$ propellant.

Minimum Drag (C_{Do}) Trade. As the propellant split ratio was increased from zero to 1, the required propellant volume decreased and permitted overall reduction in the size of the configuration. Thus, the body was reduced in diameter and the wing reduced in thickness (since reference wing area was held constant for a take-off speed of 183 m/sec (600 fps) at 15° angle of attack, and re-entry planform loadings were held approximately constant for entry temperature constraints). These reductions in body fineness ratio and wing thickness ratio produced decreases in the minimum drag coefficient, C_{Do}, as shown in Figure 10. The decreased aerodynamic drag in turn improved vehicle ascent performance by increasing the injected weight. These effects were included in the final injected weight variations with propellant split ratio.

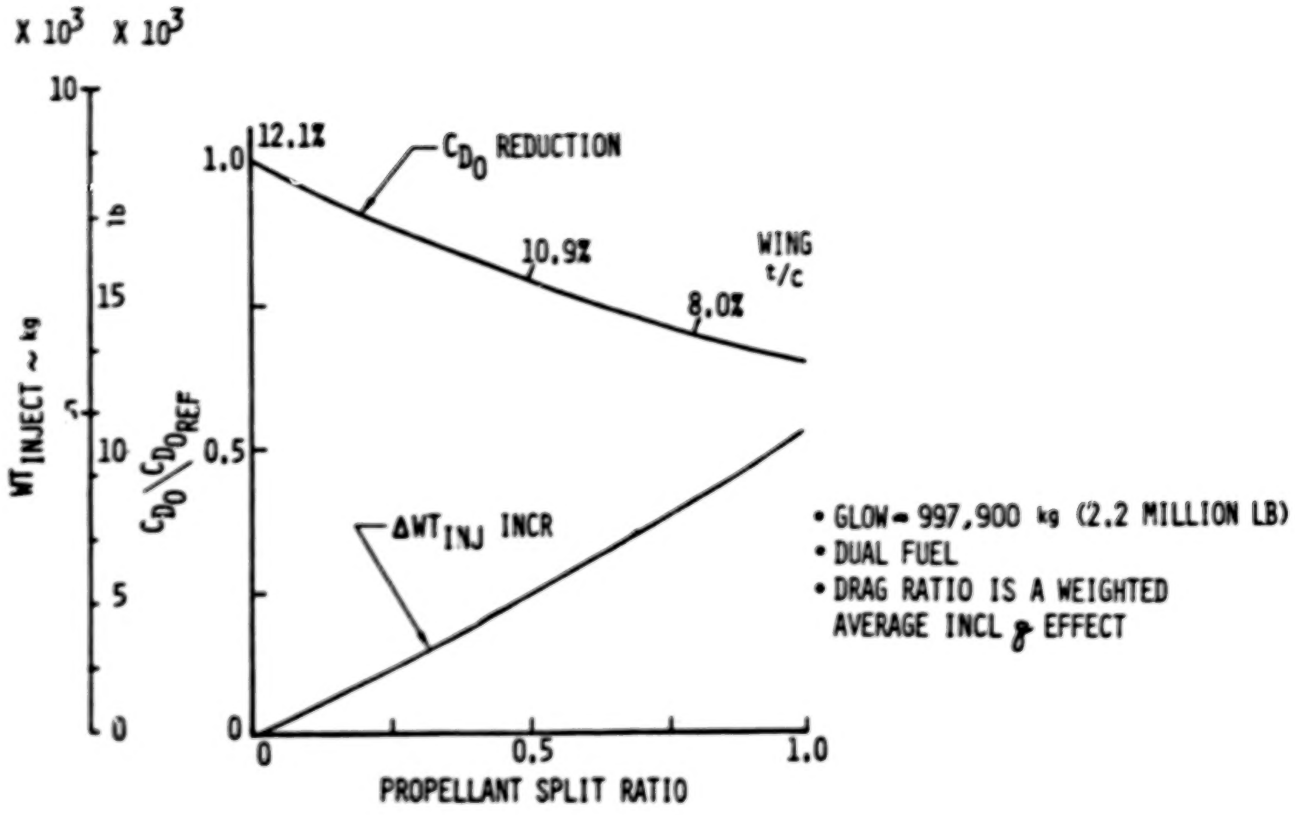

FIGURE 10 MINIMUM DRAG (C_{DO}) TRADES

Series Burn Engine Transient Analysis. The estimated shutdown/start-up transient is shown in Figure 11 and for vehicle ascent performance effectively amounts to about 3.5 seconds of coast between propellant phases. This coast reduced injected weight or payload by about 181 kg (400 lb).

SHUTDOWN/START-UP TRANSIENTS FOR CONVERSION FROM $LO_2/RP-1$ BURN TO LO_2/LH_2 BURN. ASSUME A 2-SECOND SHUTDOWN AND A 3-SECOND START.

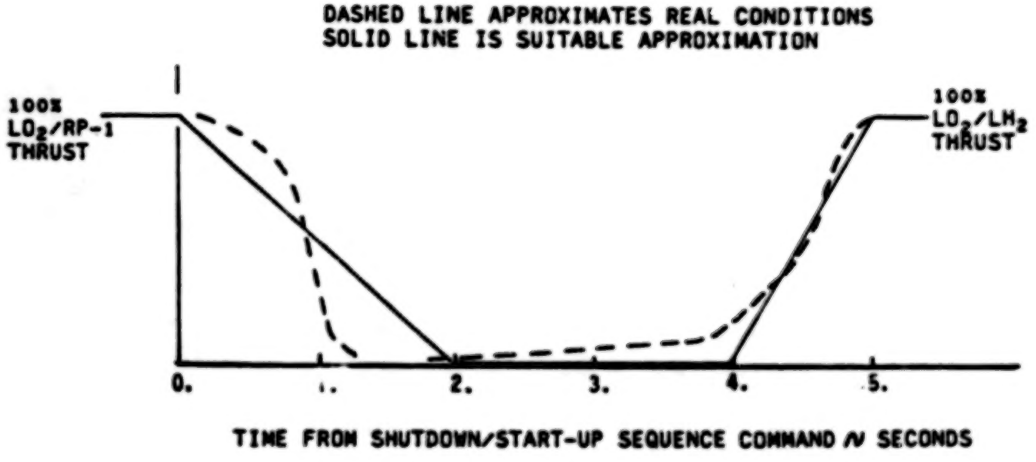

FIGURE 11 SERIES BURN ENGINE TRANSIENT ANALYSIS

Propulsion Analysis

This section provides parametric data on candidate Mode 1 and Mode 2 bell nozzle rocket engine concepts for mixed mode, Single Stage to Orbit vehicles. The majority of data was generated by the Aerojet Liquid Rocket Company as part of the study on advanced high pressure engines (Reference 2). An assessment was conducted to determine the impact on previous weight estimating relationships developed during the course of studying technology requirements for advanced Earth-orbital transportation systems which was limited to LO_2/LH_2 propellants. The results of the engine weight assessment indicated that the Aerojet data showed an increase in engine weight per unit thrust while Rocketdyne showed a decrease. In addition, the Rocketdyne data indicated a much greater weight increase than the Aerojet data as the expansion ratio increased.

Since it was desired that consistent engine weights be used in the dual fuel study, agreement was reached between NASA Langley and Boeing study personnel as to compromise assumptions. The weight estimating relationships discussed in this section reflect these compromise weights. The elements of engine weight included in the parametric analysis are defined in Table 2. A fixed 90% bell nozzle was assumed for the Mode 1 engines and a fixed 90% bell to an area ratio of 40:1, and an extendable 90% bell beyond 40:1 was assumed for the Mode 2 and dual fuel engines.

For purposes of the Parametric Weight Study, the engine is assumed to be composed of the following components:

- Regeneratively Cooled Combustion Chamber
- Regeneratively Cooled Thrust Chamber Fixed Nozzle
- Thrust Chamber Nozzle Extension (Mode 2)
- Nozzle Extension Deployment System (Mode 2)
- Main Injector
- Main Turbopumps
- Boost Pumps
- Preburners (or Gas Generator)
- Propellant Valves and Actuation
- Gimbal
- Hot Gas Manifold (if required)
- Propellant Lines
- Ignition System
- Miscellaneous (Electrical Harness, Instrumentation, Brackets, Auxiliary Lines and Controls)

Engine Dry Weights do not include:

- Gimbal Actuators and Actuation System
- Engine Controller
- Pre-Valves
- Tank Pressurant Heat Exchangers and Associated Equipment
- Contingency (A total contingency is normally included in the Vehicle Weight Statement)

TABLE 2 ENGINE WEIGHT DEFINITION

Dual Fuel Engine. Oxygen is utilized to cool the thrust chamber in both modes of operation. This is a staged combustion cycle concept in which Mode 1 turbine power is obtained from the combustion products of the total oxygen and Mode 1 fuel flow in the Mode 1 feed system preburners. Upon completion of the Mode 1 burn, the Mode 1 fuel feed system is shut down and isolated. In Mode 2 operation, turbine power is obtained from the combustion products of the total oxygen and hydrogen flow in the Mode 2 feed system preburners. An extendable nozzle is usually deployed for the Mode 2 operation.

Specific impulse in each mode is shown on Figure 12. Due to pump power requirements the weight flow of $LO_2/RP\text{-}1$ = 1.68 times the weight flow of LO_2/LH_2 and the thrust of $LO_2/RP\text{-}1$ = 1.375 times the thrust of LO_2/LH_2 at vacuum conditions. The engine dry weight which includes the nozzle, nozzle actuator, contingency controller pressurization components and thrust vector control components is:

$$W = 3.21\ \dot{W} + .002\ \epsilon_1\ \dot{W} + .0033$$

$$(\epsilon_2-\epsilon_1)\ \dot{W} + .82\left(\sqrt{\epsilon_2}-1\right)\sqrt{\dot{W}} + .24\ \dot{W} \quad (\dot{W} \text{ in kg/s})$$

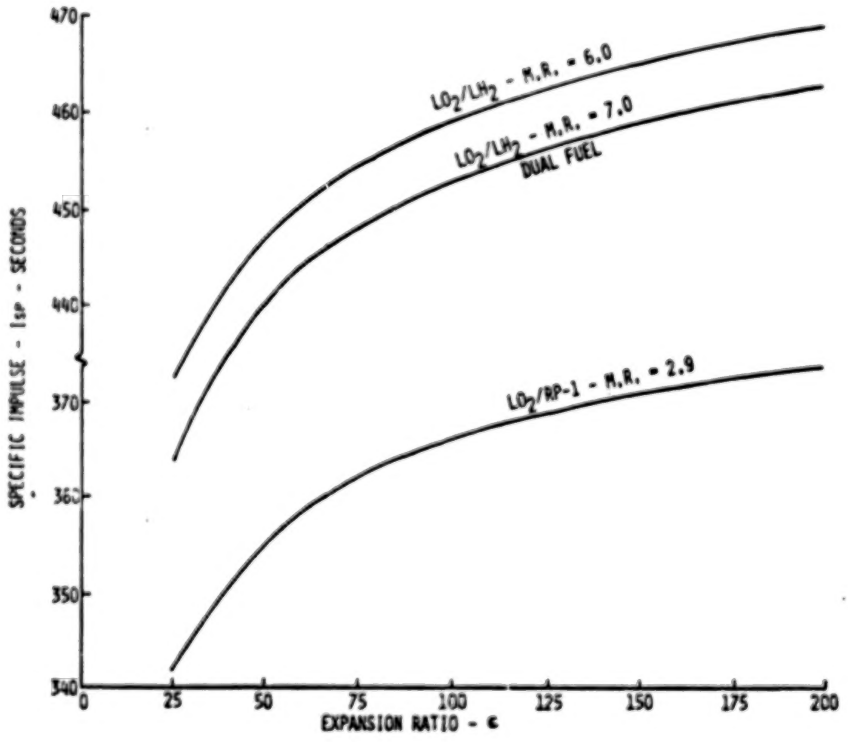

FIGURE 12 PROPULSION SYSTEM PERFORMANCE CHARACTERISTICS

The total elements of engine weight that make up the first four terms of the equation are defined in Table 2. The fifth term of the equation accounts for thrust vector control components. In the equation $\dot{W}$ is the LO_2/LH_2 flow rate and the engine chamber pressures are 27.58 MN (4000 psia) for LO_2-RP-1 and 20.68 MN (3000 psia) for LO_2/LH_2 and ϵ_1 and ϵ_2 are the retracted and extended nozzle expansion ratios, respectively.

Single Fuel Engines. The Mode 1 LO_2/RP-1 engine has a maximum recommended chamber pressure 27.58 MN (4000 psia) at a O/F mixture ratio of 2.9:1. Oxygen is utilized to cool the thrust chamber. This is a staged combustion cycle concept in which turbine power is obtained from the combustion products of the total engine flow in oxygen-rich and fuel-rich preburners. The weight estimating relationship (WER) for this engine is:

$$W = 1.18\,\dot{W} + .0012\,\epsilon_1\,\dot{W} + .0014\,(\epsilon_2-\epsilon_1)\,\dot{W} \qquad (2)$$

$$+ .67\,(\sqrt{\epsilon}_2-1)\,\sqrt{\dot{W}} + .15\,\dot{W} \qquad (\dot{W} \text{ in kg/s})$$

where the specific impulse is shown on Figure 12. For the gas generator cycle where hydrogen is utilized to cool the thrust chamber subtract .4 W in weight from first term in the above equation. The hydrogen coolant is burned in a hydrogen-rich gas generator to provide the combustion products for turbine power. The turbine exhaust gases are then expended in the main chamber nozzle. The main chamber impulse should be reduced by 1.2 seconds due to chamber heat loss to hydrogen coolant. Thrust of the turbine exhaust products should be determined by adding an LO_2/LH_2 flow rate of 23.6×10^{-6} kg (52×10^{-6} lb) x vacuum thrust with a specific impulse of 255.5 seconds.

Both the gas generator and staged combustion cycle engines were evaluated. Although the staged combustion cycle did not offer any significant overall saving over the gas generator cycle it was used for all the subsequent analysis.

The Mode 1 LO_2/LH_2 engine has a chamber pressure of 20.68 MN (3000 psia) at a O/F mixture ratio of 6:1. Hydrogen is utilized to cool the thrust chamber. This is a staged combustion cycle concept in which turbine power is obtained

from the combustion products of the total engine flow in oxygen-rich and hydrogen-rich preburners. An extendable nozzle is deployed for the Mode 2 operation. Parametric weights are determined by the following:

$$W = 2.39\ \dot{W} + .002\ \epsilon_1\ \dot{W} + .0033\ (\epsilon_2-\epsilon_1)\ \dot{W} \qquad (3)$$

$$+ .82\ \ (\sqrt{\epsilon_2}-1)\ \ \sqrt{\dot{W}} + .24\ \dot{W} \quad (W \text{ in kg/s})$$

where the specific impulse is shown on Figure 12.

Figure 13 reflects the results of the parametric en ine sizing and weights which was accomplished on the various parametric configurations.

Configuration Analysis

It is important to note that the basis for the structural concept and baseline configuration for the dual mode propulsion studies was the horizontal SSTO vehicle which Boeing had selected as the recommended all LO_2/LH_2 system concept during the earlier study to identify cost effective technology requirements for advanced earth-orbital transportation systems.

Baseline System Concept. The SSTO technology development and past study effort are based on the belief that there is (1) a continued requirement for lower cost space transportation and that (2) a fully reusable, airplane type operation of aerodynamic transportation vehicles will allow considerable improvement in cost per flight and mission flexibility. Earlier studies indicated that to provide a useful payload to orbit with a Single Stage to Orbit concept, operating in any launch mode, structural weight must be significantly reduced. Consequently, the study baseline concept uses a single structural system to serve functions which previously required four separate systems: thermal protection, airframe, cryogenic tankage, and cryogenic insulation.

THRUST $_{S.L.}$/GLOW = .78

GLOW .9979 x 10^6 kg (2.2 x 10^6 lb) EXCEPT AS NOTED

ENGINE ε = 50 & 150 MIXTURE O/F RP-1 = 2.9:1, LO_2 = 6:1

MODE	PROP. SPLIT RATIO	WEIGHT INJECTED kg (LB)	LO_2 kg (LB) x 10^3	PROPELLANT LH_2 kg (LB)x10^3	RP-1 kg (LB) x 10^3	QTY TYPE	ENGINES THRUST-NEWTONS (LB) S.L.	VAC	kg/SEC (LB/SEC)	WEIGHT kg (LB)
SERIES BURN	.5	124621 (274742)	698.9 (1540.9)	62.4 (137.5)	111.9 (246.795)					
	.3	125416 (276495)	718.1 (1583.2)	87.3 (192.4)	66.6 (146.795)	(3) DUAL FUEL RP-1 LH_2	2.544 x 10^6 (572000) 1.824 x 10^6 (410.049)	3.004 x 10^6 (675398) 2.161 x 10^6 (485906)	803 (1771) 473 (1044)	4051 (8930)
	.79	114106 (251560)	678.2 (1495.2)	26.4 (58.3)	179.1 (394.872)					
▶	.613	172491 (380278)	947.0 (2087.8)	66.5 (146.6)	189.0 (416.609)	(4) DUAL FUEL RP-1 LH_2	2.629 x 10^6 (591031) $_6$ 2.092 x 10^6 (470297)	3.030 x 10^6 (681217) 2.458 x 10^6 (552487)	833 (1836) 539 (1188)	4880 (10758)
PARALLEL	.5	123457 (272176)	699.9 (1543)	62.5 (137.7)	112.1 (247.077)	(2) RP-1 (2) LH_2	2.257 x 10^6 (507409) $_6$ 1.56 x 10^6 (350733)	2.601 x 10^6 (584835) 1.849 x 10^6 (415617)	715 (1576) 405 (893)	3126 (6892) 2748 (6058)
	.3	133436 (294175)	711.5 (1568.6)	86.4 (190.5)	66.5 (146.667)	(1) RP-1 (2) LH_2	2.680 x 10^6 (602404) 2.477 x 10^6 (556951)	3.088 x 10^6 (694323) 2.936 x 10^6 (659985)	849 (1871) 644 (1419)	3679 (8111) 4290 (9458)
	.16	139047 (306547)	720.5 (1588.4)	103.0 (227.1)	35.3 (77.846)	(1) RP-1 (3) LH_2	1.422 x 10^6 (319737) 2.071 x 10^6 (465528)	1.639 x 10^6 (368525) 2.454 x 10^6 (551646)	450 (993) 538 (1186)	2024 (4463) 3608 (7954)

▶ 1.37497 x 10^6 kg (3.0313 x 10^6)GLOW

FIGURE 13 DUAL FUEL ENGINE CHARACTERISTICS

The baseline study vehicle including its major characteristics is shown in Figure 14. It is a delta winged aero-spacecraft that takes off and lands horizontally and is powered by rocket engines. It is supported on a ground accelerator during the takeoff run. The accelerator provides three main functions: (1) aid in initial horizontal acceleration; (2) distributed support to the air vehicle during takeoff run; and (3) air vehicle rotation at liftoff.

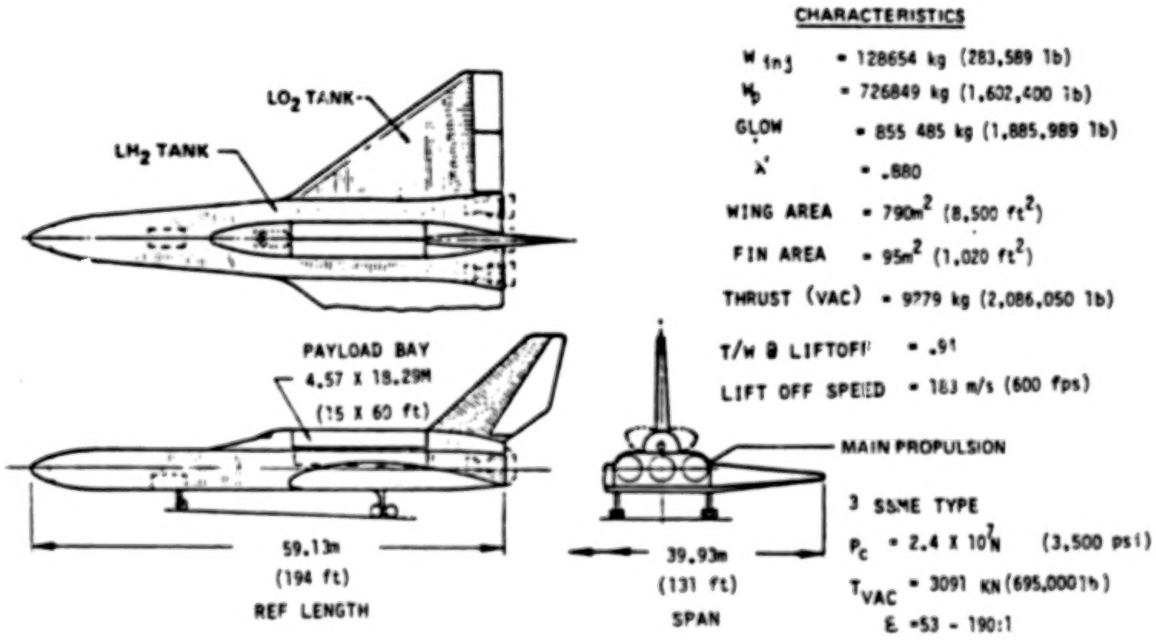

FIGURE 14 BASELINE SYSTEM CONCEPT.

The Boeing SSTO configuration utilizes integral wing liquid oxygen and body liquid hydrogen tanks. The tank walls are of multi-functional metallic surface panels. One of the key issues regarding feasibility of this type of vehicle is the ability to integrate the propellant tankage with load carrying structure. Thus, the propellant is contained by aerodynamically shaped structure rather than more conventional cylindrical pressure vessels used on current space boosters. The resultant primary structure consists of an outer shell of load bearing surface panels stabilized by ring frames with truss type internal tension struts where required.

The exterior surface of the vehicle is made from Rene'41 and titanium surface panels. Material selection is based upon the temperature attained during ascent or reentry. The Rene'41 material was developed for use on the X-20 program. The multi-function titanium surface panel development was sponsored by the Department of Transportation on the Supersonic Transport program.

By reshaping the typical cylindrical cryogenic tankage in the form of an aerodynamic type wing airframe, the vehicle can reenter the earth's atmosphere with a planform loading which allows the use of proven materials technology.

The multi-functional panel skins are stabilized by internal circumferential frames at approximately 30 inch spacing. The frames are made from Rene'41 at the lower surface and titanium at the upper surface, spliced mechanically at the halfway waterline. All of the internal body frames are truss (wing carry through structure) and ring types except for the solid bulkheads at the forward and aft ends of the tank.

The wing contains LO_2 and uses the same structural system as the body. The LO_2 is located to provide load relief from the aerodynamic lift and reduce wing bending loads. The wing bending loads are carried by a series of truss wing spars located at the same body station as the body frames. The wing bending loads are carried through the body by beams, stabilized by the body frame struts. The wing leading edge temperatures exceed the capability of Rene'41 and so a columbium alloy is used. Leading edge construction consists of integrally stiffened coated columbium alloy overlapping segments supported by a determinate truss system. The relative low thermal conductivity of the multi-functional metallic surface panels prevents formation of liquid air on the outside of the vehicle and prevents excessive boil-off of the LH_2 and LO_2.

Dual Fuel Vehicle Configuration Constraints. Prior to proceeding with the discussion of the configuration design analysis, one should consider the configuration constraints on dual fuel design activities. When projecting structures technology to the 1985 time period, the unit weights or sensitivity of structures weight to propellant volume is reduced. The overall objective of the dual fuel concept is to reduce vehicle volume and thus vehicle weight. Past

and previous technology indicates that structural unit weights of 31.74 kg/m^2 (6.5 lb/ft^2) to 39.06 kg/m^2 (8.0 lb/ft^2) could be used in the trade for launch vehicles. Use of multifunctional surface panels, composite materials and advanced insulation schemes projected during the previous study indicate that structural unit weights of 26.85 kg/m^2 (5.5 lb/ft^2) to 31.74 kg/m^2 (6.5 lb/ft^2) are obtainable in the future. Thus the area savings resulting from the propellant volume reduction do not provide as significant savings in terms of weight as previous studies would have projected.

Wing area as a function of vehicle GLOW and entry planform loading are major constraints which are peculiar to the all-metallic horizontal takeoff design concept. Further details of these items will be developed later in the report. A horizontal takeoff vehicle requires a certain reference wing area for takeoff from the ground accelerator dependent upon takeoff speed and vehicle angle of attack to observe buffet limitations. For a constant GLOW the wing reference area remains the same, and when reducing volume in the body, the vehicle becomes essentially thinner but without any significant reduction in wetted area. This in turn causes a redistribution of oxygen in the wing which changes the distribution of the inertial weight and lift, which is very important with respect to wing bending loads. The baseline takeoff speed for previous studies, as well as the dual fuel configuration, was 182.9 m/s (600 fps). When considering a reduction in the takeoff reference wing area, by increasing takeoff speed, the entry planform loading limits must be observed to remain within the temperature capability of the vehicle materials.

Another major constraint on the all-metallic "hot" structure concept for dual fuel design is the RP tank temperature limitation to prevent coking of propellant residue. The Rocketdyne Division of Rockwell International has recommended a 589K (600°F) limitation on RP lines and tankage to prevent this occurrence. This requires complete thermal isolation of the RP tankage from the remaining structure.

The addition of a separate fuel requires more feed lines, valving, antivortex and quantity measuring equipment. The vehicle configuration must be balanced for ascent as well as reentry to keep flight control requirements at a reasonable level. This problem is a bit more pronounced on the horizontal takeoff type vehicles but somewhat complicates the configuration arrangement of

all vehicles. Finally, in the series burn mode the penalties involved with hydrogen storage for the Mode 1 burn (hydrogen boiloff versus insulation) have a weight impact on the vehicle not normally encountered during the all LO_2/LH_2 operation or parallel burn concept.

Dual Fuel Vehicle Design. As indicated previously, several configurations were developed to understand the specific design features and peculiarities associated with a dual fuel vehicle configuration. All configuration effort was associated with a vehicle GLOW of 997,900 kg (2.2 million lb). The reasoning supporting this selection of GLOW are (1) preliminary cost tending indicated that the dual fuel vehicle GLOW would have to be under 1,360,770 kg (3.0 million lb) to be cost competitive with an all LO_2/LH_2 vehicle; (2) weight trending data developed for structures weight versus vehicle GLOW indicate a direct correlation and that weight within this area of interest could be scaled either up or down, and (3) the technical understanding and background associated with this size of vehicle would contribute to a more rapid and detailed design solution.

Specific design parameters which were used to constrain the design were wing reference area = 882.55 m^2 (8500 ft^2), leading edge sweep = 52° to 60°, section thickness = 10% to 12%, fin reference area = 14% of wing, payload bay = 6.57m (15 feet) x 18.29m (60 feet), crew cab and wheel wells are constant volume. Vehicle propulsion system thrust to weight (T_{SL}/GLOW) ratios were investigated at .78, .88 and .94. Subsystems installations and weights were derived by utilizing the previous results of the all LO_2/LH_2 vehicle study.

A series of variations from a ALRS-205 generic configuration were intuitively assessed to see if the more dense fuel loading associated with the dual fuel system could provide significant inert weight reductions (holding GLOW/constant). In general, each of the preliminary configurations incorporating these variations had aerodynamic instability characteristics that indicated further evaluation would be of no value. The conclusion from this assessment was that weight trending versus propellant split for both series and parallel burn systems would be developed using a configuration generic to the ALRS-205. Prior studies (Ref. 1) had shown that with proper center of gravity position this configuration had acceptable aerodynamic characteristics.

The arrangement and configuration shown in Figure 30 is representative of those used in developing weight trending data. Fuel tank volumes were

varied as required for propellant split ratios. However, due to the prior discussed system design constraints the primary change in vehicle configuration was in body and wing depth.

The following discussion presents the general approach used in developing detail technical data to establish subsystem weight trending.

Loads and Dynamics. Airloads were computed using a program based on the aerodynamic influence coefficient method of Woodward. Fifty panels, including twelve elevon panels, were used for the half vehicle planform. Inertia loads and centers of gravity were computed based on actual propellant tank geometries with preliminary estimates of structure and subsystem weights. Design criteria and analysis methods used were consistent with previous SSTO studies (Reference 1).

Wing limit loads were developed for conditions making up the design envelope. Positive wing bending loads are higher on these vehicles than on the ALRS-205 SSTO described in Reference 1. This is due to the greater amount of LOX in the ALRS-205 wing which provides greater inertia relief. However, the negative bending loads are lower than on the ALRS-205 since these are inertia loads.

Body limit loads were analyzed for typical configuration designs. The center of gravity at lift-off was computed to be well aft of the center of pressure. Up to 16 degrees of thrust vectoring was required for trim on some of the vehicles analyzed, assuming no elevon deflection. Since gimbal limits will be no more than 10 degrees, elevons would have been required for those configurations.

The effect of reducing wing thickness on wing loads was also analyzed. More LOX would be in the body with the thin wing, eliminating a dry bay and the associated bulkhead weight. However, wing loads would increase due to the decrease in inertia relief in the 1.75 g pullup condition.

Increasing wing thickness and reshaping the wing tank to move the effective LO_2 inertia outboard to achieve a better balance between air loads and inertial loads was attempted. However, the penalities associated with the thicker wing on a horizontal take-off vehicle (which is sensitive to drag) and the structural penalties of additional bulkheading offset the reduction in wing loads.

The vertical fin loads and rudder hinge moment loads were obtained by scaling from the ALRS-205 loads given in Reference 1.

Main gear impact loads are similar to ALRS-205 as landing weight, gear stroke, and sink rate are very similar.

The two main conclusions reached during the preceding analysis were as follows:

(1) reduction of the amount of LO_2 in the wing tanks which are sized by the entry or takeoff requirements tends to develop structural penalties in this area.

(2) The additional weight of the dual fuel engines in conjunction with the shorter vehicle length leads to excessive gimbal requirements. These requirements can somewhat be offset by shifting of propellants in the wing tanks which then must be balanced against the loads.

Weights Analysis

Subsystems Weight Trending. Figure 15 depicts The various design points and resulting trend line for subsystem parametric weights as a function of propellant split for a constant vehicle GLOW of 997,900 kg (2.2 million lb). Control surfaces, landing gear, reaction control system, orbital maneuvering system, accessory power unit, electrical power and thermal control system weights were developed as a function of the vehicle performance injected weights. Avionics, environmental control system and vehicle personnel provisions are fixed weights and are not sensitive to the changes in configuration due to dual fuel. Feed and vent system pressurization, tank insulation and RP tank pressurization are configuration sensitive and were developed by actual layout and assessment. Figure 16 illustrates a typical feed system point design for a series burn 50/50 propellant split. This arrangement is a generalized approach and was used for analysis of the parametric trending development. The resultant subsystems weight trend saving varies from 0 kg to 1018.3 kg (2245 lb) as the propellant split ratio varies from 0 to .79.

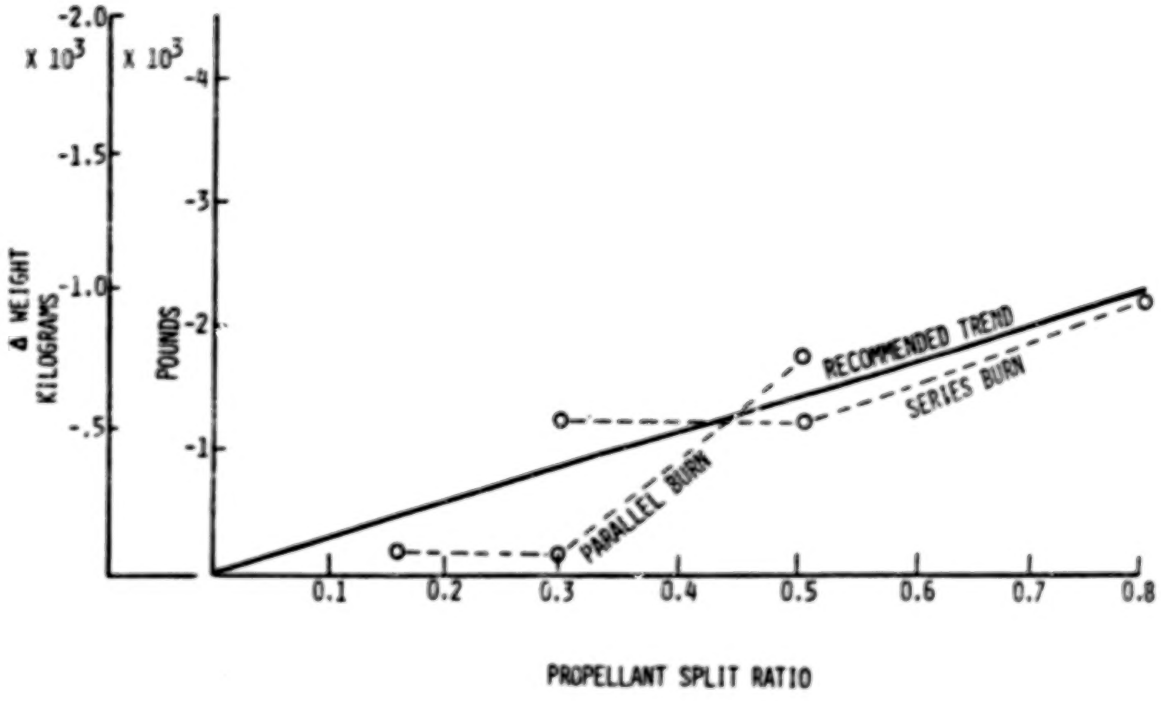

FIGURE 15 SUBSYSTEMS WEIGHT TRENDING

Fluids Weight Trending. Figure 17 illustrates the various assessment points and resulting trend line for fluids parametric weights as a function of propellant split for a constant GLOW of 998,100 kg (2.2 million lb). Residual weights are made up of the liquid residuals, the pressurant remaining in the tank at burnout and the propellant utilization error. The liquid residuals reflect an immediate increase when adding an additional RP tank. This additional tank causes an increase of 717.1 kg (1581 lb) which results from line configuration, not tank volume or size. The liquid residuals in the LO_2 and LH_2 tank remain the same as the previous all LO_2/LH_2 baseline concept. Pressurant residuals are reduced as the LO_2/RP-1 propellant split is increased because of the reduction in LO_2 and LH_2 tankage. This reduction is a direct function of the propellant volume reduction. Propellant utilization error varies slightly and is .068% of the total propellant weight. OMS propellant is based on a ΔV requirement of 198.1 m/s (650 fps) and decreases for increased LO_2-RP-1 propellant splits due to the reduction in

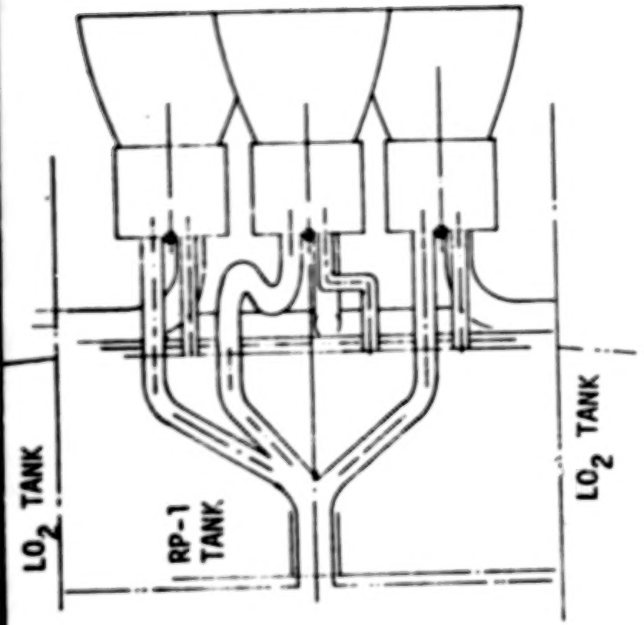

DUAL FUEL - SERIES BURN
.50 PROPELLANT SPLIT RATIO
FUEL FEED SYSTEM

RP-1 SYSTEM 27.9 CM (11 IN.) DIA. TITANIUM DUCTS WITH 30.5 CM (12 IN.) LONG FLEX SECTIONS	53.6 kg (118.2 LB)
LO_2 SYSTEM 55.9 CM (22 IN.) DIA. MANIFOLD TO 45.7 CM (18 IN.) DIA. STEEL DUCTS WITH 30.5 CM (12 IN.) LONG FLEX SECTIONS AND 24.4 CM (.8 FOOT) WIDE SUMP PLATES	450.6 kg (993.5 LB)
LH_2 SYSTEM 66 CM (26 IN.) DIA. MANIFOLD TO 38.1 CM (15 IN.) DIA. VACUUM JACKETED TITANIUM DUCTS WITH 30.5 CM (12 IN.) LONG FLEX SECTIONS AND 1.52 CM (5 FOOT DIA.) SUMP PLATE	408.9 kg (901.5 LB)

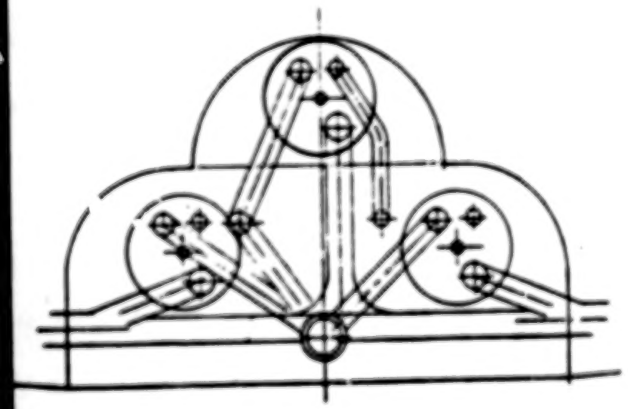

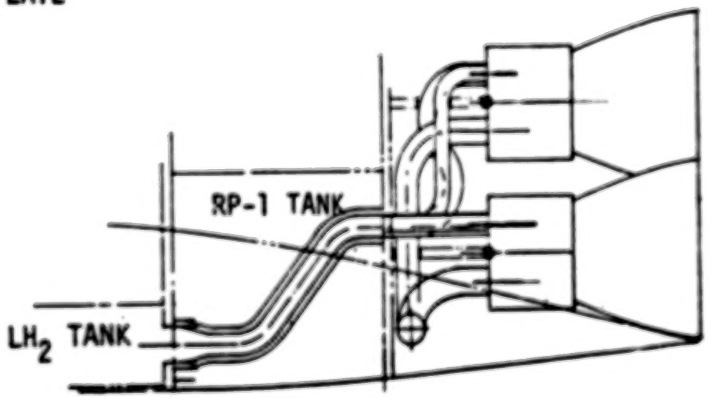

FIGURE 16 DUAL FUEL FEED SYSTEM POINT DESIGN

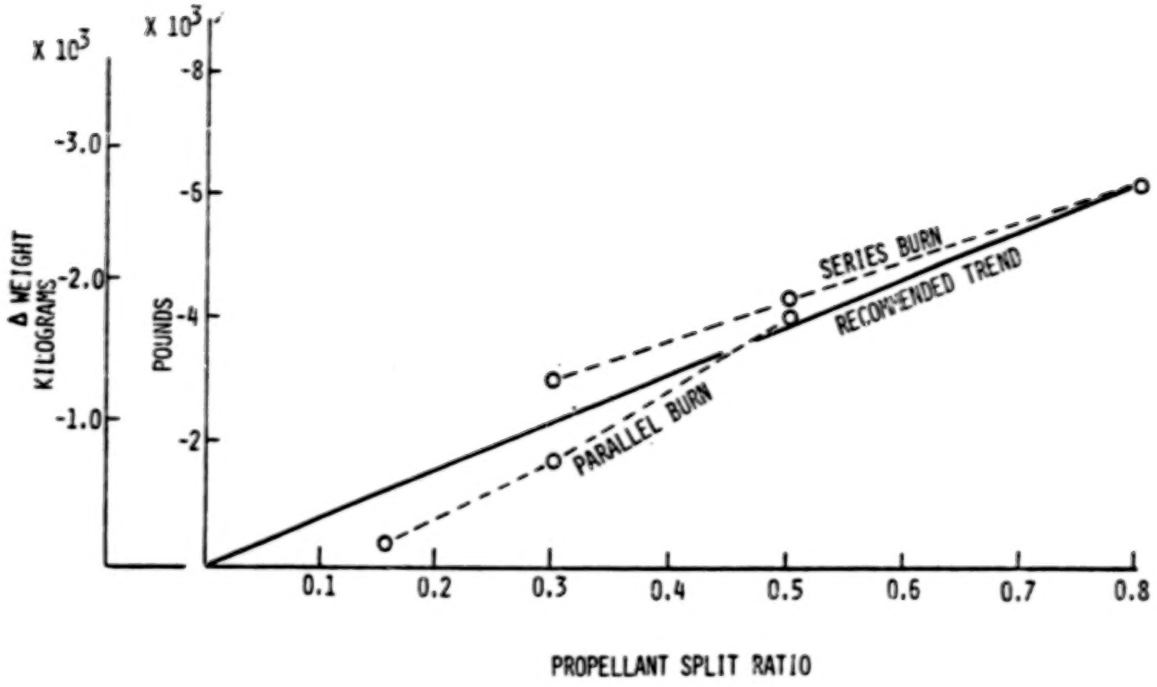

FIGURE 17 FLUID WEIGHT TRENDING

injected weight. Flight performance reserves, which are determined as .085% of the total ascent ΔV requirements, follow the same trend as the OMS as well as the subsystems fluids and reaction control propellants which are directly proportional to the performance injected weight. The resultant fluids weight trend savings vary from 0 kg to 2873 kg (6333 lb) as the propellant split ratio varies from 0 to .79.

Structures Weight Trending. Figure 18 illustrates the various assessment points and resulting trend lines for structures parametric weights as a function of propellant split. The solid preliminary line indicates structures weight estimates that when closely assessed showed the 50/50% propellant split to be nearly optimum for the tankage design for this family of vehicles. The lower propellant split design point tended to penalize the structure for initial tank installation penalties and those above 50% tended to penalize the larger tanks in terms of tank efficiency. The tankage arrangements for the propellant split ratios above .5 were large cylindrical tanks which tended to be rather inefficient due to integrating them around the payload bay. Tankage

arrangements for split ratios less than .5 were smaller tanks located between the payload and the engine compartment. This tank arrangement is similar to that shown in Figure 30. A review of the structural assessment resulted in the final curve where the initial penalties and tank inefficiency were relaxed. The maximum weight saving remained at an approximate 50/50% propellant loading indicating that the tankage installation was nearly optimum at that point.

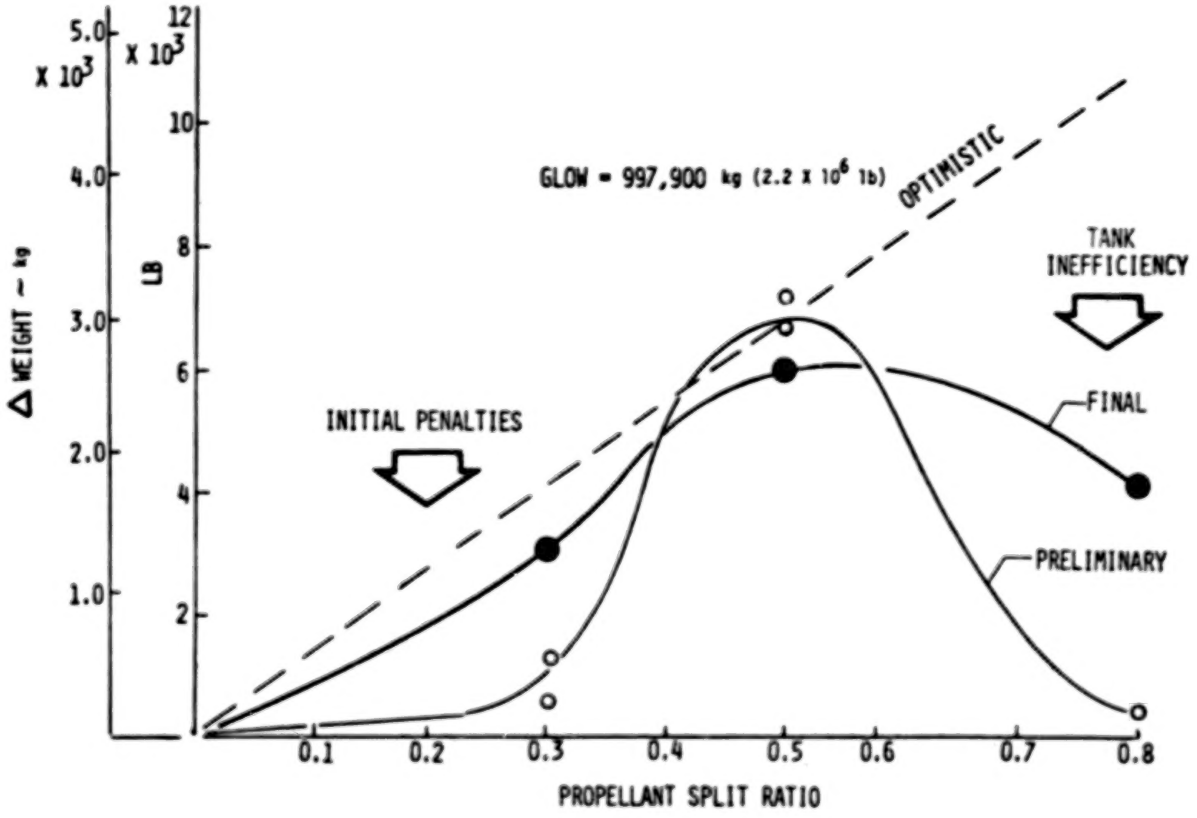

FIGURE 18 STRUCTURES WEIGHT TRENDING

All trending lines developed to this point reflected a normal technology projection in all areas. Figure 19 reflects a summation of all the partial trending data including the propulsion system weight savings shown separately. In addition, weight savings have been included to account for accelerated technology as was the case in Task 4 of the previous study. These trend data were then integrated with the performance program to derive the data shown on Table 3 for series burn and parallel burn. Payload varies as a function of the calculated inert weight for a fixed GLOW of 997,900 kg (2,200,000 lb).

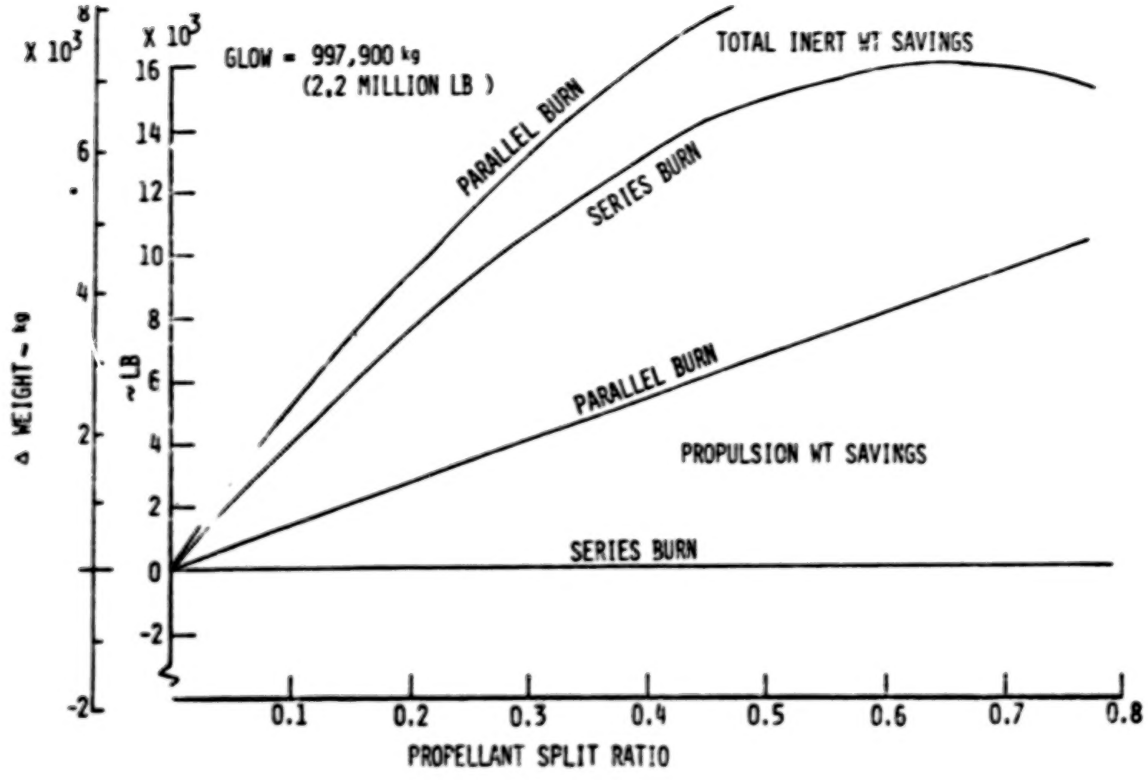

FIGURE 19 DUAL FUEL SYSTEM INERT WEIGHT TRENDING

FIXED GLOW = 997,900 kg (2.2 MILLION lb)

SERIES BURN DUAL FUEL ENGINES:

PROP SPLIT RATIO	WT PROP kg	WT PROP LB	WT LO_2/RP kg	WT LO_2/RP LB	WT ENG kg	WT ENG LB	WT INERT kg	WT INERT LB	PAYLOAD kg	PAYLOAD LB
0.000	898,973	(1,981,985)	0	(0)	14,179	(31,259)	114,250	(251,780)	13,302	(29,325)
0.115	870,120	(1,918,237)	99,790	(220,000)	14,179	(31,259)	112,057	(247,044)	15,726	(34,669)
0.229	870,164	(1,918,384)	199,580	(440,000)	14,179	(31,259)	110,273	(243,111)	17,465	(38,504)
0.344	870,240	(1,918,551)	299,371	(660,000)	14,179	(31,259)	108,824	(239,917)	18,839	(41,533)
0.459	870,388	(1,918,876)	399,161	(880,000)	14,179	(31,259)	107,714	(237,469)	19,802	(43,655)
0.572	871,775	(1,921,934)	498,952	(1,100,000)	14,179	(31,259)	107,053	(236,011)	19,053	(42,054)
0.684	875,114	(1,929,297)	598,742	(1,320,000)	14,179	(31,259)	106,900	(235,674)	15,889	(35,029)
0.798	881,117	(1,942,530)	698,532	(1,540,000)	14,179	(31,259)	107,304	(236,564)	9,483	(20,906)
0.896	890,489	(1,963,191)	798,323	(1,760,000)	14,179	(31,259)	108,302	(238,766)	-888	(-1,958)

PARALLEL BURN:

PROP SPLIT RATIO	WT PROP kg	WT PROP LB	WT LO_2/RP kg	WT LO_2/RP LB	WT ENG kg	WT ENG LB	WT INERT kg	WT INERT LB	PAYLOAD kg	PAYLOAD LB
0.000	902,204	(1,989,197)	0	(0)	14,411	(31,771)	113,030	(249,221)	27,888	(61,482)
0.116	858,522	(1,892,716)	99,790	(220,000)	9,113	(30,090)	110,369	(243,324)	29,012	(63,961)
0.232	861,775	(1,899,888)	199,580	(440,000)	17,472	(28,519)	108,197	(238,536)	27,930	(61,576)
0.346	866,029	(1,909,267)	299,371	(660,000)	12,300	(27,118)	106,532	(234,863)	25,342	(55,870)
0.458	871,072	(1,920,386)	399,161	(880,000)	11,461	(25,267)	105,062	(231,623)	21,768	(47,991)
0.569	876,783	(1,932,976)	498,952	(1,100,000)	10,822	(23,859)	104,173	(229,663)	16,947	(37,361)
0.678	883,077	(1,946,852)	598,742	(1,320,000)	9,985	(22,013)	103,448	(228,065)	11,378	(25,084)
0.785	889,887	(1,961,865)	698,532	(1,540,000)	9,322	(20,552)	103,244	(227,616)	4,771	(10,518)
0.890	897,154	(1,977,888)	798,323	(1,760,000)	9,322	(20,552	104,035	(229,359	-3,287	(-7,247)

TABLE 3 DUAL FUEL WEIGHT/PERFORMANCE TRENDING

Scaling these data based on previous experience to a constant 29,484 kg (65,000 lb) payload results in gross liftoff weight comparions for both dual fuel concepts as shown in Figure 20. The all LO_2/LH_2 vehicle of the previous study (Ref. 1) resulted in a GLOW of 816,900 kg (1.8 million lb) when projected with the appropriate "advanced" or recommended technology improvements.

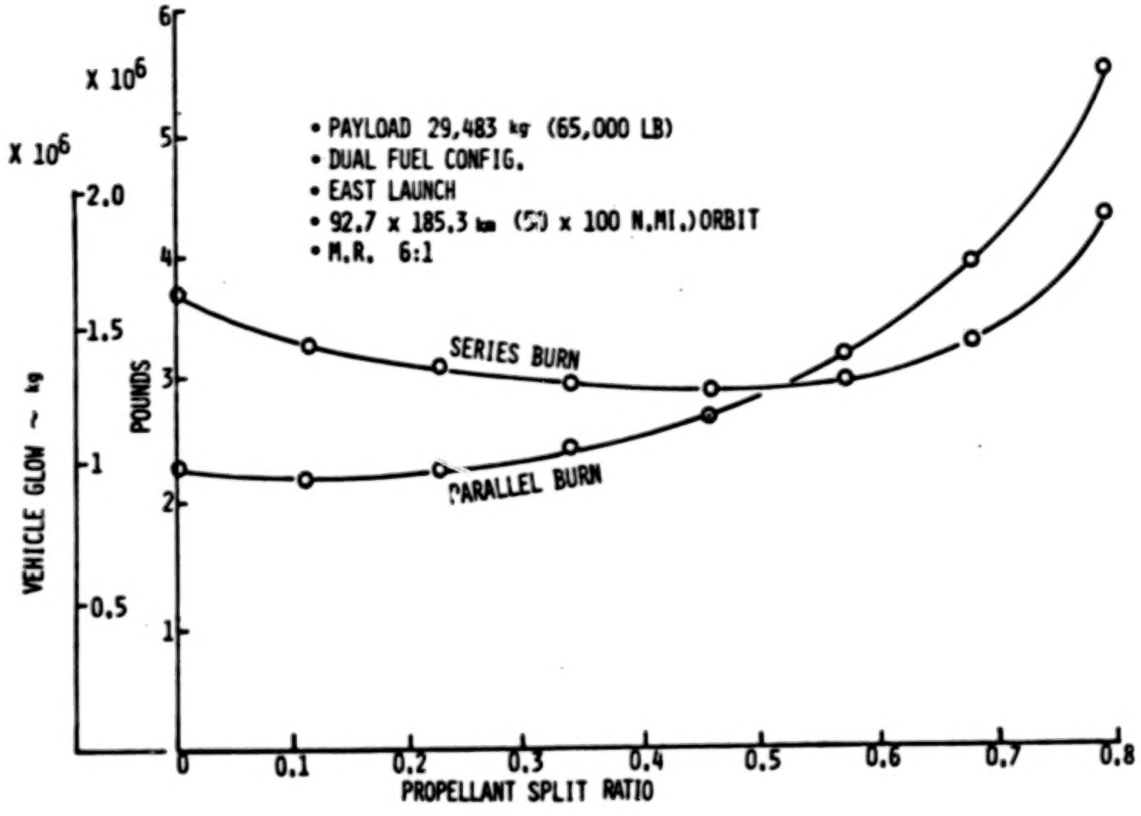

FIGURE 20 DUAL FUEL GROSS LIFTOFF WEIGHT COMPARISON

Without the "advanced" or technology improvements, the all LO_2/LH_2 vehicle, GLOW is 1.04 million kg (2.3 million lb) as indicated by the intersection of the parallel burn curve with the zero propellant split ratio line. This update or difference from Reference 1 is caused by the incorporation of (1) new aerodynamic drag data which were developed during model testing in the Unitary Plan Wind Tunnel at NASA/Langley and (2) use of the new propulsion system weight data derived for this study rather than the previous Rocketdyne data. The parallel burn concept minimizes GLOW at 1.01 million kg (2.22 million lb) at a propellant split ratio of about .1. The series burn concept minimizes GLOW at 1.31 million

kg (2.88 million lb) at a propellant split ratio of approximately .45. The shapes of the curves are driven by the performance of the dual fuel propulsion systems as detailed in the performance analysis discussion previously.

Cost Analysis

To determine the cost effectiveness of each of the dual fuel options it was necessary to develop parametric cost estimating relationships for vehicle systems. The cost estimating relationships developed are for design, development, test and evaluation (DDT&E), production and operations.

DDT&E Costs. The vehicle costs including the ground accelerator were developed as a function of inert weight during the previous study and are shown in Figure 21. Propulsion system development costs are not included.

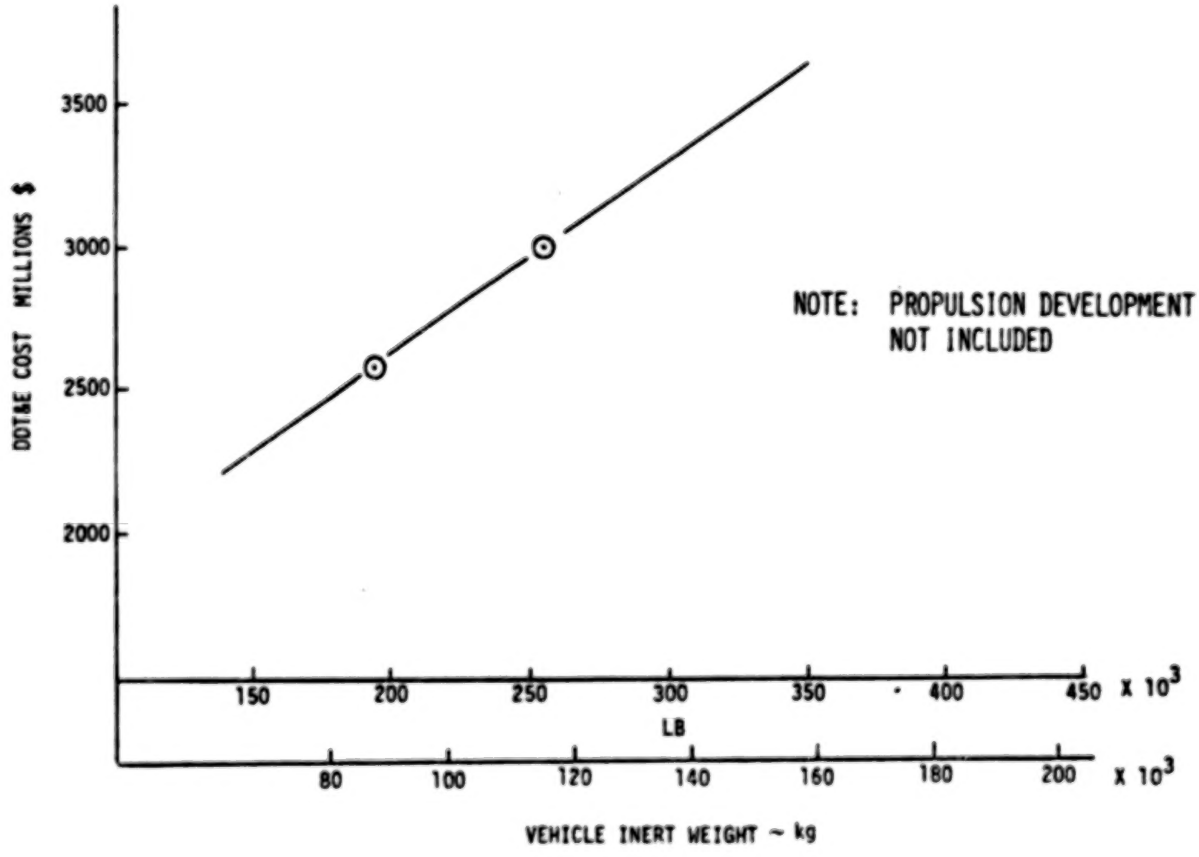

FIGURE 21 VEHICLE DEVELOPMENT COST ESTIMATING RELATIONSHIPS

Propulsion system costs are shown on Figure 22 based on a review of NASA, Boeing and engine contractor cost estimating relationships. The $LO_2/RP-1$ and LO_2/LH_2 engine development costs are taken from a 1971 NASA/OART report (Reference 3) and the cost factored to 1976 dollars.

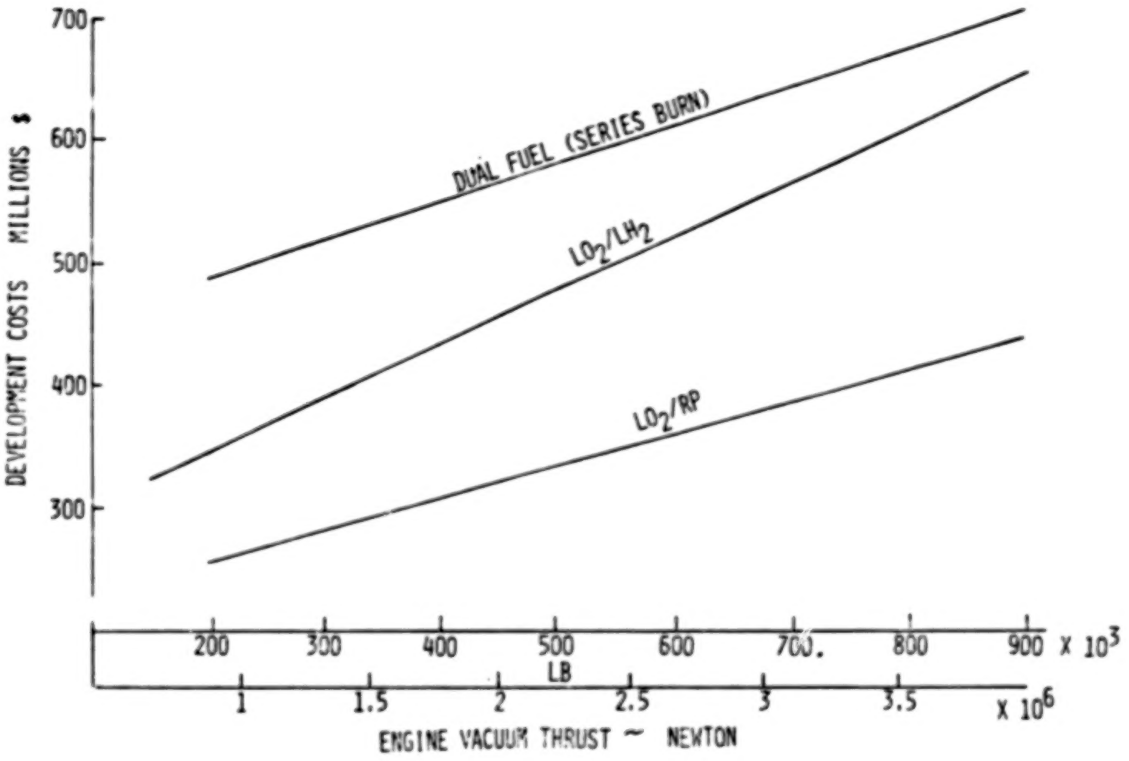

FIGURE 22 PROPULSION DEVELOPMENT COST ESTIMATING RELATIONSHIPS

The equation for a regeneratively cooled, pump fed, storable engine (LO_2/RP) is: $1.3\ [50 \times 10^6 + 4.61 \times 10^5\ (T)^{.422}]$. (T in newtons)

The equation for a regenerative cooled, pump fed, oxygen/hydrogen engine is: $1.3\ [50 \times 10^6 + 7.48 \times 10^5\ (T)^{.422}]$. (T in newtons)

The dual fuel engine development cost is based on the proportional difference between dual fuel engines and LO_2/LH_2 engines as developed by Aerojet-General. The cost difference looks rather low but since Aerojet has the most experience with this type of engine it was used to provide an optimistic assessment of program development costs.

Not noted on the figure but an important factor is that the majority of cost estimating relationships tend to cross at a thrust level of 181,436 to 362,872 kg (400-800,000 lb). Because of this fact, and because the weight estimating relationships followed a similar trend, it was decided that parametric trending data stay within this region so that scale-up or scale-down errors were minimized.

Production Costs. The dual fuel vehicle costs, including the ground accelerator, were developed as a function of inert weight during the previous study and are shown in Figure 23. These costs have the previous Rocketdyne propulsion production costs removed. The cost estimate reflects the same type of groundrules and rationale used on the previous assessment of an all LO_2/LH_2 vehicle. Four production vehicles were included in the program.

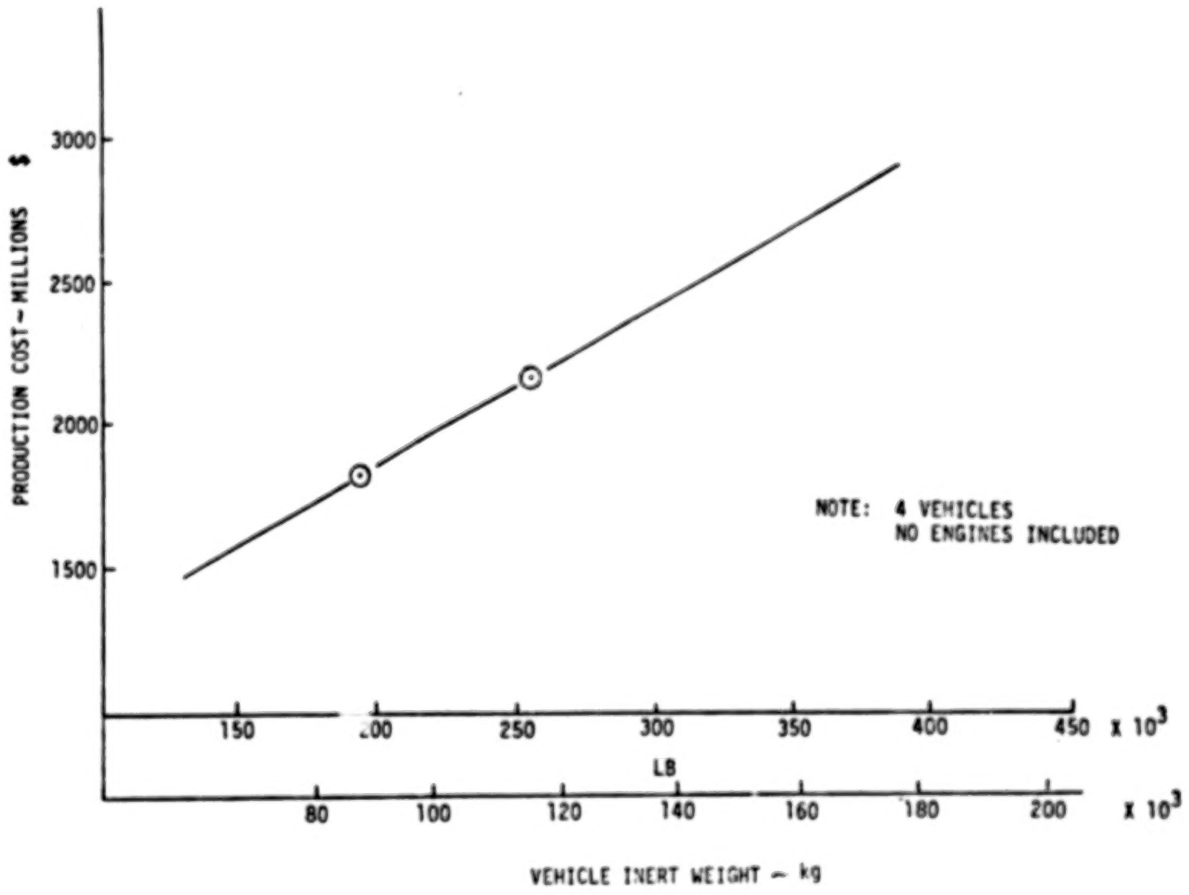

FIGURE 23 VEHICLE PRODUCTION COST ESTIMATING RELATIONSHIPS

Propulsion unit costs are shown on Figure 24. These relationships again were based on a review of NASA, Boeing, and engine contractor cost estimating relationships. The LO_2/RP-1 and LO_2/LH_2 engine unit costs are taken from the same NASA/OART report and factored to 1976 dollars. The equation for a regeneratively cooled, pump fed storable engine (LO_2/RP-1) is: $1.3\ [270{,}000 + 79.2\ (T)^{.8}]$. (T in newtons)

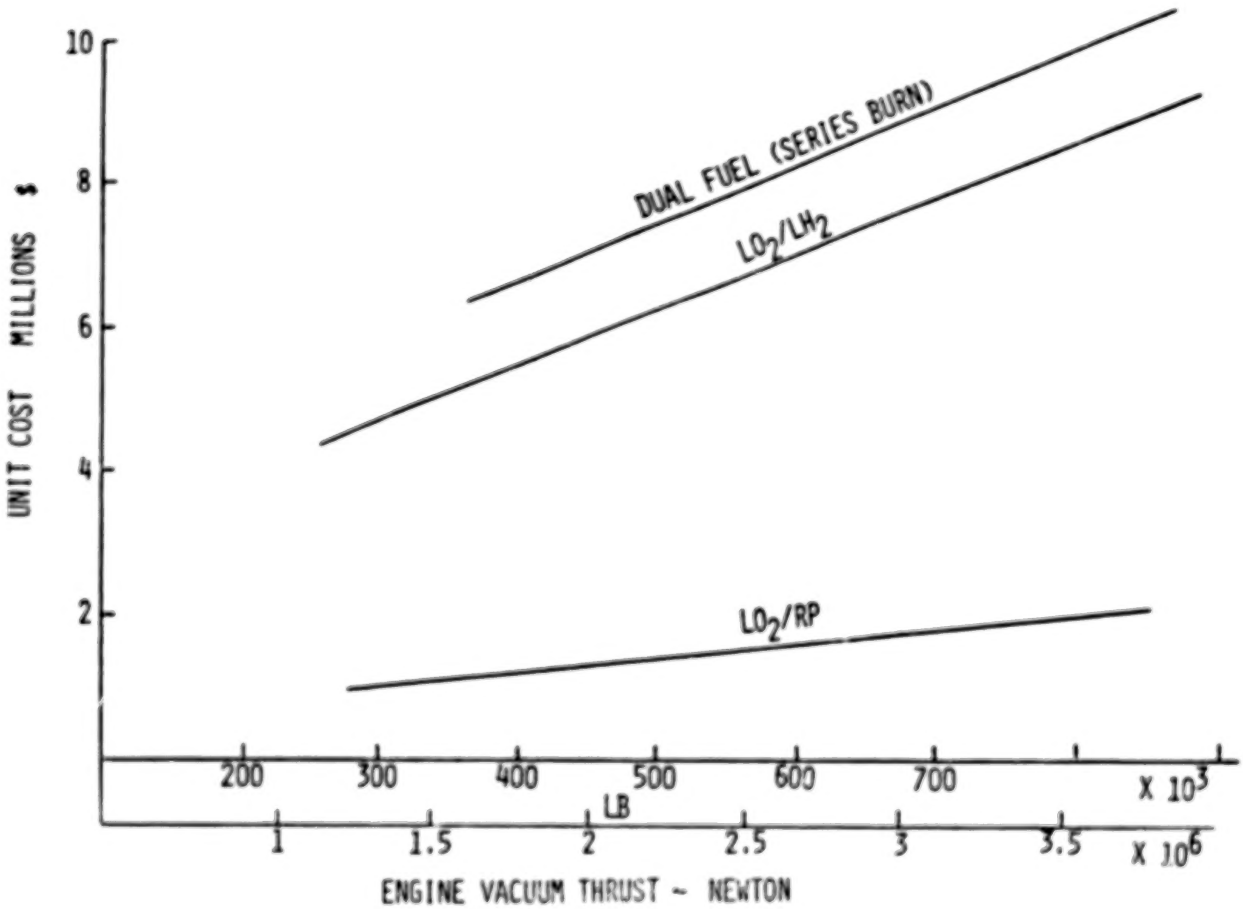

FIGURE 24 PROPULSION PRODUCTION COST ESTIMATING RELATIONSHIPS

The equation for a regeneratively cooled, pump fed oxygen hydrogen engine is: $1.3\ [350{,}000 + 1350\ (T)^{.7}]$. (T in newtons)

The dual fuel engine unit costs are based on the proportional difference between dual fuel engines and LO_2/LH_2 engines as developed by Aerojet-General.

Operations Costs. Operations costs were developed as a function of inert weight after a review of previous program estimates on the same type of system. The ground operations costs were scaled directly as were the spares and refurbishment and program support costs. Fuels and propellant costs were \$2.20/kg (\$1.00/lb) for LH_2, \$.044/kg (\$.02/lb) for LO_2 and \$.132/kg (\$.06/lb) for RP-1. LH_2 and LO_2 propellant usage was factored by 125% to reflect storage and transfer losses. RP-1 utilized a 105% factor. Figure 25 reflects the operations cost estimating relationships for dual fuel without the propellants and gases and main engine maintenance costs.

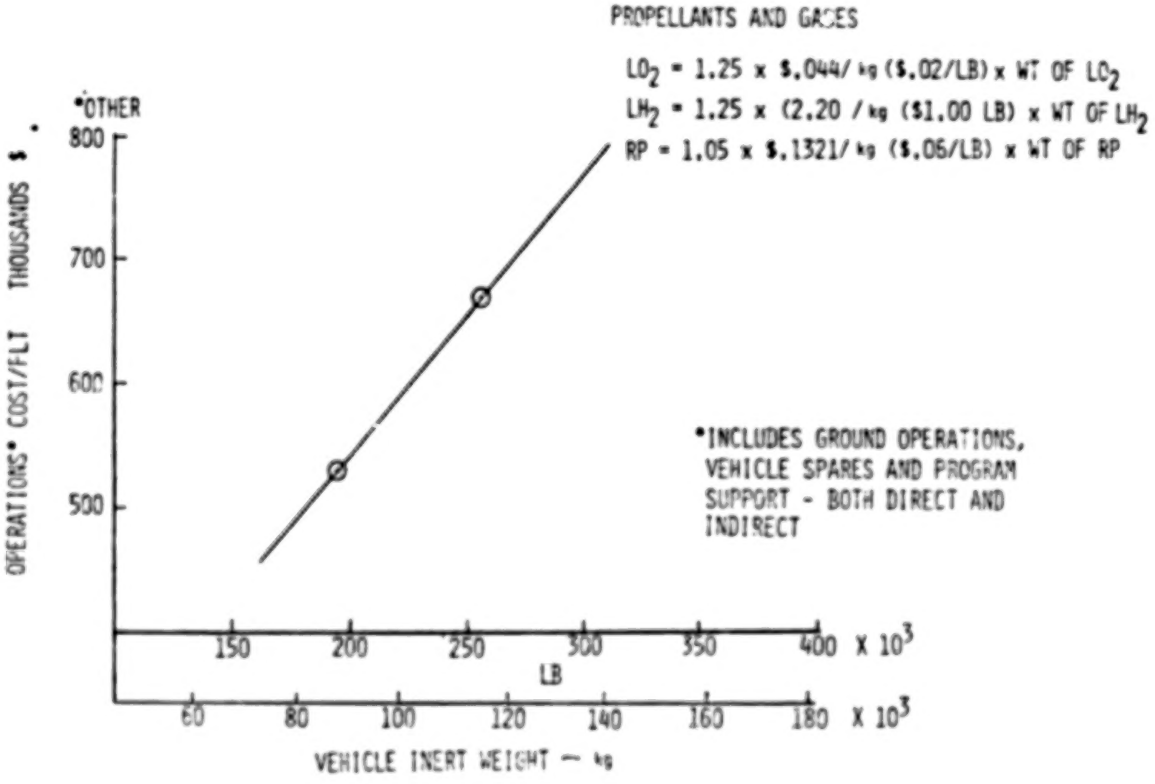

FIGURE 25 OPERATIONS COST ESTIMATING RELATIONSHIPS

The main engine operations and maintenance cost estimating trends are shown in Figure 26. This LO_2/LH_2 engine estimate was developed by reviewing the Rocketdyne preliminary estimates for the Space Shuttle and projecting

modest improvements in learning and engine wear due to equipment modification and maturity. LO_2/RP-1 maintenance costs were assumed to be the same as for a LO_2/LH_2 engine. Dual fuel engine maintenance costs were projected at 150% of the all LO_2/LH_2 or LO_2/RP-1 engine maintenance costs.

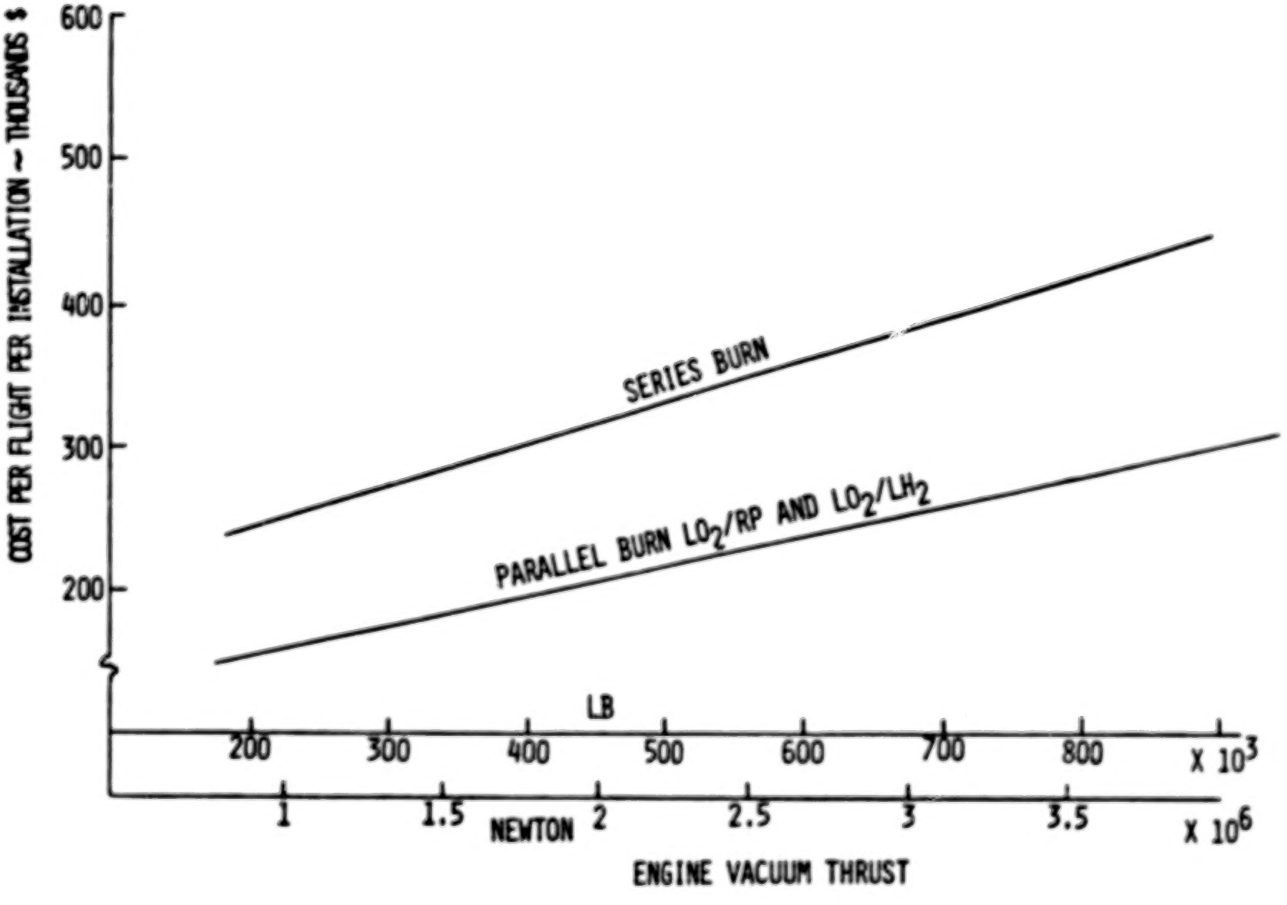

FIGURE 26 ENGINE OPERATIONS COST ESTIMATING RELATIONSHIPS

Program Cost Comparisons. Total program costs were developed for the dual fuel series burn and parallel burn system concepts to determine the propulsion system type and propellant fuel split to be examined in detail during Task 3. Figure 27 shows the life cycle cost results obtained by using the previously discussed costing trends. The parallel burn concept has a minimum program cost at 0 propellant split ratio or essentially the all LO_2/LH_2 propul-

sion system concept. The series burn configuration minimizes at .50 propellant split ratio. The cost curves are strongly impacted by inert weight and associated GLOW. This explains the high program costs associated with low propellant split series burn configurations. Increasing the thrust/weight ratio at sea level to offset early thrust mismatch, and, as a result increase performance, has a significant impact on life cycle costs up to 50%.

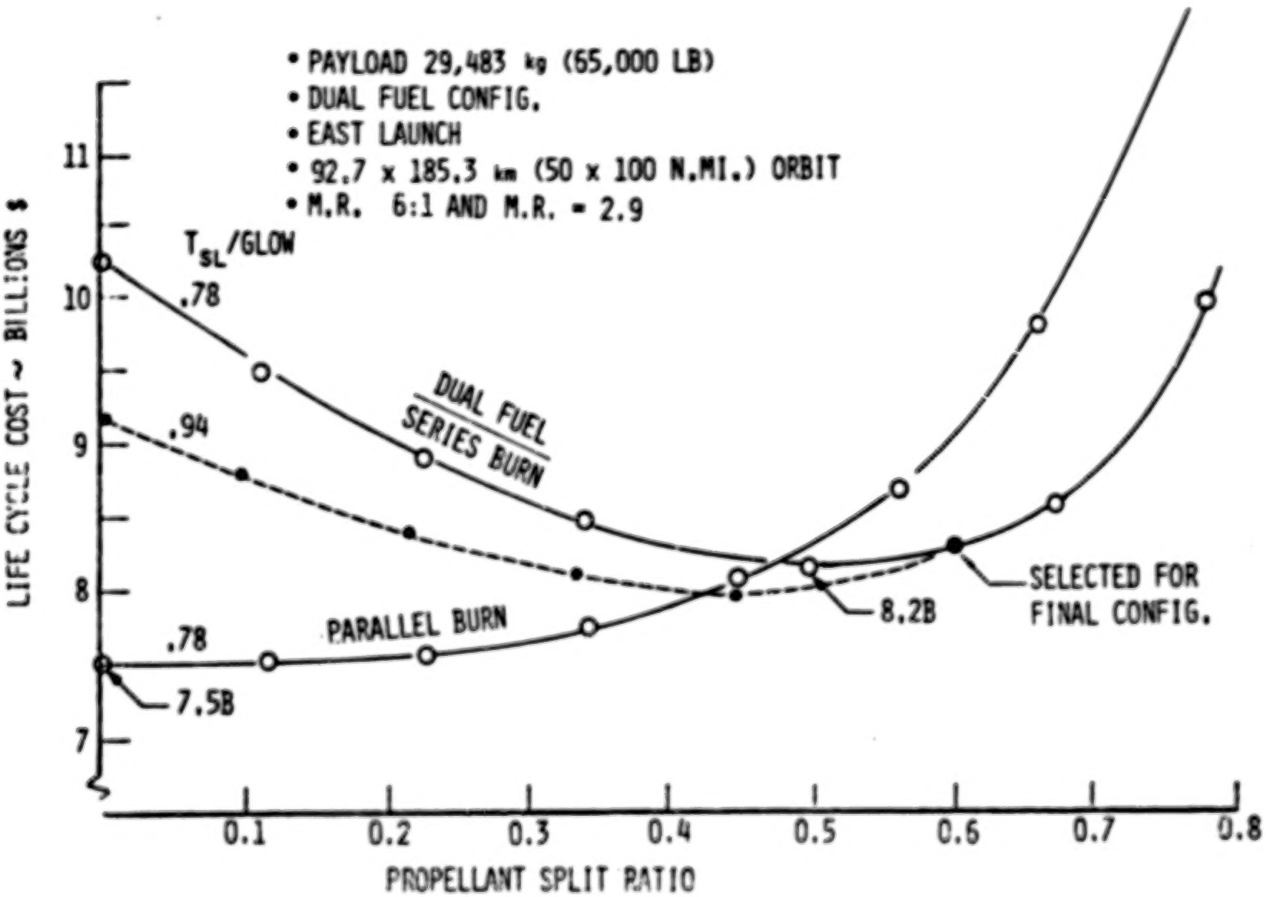

FIGURE 27 DUAL FUEL LIFE CYCLE COST COMPARISON

Figure 28 shows the sensitivity of inert weight savings on life cycle costs. The inert weight factors shown (1.0 and 1.4) reflect the baseline inert weight savings and a 40% increase in inert weight savings respectively. Both concepts are much more sensitive to increased weight savings at the higher split ratios. Increased weight savings have little effect on reducing the

minimum cost of a parallel burn system but do have a significant impact on reducing the lowest life cycle costs of the series burn concept. The minimum "bucket" increases in propellant split ratio somewhat from .50 to .55.

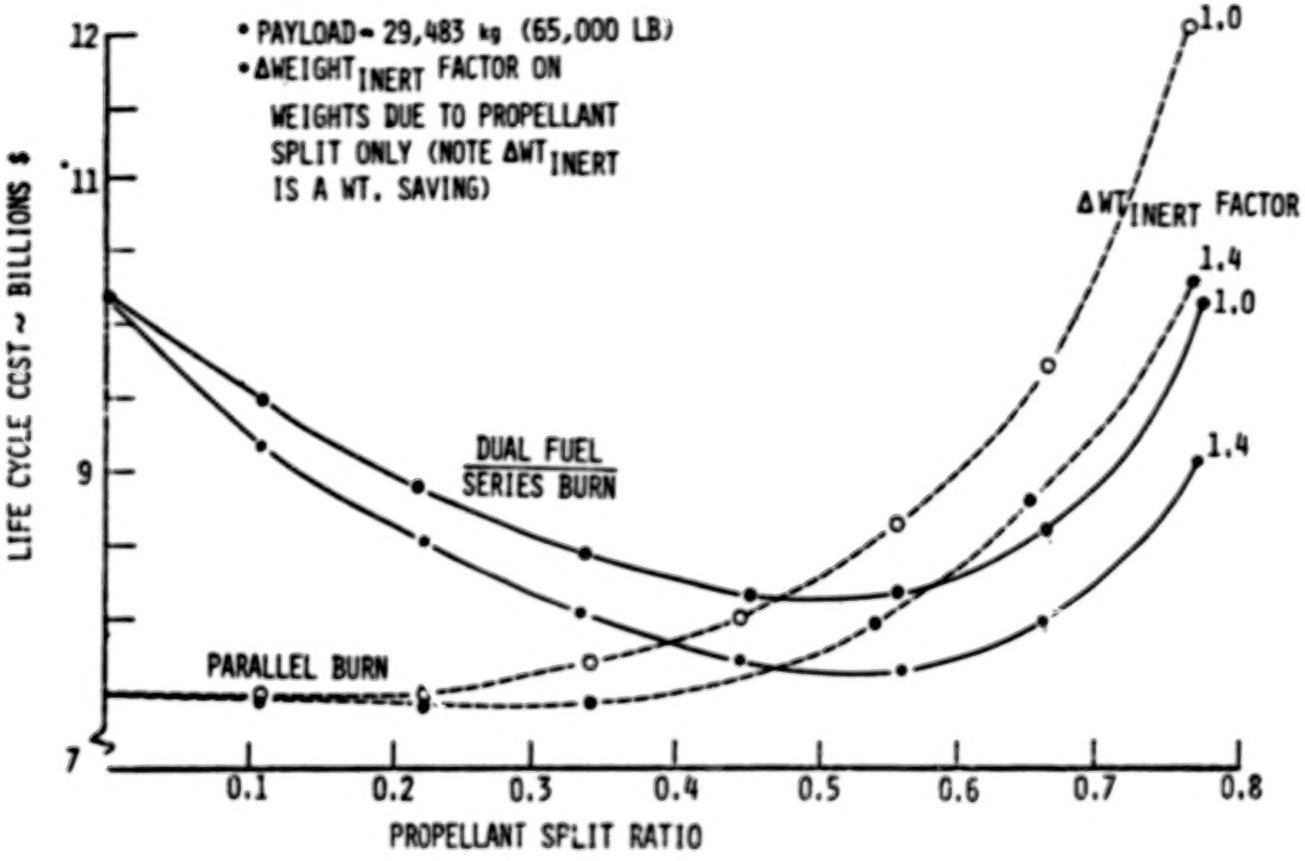

FIGURE 28 DUAL FUEL INERT WT. SENSITIVITY TO COST

Another important factor in determining the ultimate configuration are the launch operations costs. Since the overall programs cost could vary dependent upon the assumed mission model, the operations cost for each concept was analyzed to determine its importance on configuration selection. Figure 29 shows the operations cost trends for parallel and series burn as a function of propellant split ratio. The parallel burn operations costs are minimum at a propellant split ratio slightly greater than .20 although the "bucket" is very flat. The series burn configuration "bucket" has been moved out to .60 propellant split ratio due to the larger impact of propellant cost differences between RP-1 and LH_2.

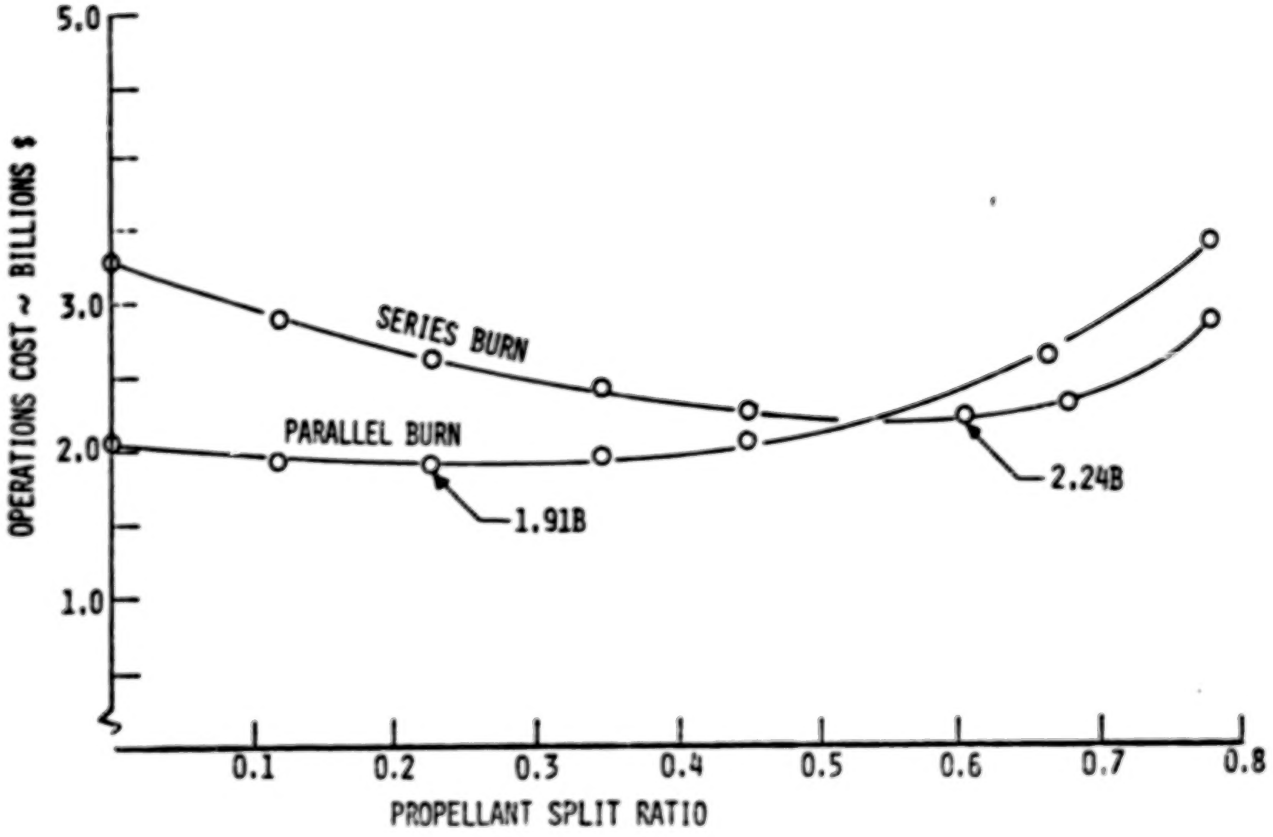

FIGURE 29 DUAL FUEL OPERATIONS COST COMPARISON

Configuration Selection. Because the parallel burn configuration at its minimum cost design point is so close to all LO_2/LH_2 vehicles in appearance and operations, the series burn configuration was selected for Step 3 evaluation. Due to the strong influence projected for operations costs of advanced transportation systems, the propellant split ratio was selected at .60 for a design point. This results in an increase in system GLOW from 1,310,000 kg (2.88 x 10 lb) to 1,374,967 kg (3.031 x 10^6 lb), Reference Figure 20.

VEHICLE DESIGN AND PERFORMANCE POTENTIAL - STEP 3

This section contains a discussion of the series burn dual fuel vehicle system design features, its mode of operation and performance characteristics, including mission profiles, as well as analysis results taking into account the operational environment and leading to the resulting system weights and costs.

Vehicle Design, Layout and Structural Analysis

Based on the generic configuration approach adopted in Reference 1 and using the parametric data from Step 2, several configurations of dual fuel vehicles were investigated leading to the final series burn dual fuel (.6 PSR) configuration described in detail in the following paragraphs. Maximum commonality was maintained with the ALRS 205 vehicle from Reference 1. The structural analysis was based on the same criteria as those used in Reference 1.

Airframe. The Dual Fuel Series Burn Vehicle Airframe structural centerlines are shown in Figure 30.

The fuelage consists of (1) a nose section running approximately twenty feet aft of the forward body end, (2) a forward LH_2 fuel tank section that houses the nose gear, (3) a mid-body dry bay section that houses the forward R-P tanks and payload bay, (4) an aft wing-body intersection area housing LH_2, and the aft RP tank and (5) an aft section housing the thrust structure, engines, aft R-P tank, body flap and vertical tail support. The crew cab is mounted on top of the forward LH_2 fuel tank section.

The wing is attached to the body at the side of the body. The wing consists of (1) a leading edge section, (2) a forward section housing LO_2, (3) an aft section housing LO_2 and the main landing gear, (4) a trailing edge section that houses the wing RCS and control surface actuation system, and (5) the elevons.

The vertical tail, mounted on top of the aft body section consists of (1) a leading edge section, (2) a main structural box, and (3) trailing edge and rudders

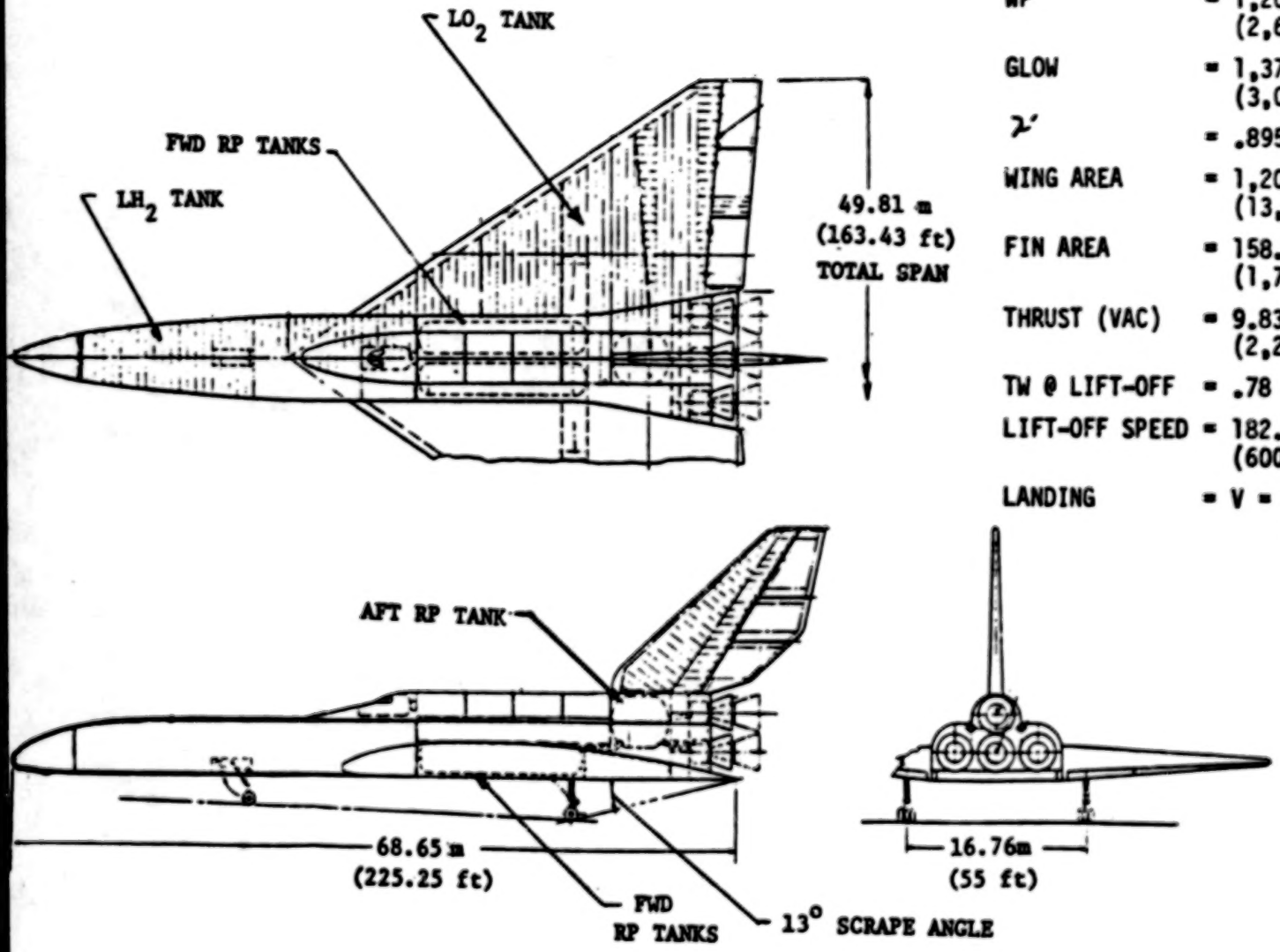

CHARACTERISTICS

W_{INJ}	= 170,051 kg (374,900 LB)
WP	= 1,204,463 kg (2,655,400 LB)
GLOW	= 1,374,967 kg (3,031,300 LB)
λ'	= .895
WING AREA	= 1,207.7 m^2 (13,000 FT^2)
FIN AREA	= 158.9 m^2 (1,710 FT^2)
THRUST (VAC)	= 9.83 MN (2,209,948 LB)
TW @ LIFT-OFF	= .78
LIFT-OFF SPEED	= 182.9 m/s (600 FPS)
LANDING	= V = 72.59 m/s (141 KNOTS) α = 8°

FIGURE 30 DUAL FUEL SERIES BURN VEHICLE CONFIGURATION

A more detailed description of representative structural sections follows. Due to the similarity between the structural system of the LO_2/LH_2 vehicle developed in Task 4 of Reference 1 much of the structural sizing for the dual fuel vehicle is obtained through size comparisons. External loads used in the analysis are extrapolated from those shown in Reference 1.

Nose Compartment. A typical fuselage nose compartment cross section is shown in Figure 31. Construction consists of integral stiffened superalloy skins supported by superalloy frames at approximately 229 mm (9 inch) spacing. The skins are attached with superalloy rivets. The forward lower portion of the nose compartment uses Columbium alloys instead of the superalloys. A coated Molydenum alloy TZM integrally stiffened nose cap is used.

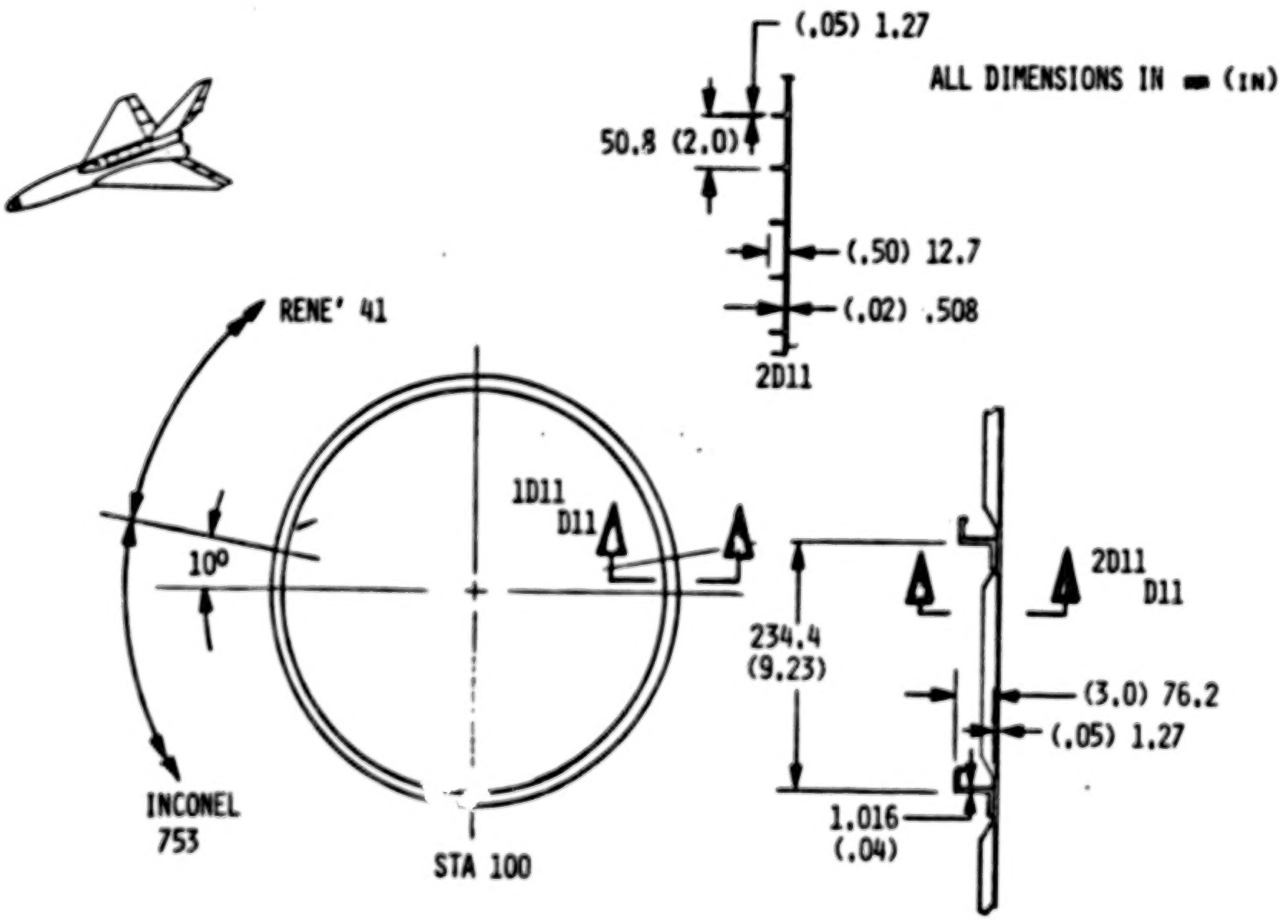

FIGURE 31 NOSE COMPARTMENT STRUCTURAL DETAILS

The stress analysis shows large margins of safety using what are generally considered to be minimum structural gages for this type of construction. The longitudinal integrally stiffened skin permits large thermal gradients between skin and frames without inducing excessive thermal stresses. The integral skin is padded at the frames to handle load distributions.

Forward Fuselage Section. The forward fuselage structural concept is shown in Figure 32. Construction consists of a multi-functional titanium (Ti-6AL-4V-ELI) upper surface and a multi-functional Rene'41 surface. Frames are I sections using titanium on the upper side and Rene'41 for the lower surface. Trusses are titanium tubes made of Ti-8AL-1V-IM. The structural system was selected as to provide adequate thermal insulation for the LH_2 during hold and ascent and handle the reentry temperatures.

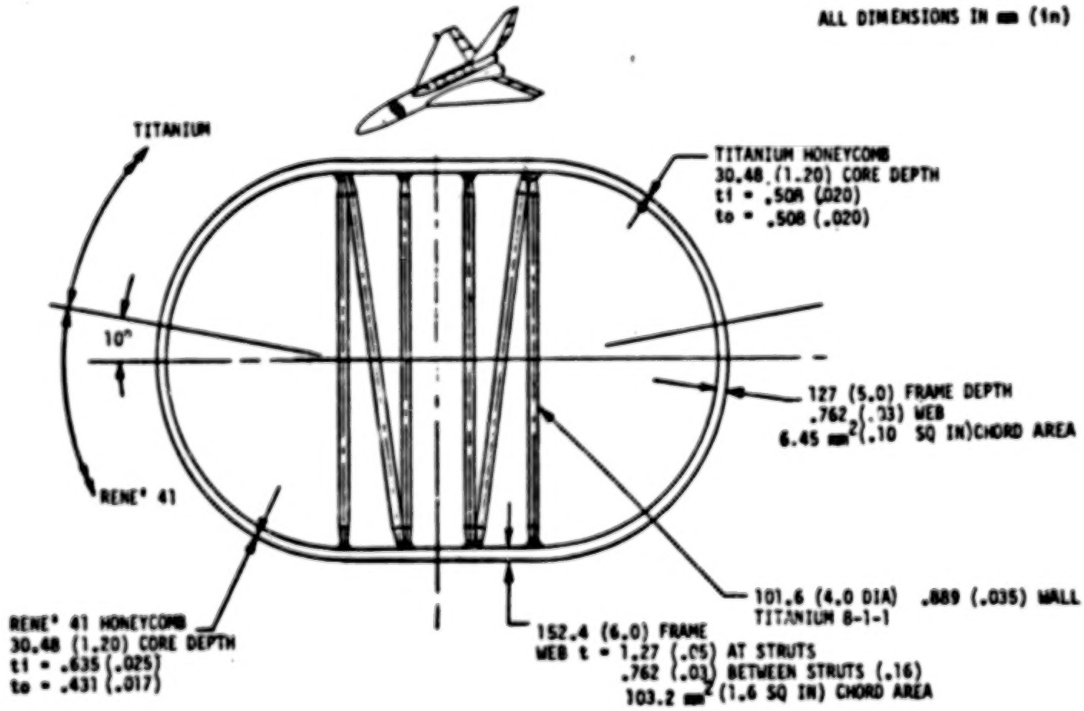

FIGURE 32 FORWARD LH_2 TANK STRUCTURAL DETAILS

The structural sizing considers both the load and thermally induced stresses. The critical condition occurs during ascent at approximately 210 seconds. At this time there is the maximum of thermal gradients in conjunction with maximum internal pressures. The load stresses incurred during reentry are very small in that maximum delta wall pressure is 10.34 k Pa. Further thermal gradients are less than those experienced during ascent. The gradients at maximum temperatures are small and do not induce critical stresses.

Mid-Body Section. The mid-body structural system is shown in Figure 33. The structural load transfer system is as follows. A structural bent is used to transfer body shear resulting from unbalanced wing moments. Use of a bent provides space for the forward RP tanks. The upper chord of the bent is a stiffened titanium frame that carries upper wing surface loads, a portion of the transverse shear and stiffens the upper body surface. The lower chord of the bent is a 10 inch deep Rene'41 stiffened I beam. The center truss permits moment redistribution, hence reducing shear spanning distances. The center trusses use boron-aluminum tubes. An upper titanium longeron is used to handle fuselage bending moments.

Structural sizing was based on a 70/100 distribution of a wing root moment per 762 mm (30 inch) spacing of .757 MN.m (6,700,000 in. lb.). This resulted in an unsymmetrical moment of .227 MN.m (.3 (6,700,000) = 2,100,000 in. lb.). Spar shears were 33.36 KN/bay (2,100,000/280 = 7,500 lb/bay).

The RP tank was considered to have vertical support at each bulkhead, i.e. every 762 mm (30 inches). The tank was supported at the side of the body and off the upper chord of the bent. Vertical load from the tanks at an ultimate load factor is 100.67 kN (22.631 lb). This load designs the bent elements.

The vertical beam at the side of the body is made from Rene'41. Critical loads result from wing tank pressures.

Aft Body Wing Carry-Thru and LH_2 Tank. The aft body wing carry-thru LH_2 tank section structural system is defined in Figure 34. The upper wing surface carry-thru also serves as the top of the LH_2 tank. Titanium (Ti-6AL-4V-ELI) panels are used for the upper surface panels and titanium (Ti-6AL-4V-ELI) spar caps are spaced at 762 mm (30 inches). The lower surface is a Rene'41 multi-functional panel with Rene'41 spar caps attached. Spar trusses are boron-aluminum tubes with titanium end fittings.

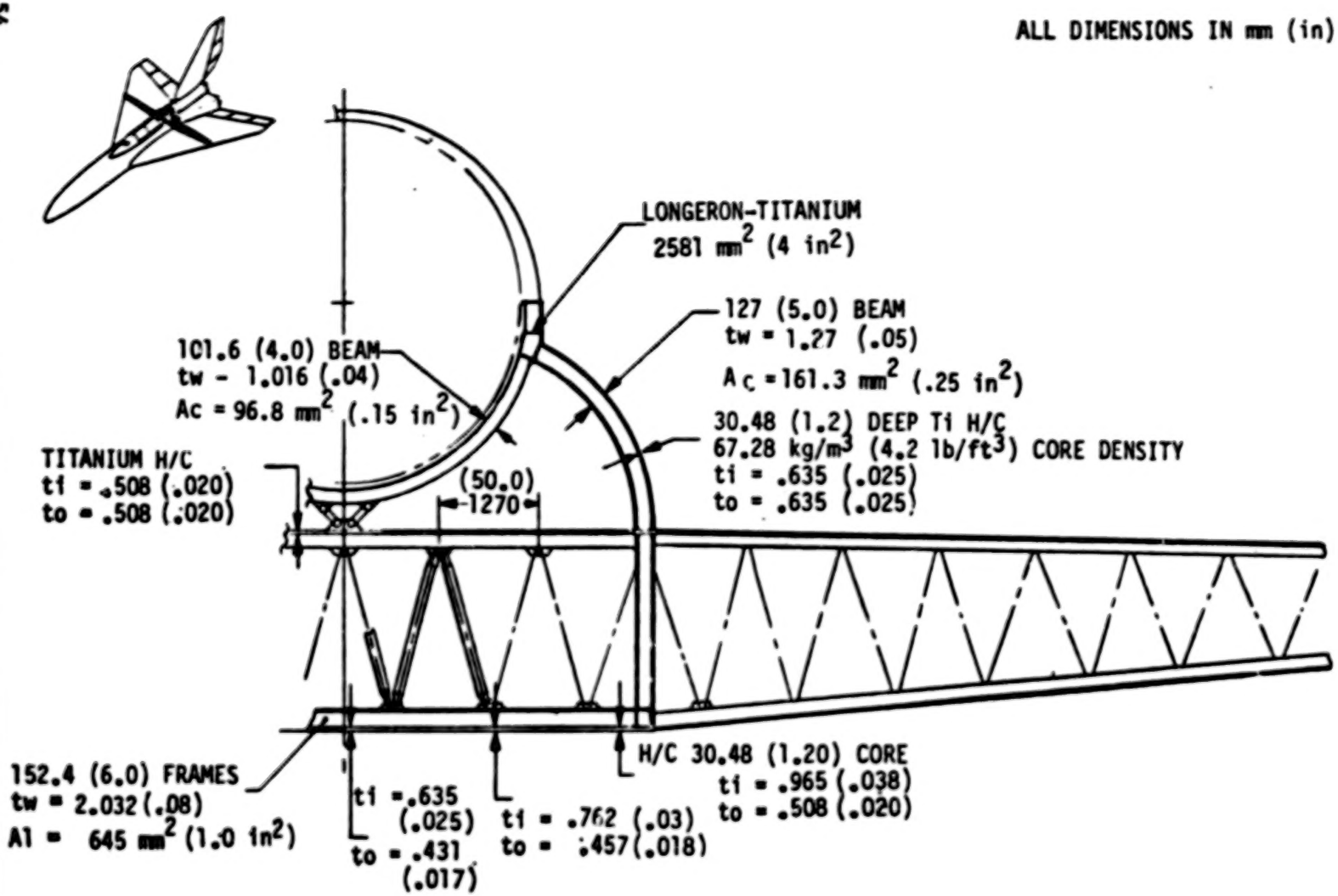

FIGURE 33 MID BODY WING CARRY THRU STRUCTURAL DETAILS

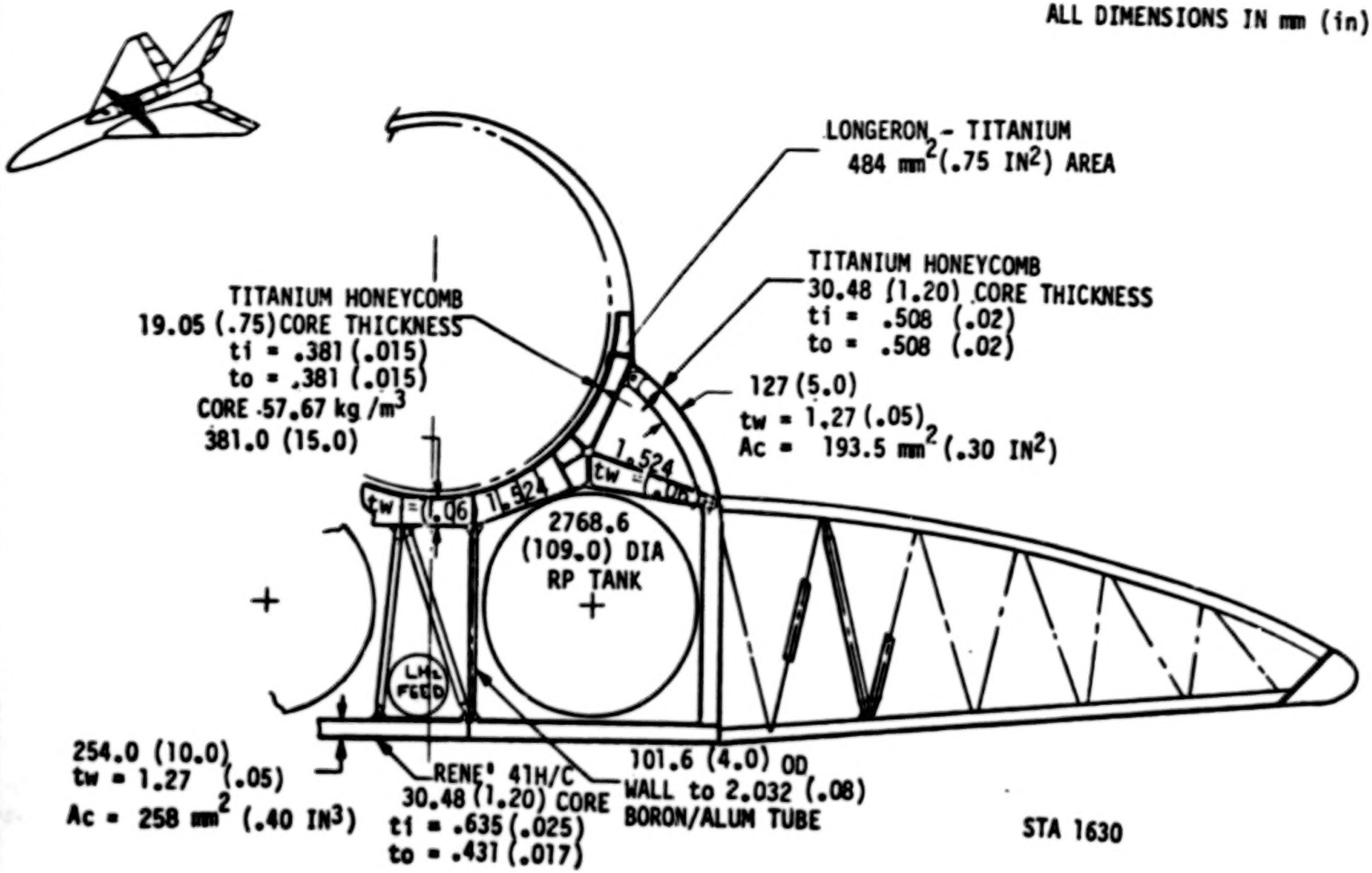

FIGURE 34 AFT BODY WING CARRY THRU STRUCTURAL DETAILS

The body upper surface (underneath the payload bay) is titanium multi-functional panel supported by titanium frames spaced at 762 mm (30 inches). An upper longeron is required to carry body bending loads.

Forward RP Tank. The forward RP tank structural system is shown in Figure 35. The structural system consists of a four longeron membrane wall tank, stiffened by frames at 381 mm spacing. Tank material is 2219 aluminum. The tank is a welded assembly. The tank is insulated with 25.4 mm (1 inch) thick Q felt to keep the tank walls below 600°F. This is to prevent coking and gumming of the residual fuel. Vertical supports are at 762 mm (30 inch) intervals.

Aft RP Tank. The aft RP tank structural details are presented in Figure 36. The structural system is similar to that used for the forward RP tanks.

Thrust Structure. The structural concept is the same as used on the ALRS 205 (Ref. 1), i.e. titanium beam with boron-aluminum reinforced chords.

Base Heat Shield Design. Figure 37 illustrates the approach used for the base heat shield. The coated Columbium should give significant service life in that for each flight peak temperatures of 1583K (2390°F) are experienced for a very short period. This unit weight is significantly less than a ceramic filled open core honeycomb as used for the S-IC base heat shield.

Heat Shield for Plume Induced Flow Separation (PIFS). Figure 38 illustrates the approach for handling temperatures resulting from PIFS (Reference: Figure 48). For the body, elevon and vertical tail the titanium panels were replaced with Rene'41 panels. A different approach was taken for the wing in that temperatures were a little lower and a lot of surface area was involved. The approach is also illustrated in Figure 38. The concept is to braze a single faced honeycomb that has been diffusion bonded to the upper surface of the standard titanium panels during their brazing cycle. This should provide adequate thermal protection during this short period of high heating.

Ground Accelerator

A ground accelerator is utilized for take-off similar to the approach used in Reference 1. The accelerator must be tailored to the specific vehicle. This can be achieved by appropriate scaling of the characteristic accelerator

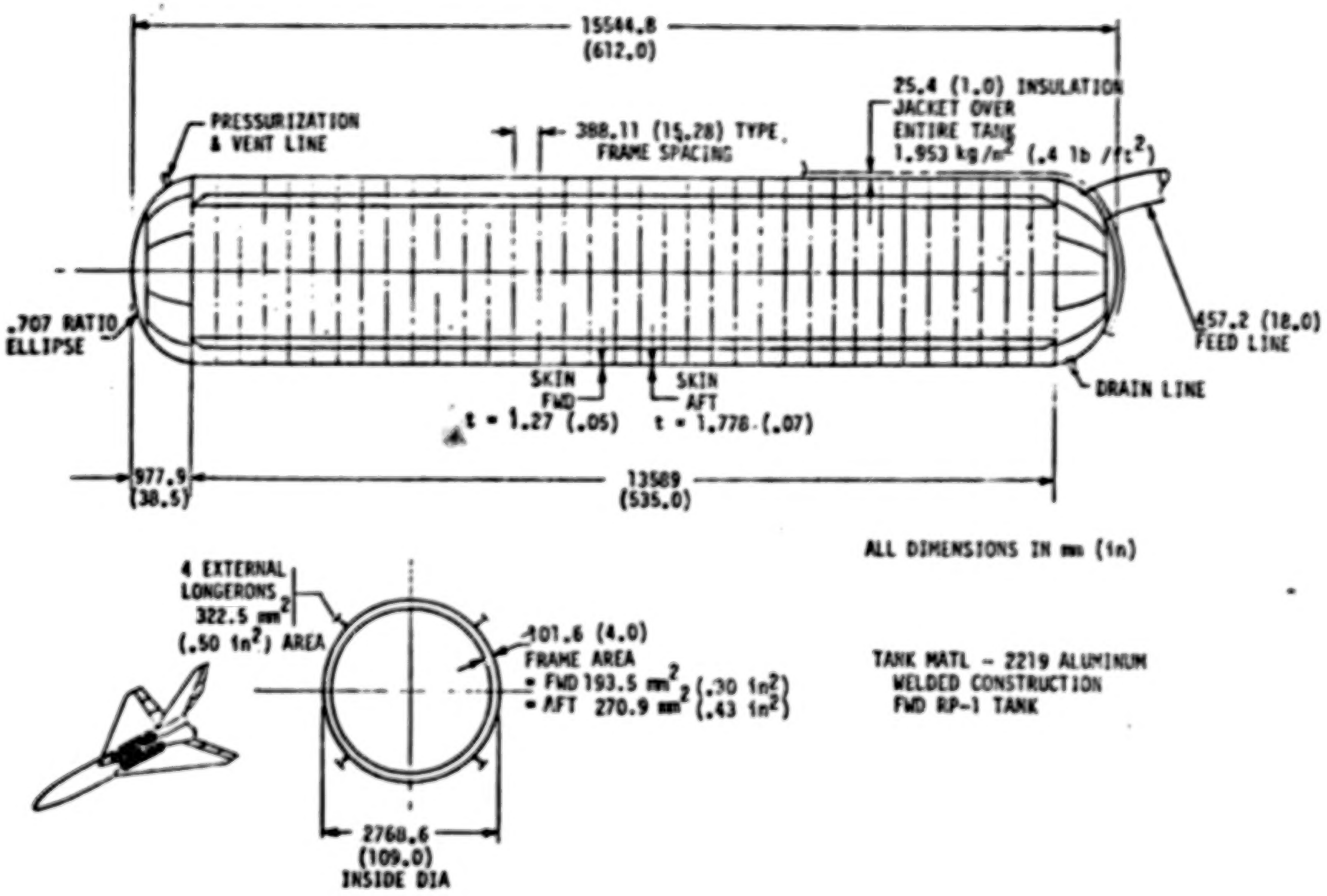

FIGURE 35 FORWARD RP TANK STRUCTURAL DETAILS

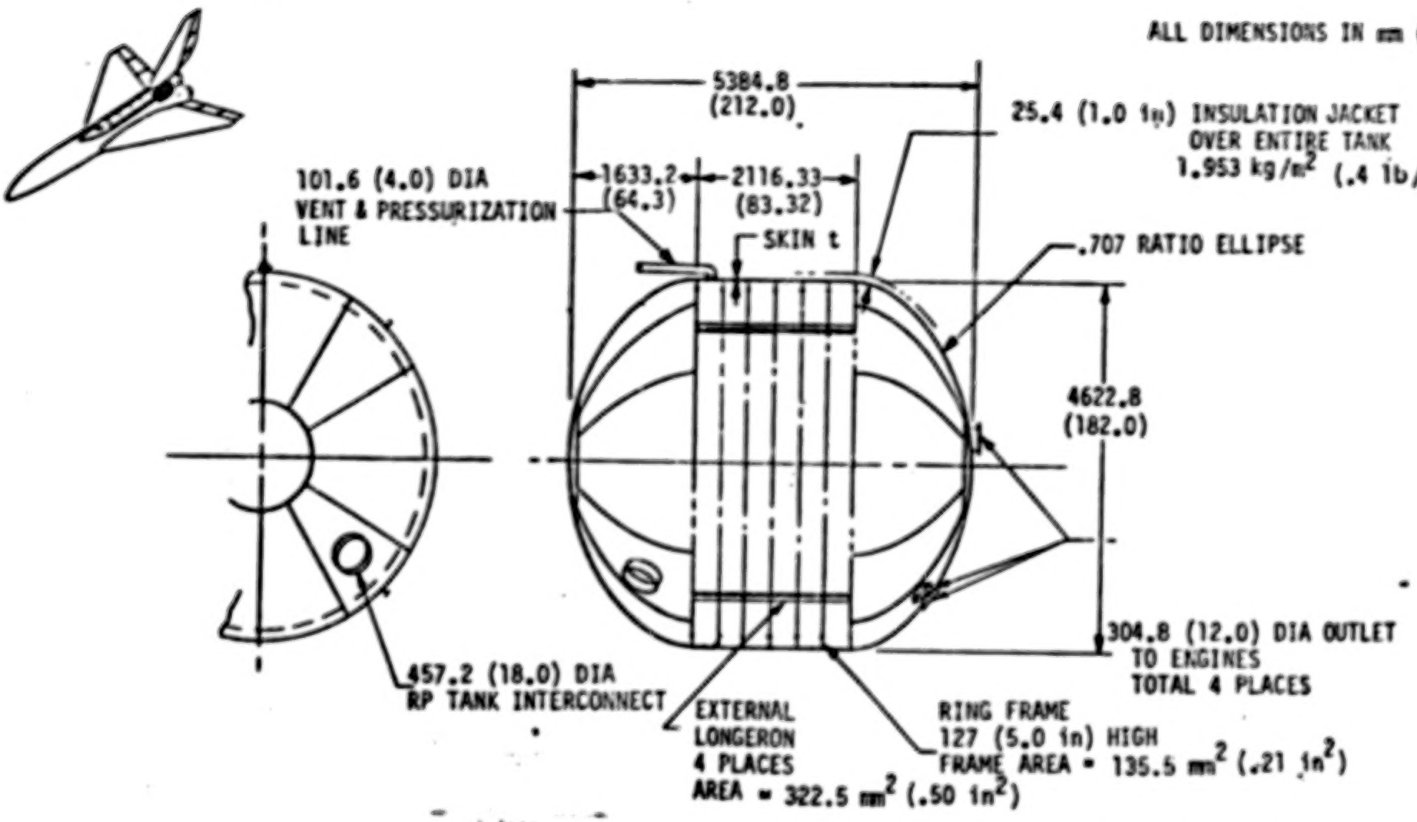

FIGURE 36 AFT RP TANK STRUCTURAL DETAILS

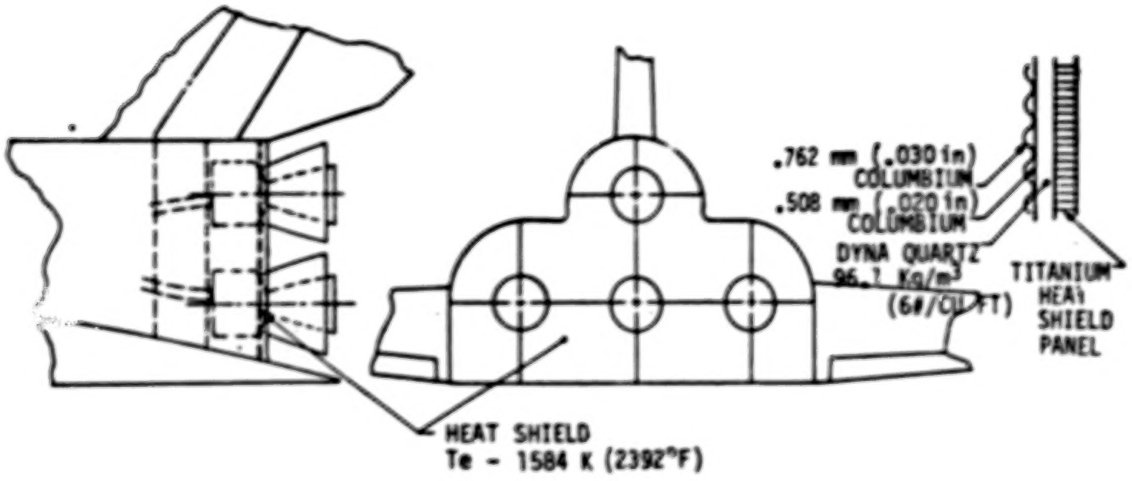

ΔWT = 56.07 kg/m^3 (3.5#/SQ FT)
TOTAL WT = 1016 kg (2240) FOR BASE HEAT SHIELD

FIGURE 37 BASE HEAT SHIELD RADIATION ASSESSMENT

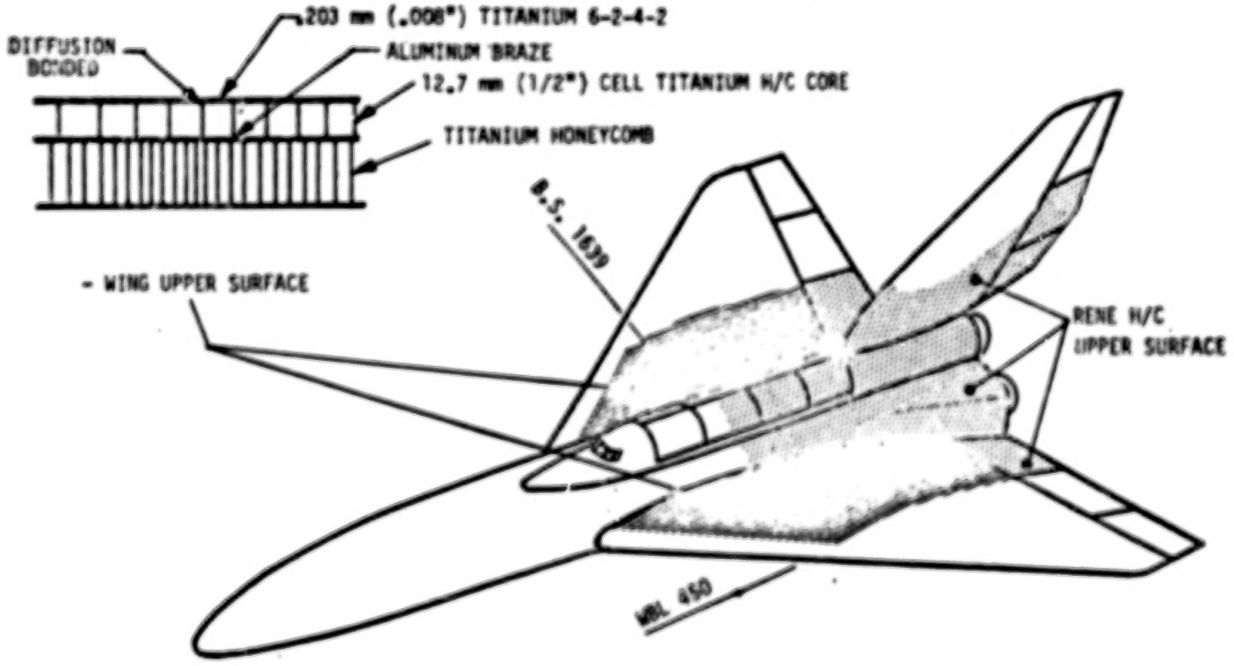

	LB/FT^2	kg/m^2	(WT~LB)	WT~ kg
WING	(.5)	2.44	(2300)	1043
ELEVON	(.55)	2.69	(130)	59
BODY	(.90)	4.39	(2700)	1225
VERT. TAIL	(.63)	3.08	(2000)	907
TOTAL			(7130)	3234

FIGURE 38 PLUME INDUCED FLOW SEPARATION ASSESSMENT

performance and configuration parameters as a function of vehicle GLOW, lift-off velocity and required thrust, support and guidance requirements as well as operational considerations. No additional new technology development is required for the scaled up version of the ground accelerator for the dual fuel vehicle.

Propulsion Design

Figure 12 provides the sizing data of the dual fuel engines required for a vehicle GLOW of 1,374,839 kg (3,031,300 lb) with a propellant split ratio of .60. Four dual fuel engines are used with extendable nozzles which change the expansion ratio from 50:1 to 150:1.

Subsystems Installation

Hydraulics System Installation. The hydraulic system illustrated on Figure 39 is an extrapolation of the system defined in Reference 1. This

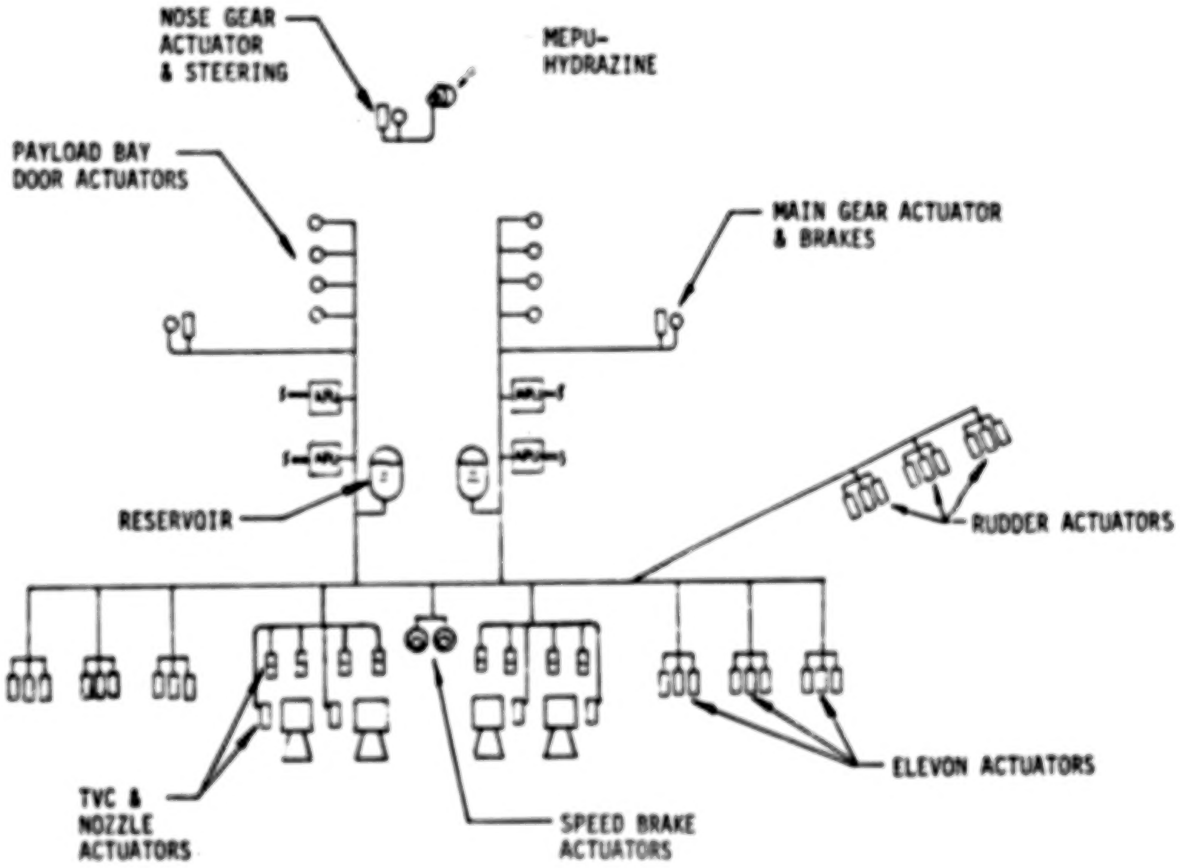

FIGURE 39 HYDRAULICS SYSTEM INSTALLATION

includes the utilization of engine driven hydraulic pumps (driven off main ascent engine propellent pumps) to provide the thrust vector control (TVC) and nozzle extension power requirements. These pumps are not shown in the schematic of Figure 39. The system is also sized by the aero-control system demands. Accumulators are used to support the peak power demands.

Main and Forward Landing. The landing gear illustrated on Figures 40 and 41 utilizes the geometry and technology definitions developed in Task 4 of Reference 1. The components and their weights have been sized up to the higher landing weight of the dual fuel vehicle. This is reflected in larger tire sizes and increased brake volume as well as a slightly longer strut length all of which are included in the increased landing gear weight. The Task 4 technology utilizes composite beams and load carrying members with titanium end fittings as well as carbon-carbon brakes to achieve the very low landing gear weight fraction.

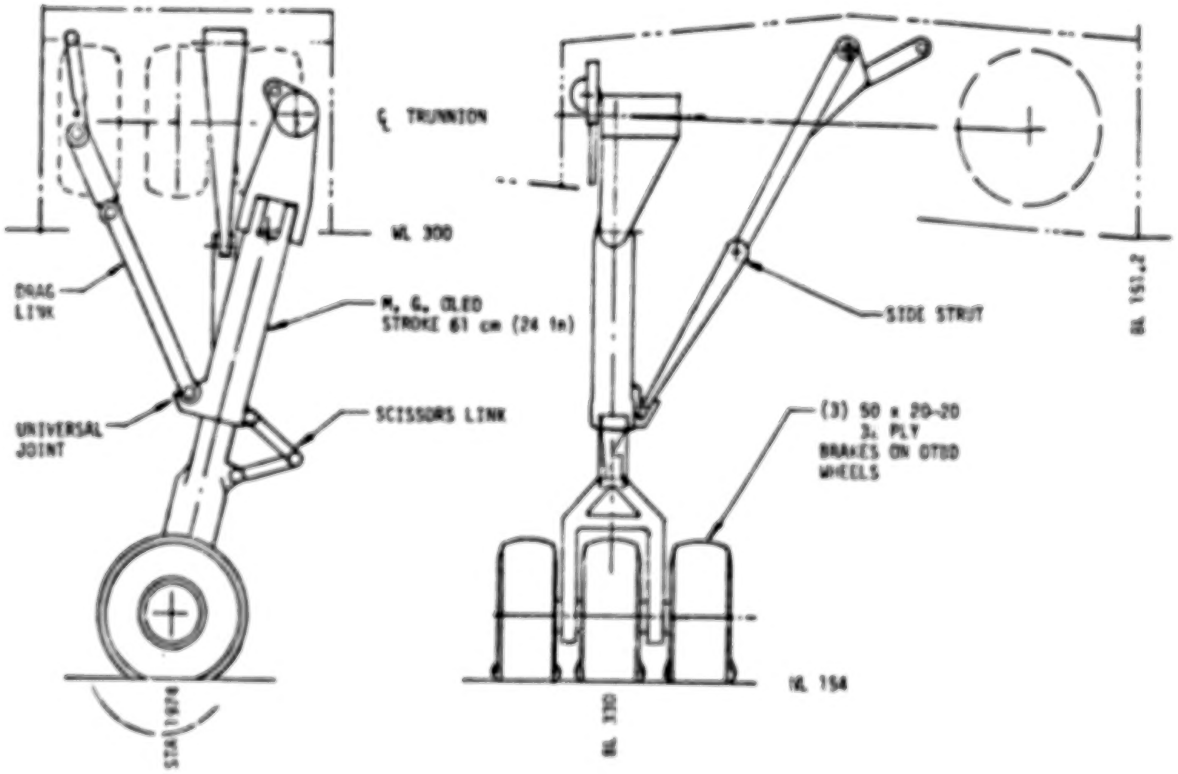

FIGURE 40 MAIN LANDING GEAR INSTALLATION

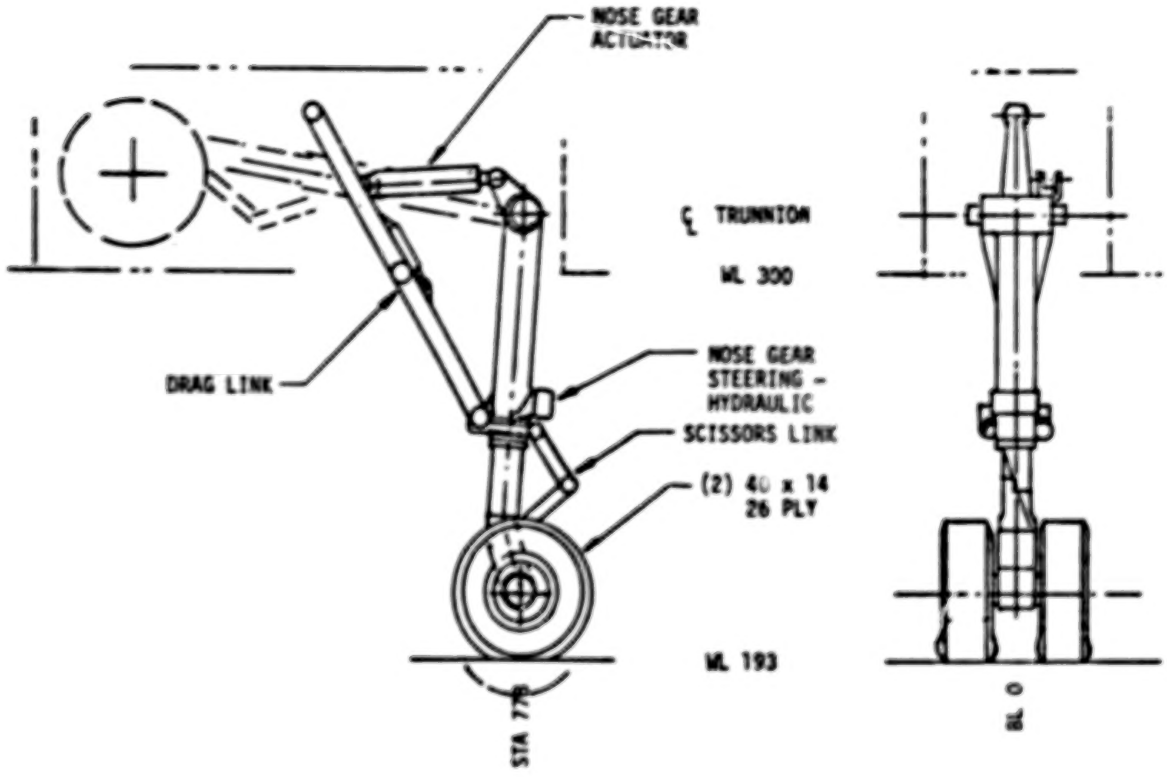

FIGURE 41 FORWARD LANDING GEAR INSTALLATION

Propulsion System Installation. The integrated auxiliary propulsion system concept selected for the dual fuel vehicle point design is illustrated on Figure 42. The design reflects a departure from the system presented in Reference 1. Trade study results indicate a LO_2/LH_2 APU and RCS is more weight competitive than the storable systems selected for the smaller all LO_2/LH_2 main engine vehicle. This change, in combination with utilizing common tankage and control elements, resulted in approximate weight savings of 680.5 kg (1500 lb) for the subsystems proposed for this vehicle.

Propulsion Tank and Feed System Installation. Figure 43 illustrates the principal features of the dual fuel tank and feed system which were identified to assess the weight increment associated with the dual fuel engine. This was referenced to the system component weight fractions developed for Task 4 of Reference 1.

The forward RCS system, although larger than the system of Reference 1, was not large enough to realize significant weight savings by a change to

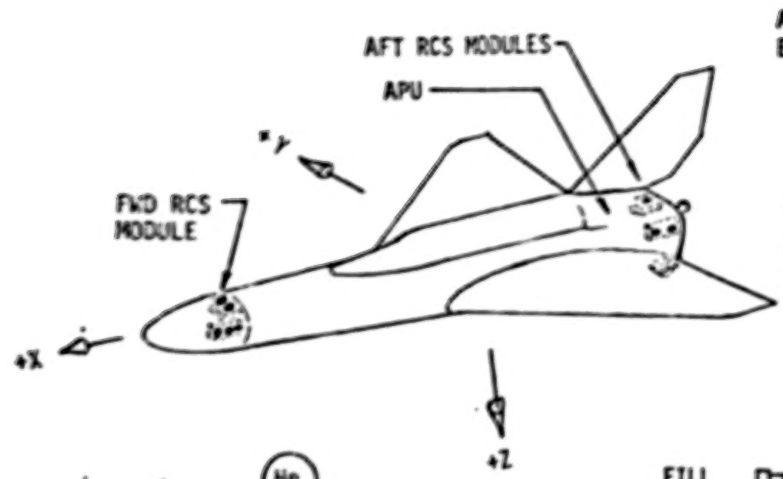

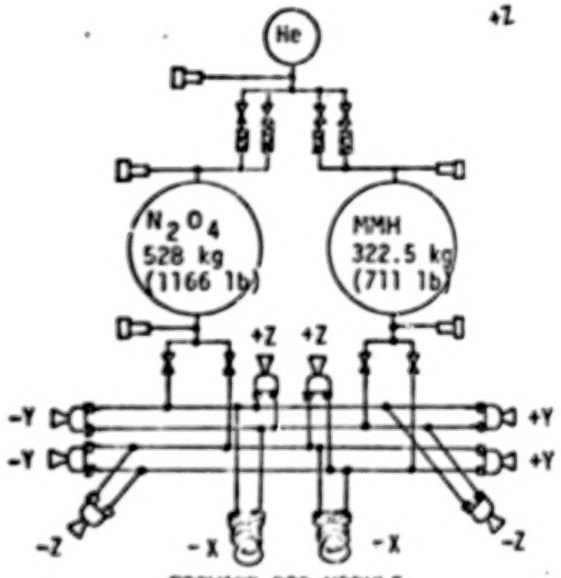

FORWARD RCS MODULE

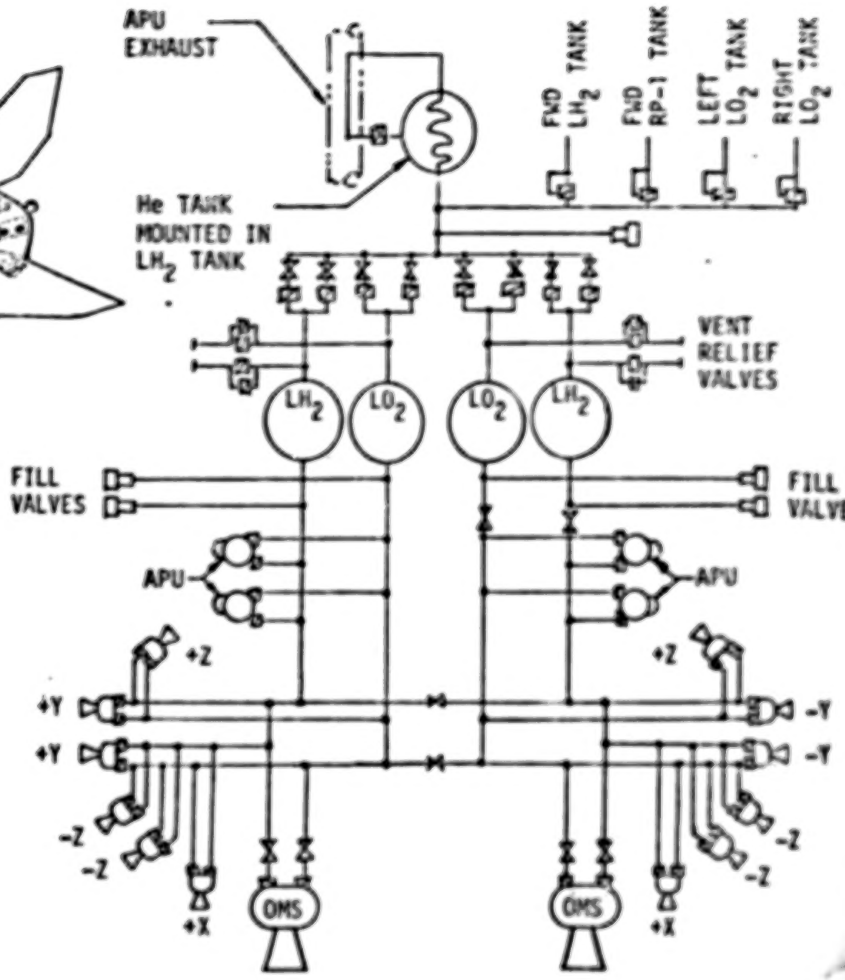

AFT RCS, OMS, APU, AND TANK PRESSURIZATION

FIGURE 42 PROPULSION SYSTEM INSTALLATION

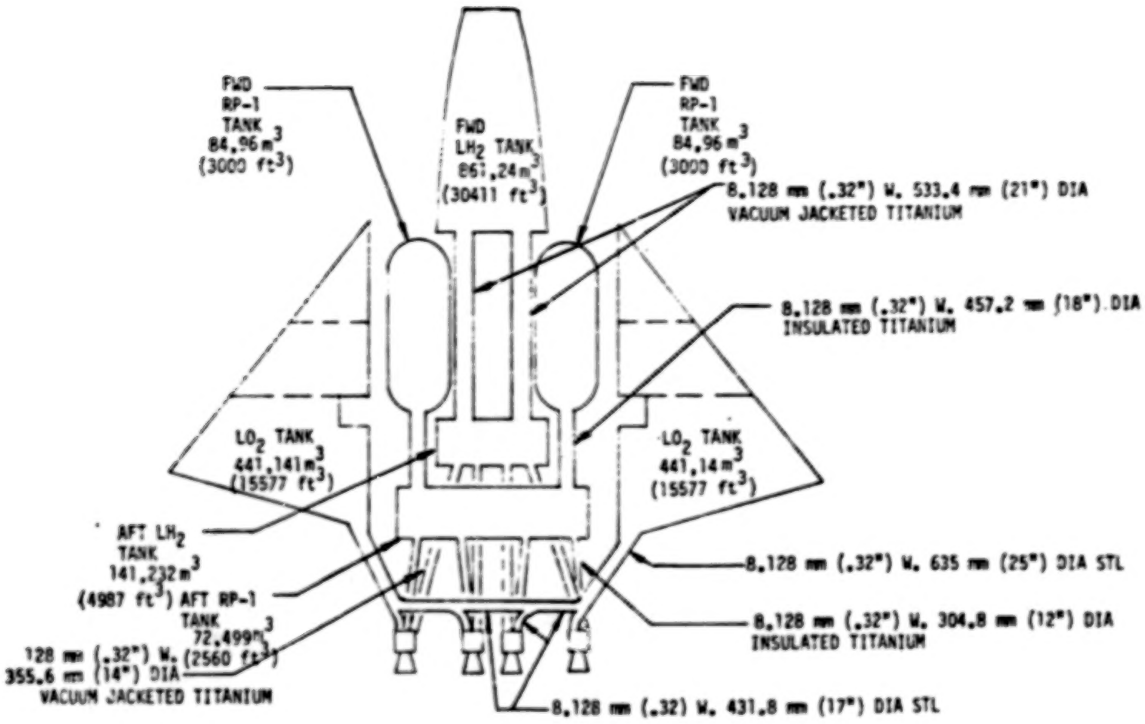
FWD RP-1 TANK 84.96 m³ (3000 ft³)
FWD LH2 TANK 861.24 m³ (30411 ft³)
FWD RP-1 TANK 84.96 m³ (3000 ft³)
8.128 mm (.32") W. 533.4 mm (21") DIA VACUUM JACKETED TITANIUM
8.128 mm (.32") W. 457.2 mm (18") DIA INSULATED TITANIUM
LO2 TANK 441.141 m³ (15577 ft³)
LO2 TANK 441.14 m³ (15577 ft³)
AFT LH2 TANK 141.232 m³ (4987 ft³)
AFT RP-1 TANK 72.499 m³ (2560 ft³)
8.128 mm (.32") W. 635 mm (25") DIA STL
8.128 mm (.32") W. 304.8 mm (12") DIA INSULATED TITANIUM
128 mm (.32") W. 355.6 mm (14") DIA VACUUM JACKETED TITANIUM
8.128 mm (.32) W. 431.8 mm (17") DIA STL

FIGURE 43 PROPELLANT TANK AND FEED SYSTEM INSTALLATION

LO_2/LH_2, therefore the lower cost N_2O_4/MMH system was retained. Both of these systems weight factors are predicated on the utilization of the Task 4 technology identified in Reference 1.

Environment

The mass properties to be determined are dependent upon the design loading and the environmental conditions. This necessitates loads, dynamics, thermal and structural analyses which result in structural sizing of the vehicle components leading to the determination of vehicle weight.

Loads and Dynamics. Loads were developed similar to those described in Step 2 since the aerodynamic shape was retained. Subsonic airloads were ratioed by gross weight and area change. Net loads were developed for each vehicle component using local weight distribution. Body load analysis results indicated shears, moments and torsions as expected from relative scale-up of the vehicle sizes. However, when analyzing wing air loads, in conjunction with LO_2 tank pressures and boost thermal environment, there were significantly different results than would be expected from area or weight scale-up.

The increase in wing lift-off bending moment of the dual fuel vehicle, as compared to the all LO_2/LH_2 Reference 1 vehicle, was caused by the increase in wing uplift loads over the LO_2 downloads. This was caused by the increased GLOW and the placement of more LO_2 inboard on the thinner wing of the dual fuel vehicle. An increase in torsion due to the dual fuel wing sweep back and LO_2 forward (ascent stability requirements) also was a negative factor in wing sizing and weight increase. Therefore a much greater portion of the dual fuel vehicle was sized by liftoff loads than for the Reference 1 SSTO vehicle.

This significant change in wing loads necessitated a re-size cycle to update wing weights. The following discussion summarizes the wing weights. The following discussion summarizes the wing resize technical approach and defines resulting wing weights.

The analysis procedure first determined the minimum skin gaging and spar sizing required to carry wing LO_2 pressure/thermal loads and stresses during boost. These loads primarily sized skins and spars of the LO_2/LH_2 vehicles of Reference 1. Using these sizings, the wing skins and spars were then checked against liftoff shears and torsional shears caused by head pressures, wing bending moments, and wing presssures. Sizings were iterated until adequate strength and balanced skin/spar sizings were obtained. The spar diagonal strut members were sized by taxi and wing liftoff shears.

Typical areas for which a stress analysis was conducted are shown on Figure 44. Typical wing pressure and thermal sizings were also developed for over the spar thicknesses of the wing. The analysis account for external and internal skin temperatures along the chord of the wing at various buttock lines as well as the LO_2 tank pressure variations as caused by relative location to pressure bulkhead.

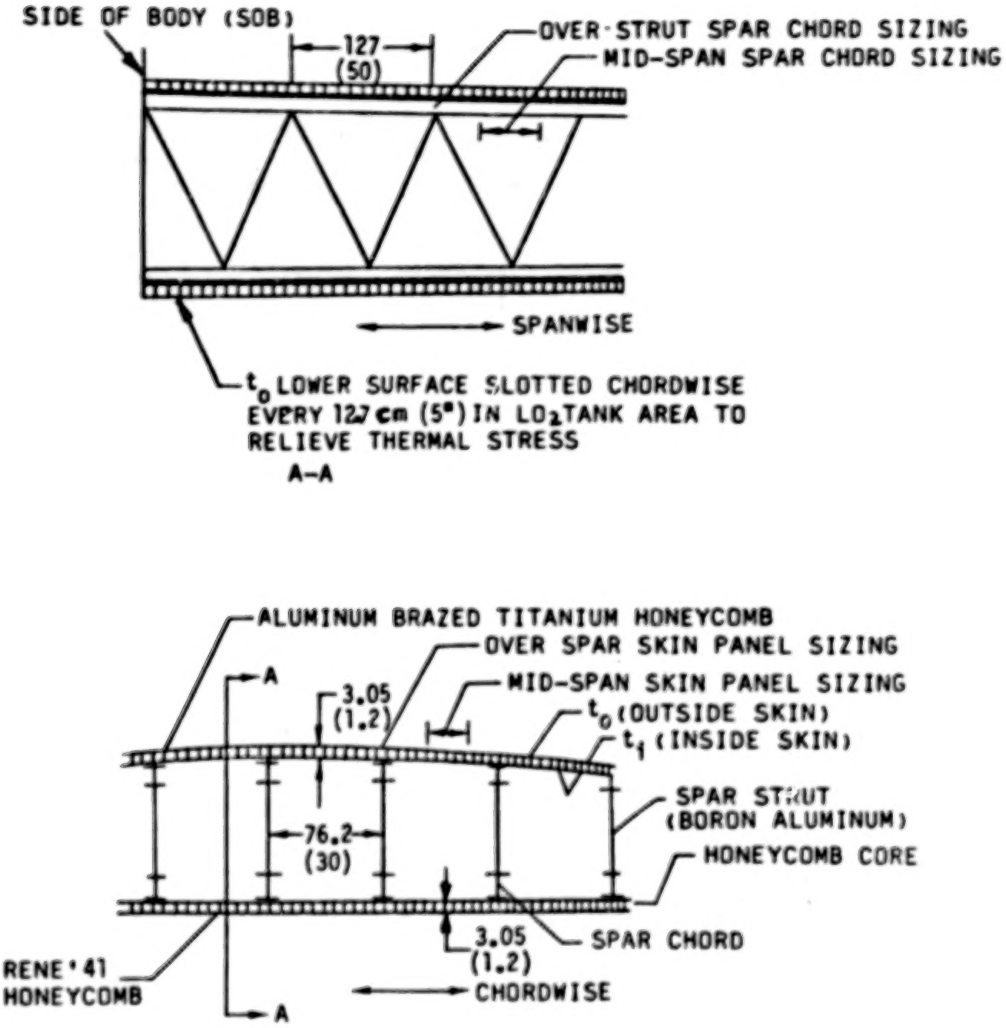

ALL XX DIMENSIONS IN CENTIMETERS
ALL (XX) DIMENSIONS IN INCHES

SKETCHES NOT TO SCALE

FIGURE 44 AREAS OF STRESS ANALYSIS

The upper and lower surface unit and total weights are shown on Figures 45 and 46, respectively.

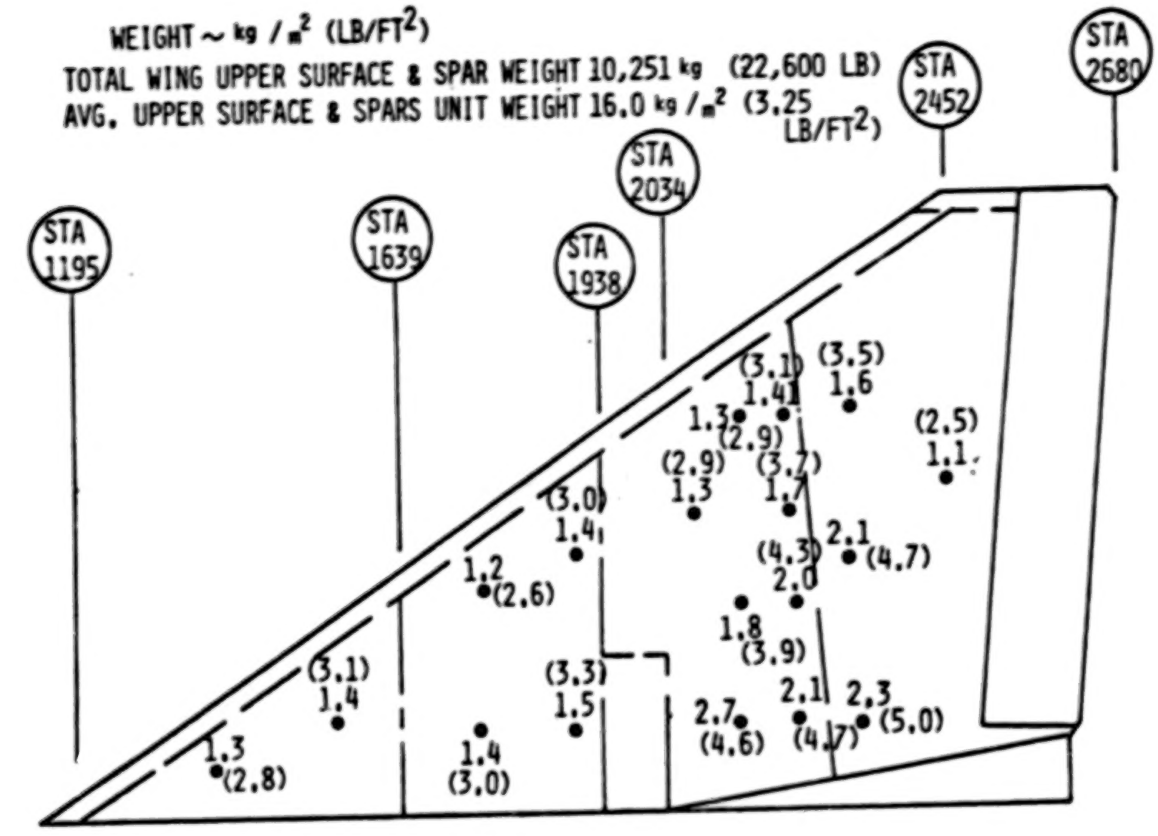

FIGURE 45 WING UPPER SURFACE WEIGHTS

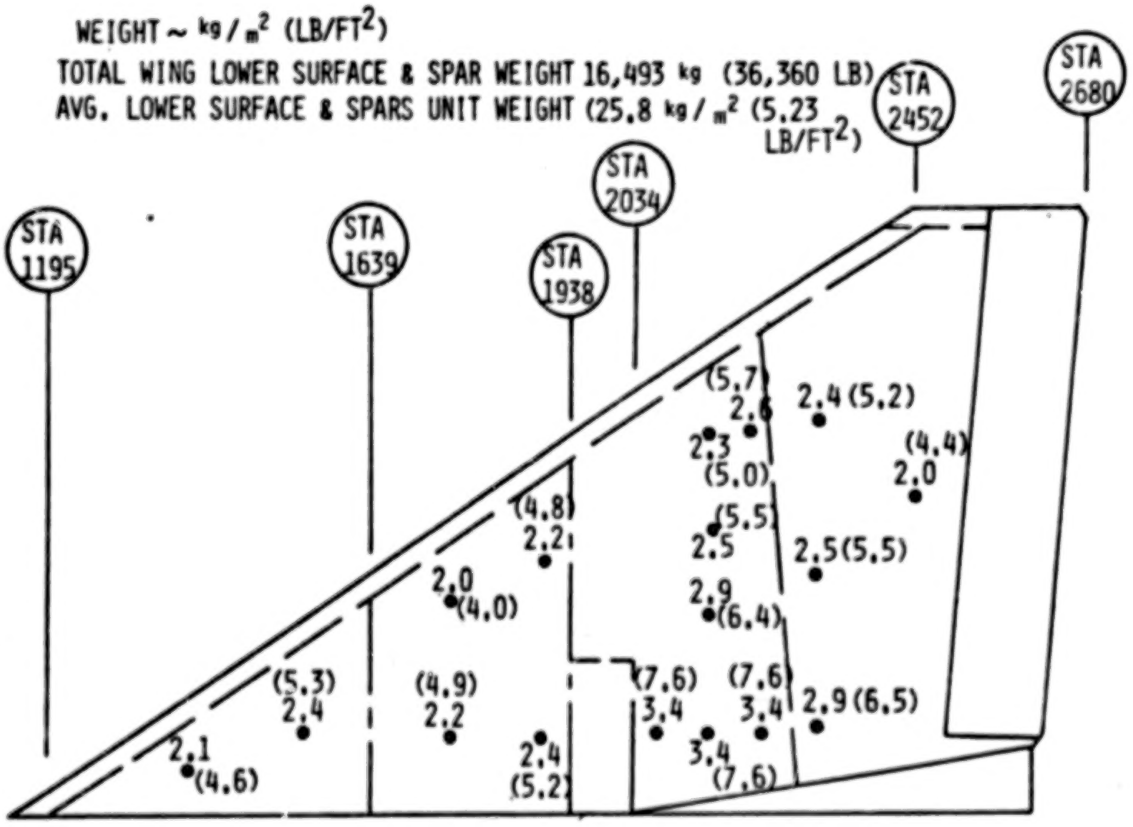

FIGURE 46 WING LOWER SURFACE WEIGHTS

It should be noted that the aft wing tank areas although nontankage become sized by bending and torsion loads. The torsion is caused by the break between balanced loads (tank weight vs air loads) and unbalanced loads (dry bay weight vs air loads). The aft wing sweep is required to get an acceptable CP/CG relationship.

These weights represent the summation of spar flange, skin honeycomb, braze alloy, spar struts and 15% of the previously mentioned weights for joint weight. These summed weights are exclusive of the overall vehicle weight growth factor.

Thermal Analysis. The thermal analysis was carried out in accordance with the criteria specified in Reference 1. Both ascent and reentry trajectories were analyzed.

Isotherms---The isotherms shown in Figure 47 are based on peak equilibrium radiation temperatures and do not account for internal radiation or material heat sink effects, nor are effects of engine plume radiation or plume induced flow separation (PIFS) included. Both ascent and reentry critical regions are

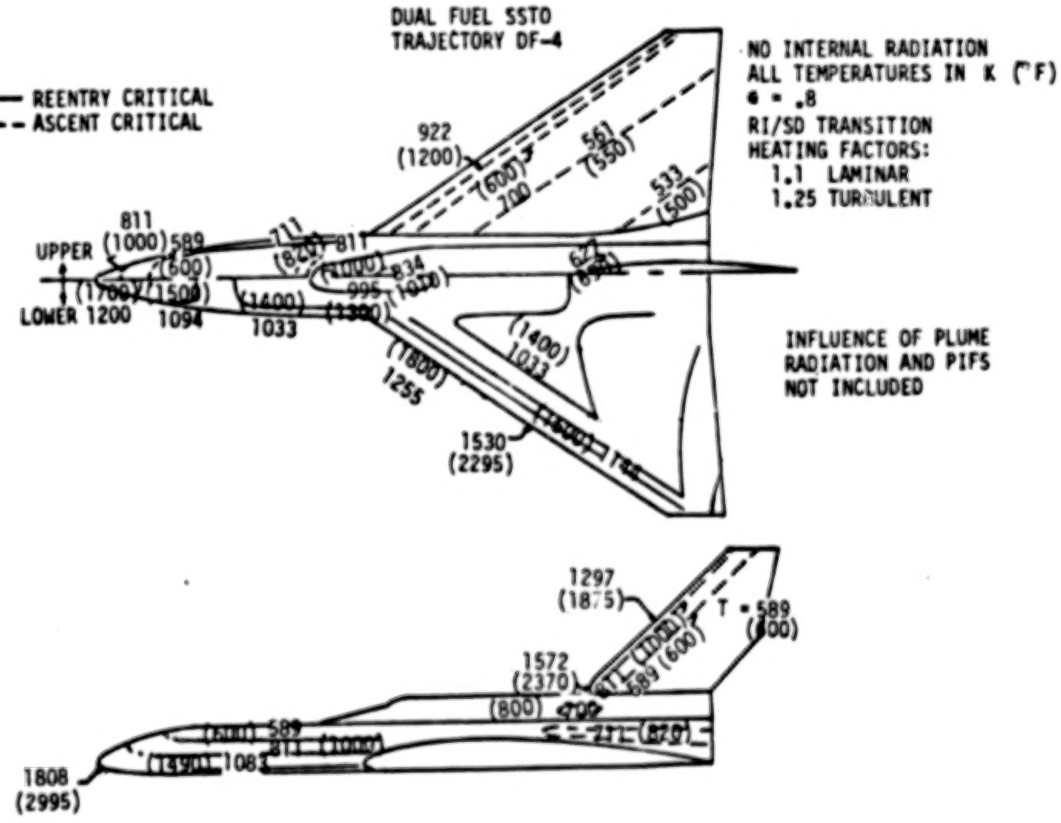

FIGURE 47 EQUILIBRIUM TEMPERATURE DISTRIBUTION

shown. The reentry trajectory is corresponding to an equilibrium glide trajectory with W/SC_L = 317.4 kg/m^2 (65 lb/ft^2) at α = 30°. The reentry angle of attack of 50° is reduced to 30° at 96.6 km (317,000 ft) altitude, and the bank angle is set at ϕ = 45°.

Computed heating rates include uncertainty factors of 1.1 for laminar and 1.25 for turbulent flow. Turbulent flow heating is predicted using the Spalding-Chi method in conjunction with a Reynolds analogy. Transition is determined using the Rockwell International/Space Division (RI/SD) transition criterion Re /Me = N, where N = 225 at the body centerline, 160 at wing mid-span, and 80 at the wing tip. The body nose radius is 51 cm (20 in). The leading edge radii are 30.5 cm (12 in) on the wing and on the vertical fin.

Interference heating was accounted for using data obtained from hypersonic tests of a representative SSTO configuration in the NASA-Ames 3.5 foot hypersonic tunnel.

Plume Radiation and Plume Induced Flow Separation (PIFS)---As compared with the LO_2/LH_2 vehicles studied in Reference 1, radiation from exhaust plumes of hydro-carbon burning engines is more than an order-of-magnitude greater than for comparable hydrogen fueled engines. An indication of the thermal environment resulting from the exhaust plume from clustered RP engines is provided by heat transfer measurements obtained from S1-C (Saturn V first stage) flights.

In addition to direct radiant heat from exhaust plumes, S1-C flight data indicate substantial increases in surface heating at high altitudes because of plume induced flow separation (PIFS). Exhaust gases are ingested into the recirculated flow, causing increased gas temperatures adjacent to the surface.

Figure 48 shows predicted peak equilibrium temperatures resulting from plume radiation and PIFS which are based on extrapolated S1-C flight data. These high temperatures, which dependent on body location occur over periods from 10 to 50 seconds, require a modification and/or thermal protection for the base heat shield, portions of the wing and body upper surfaces and on the vertical tail, as shown in Figures 37 and 38.

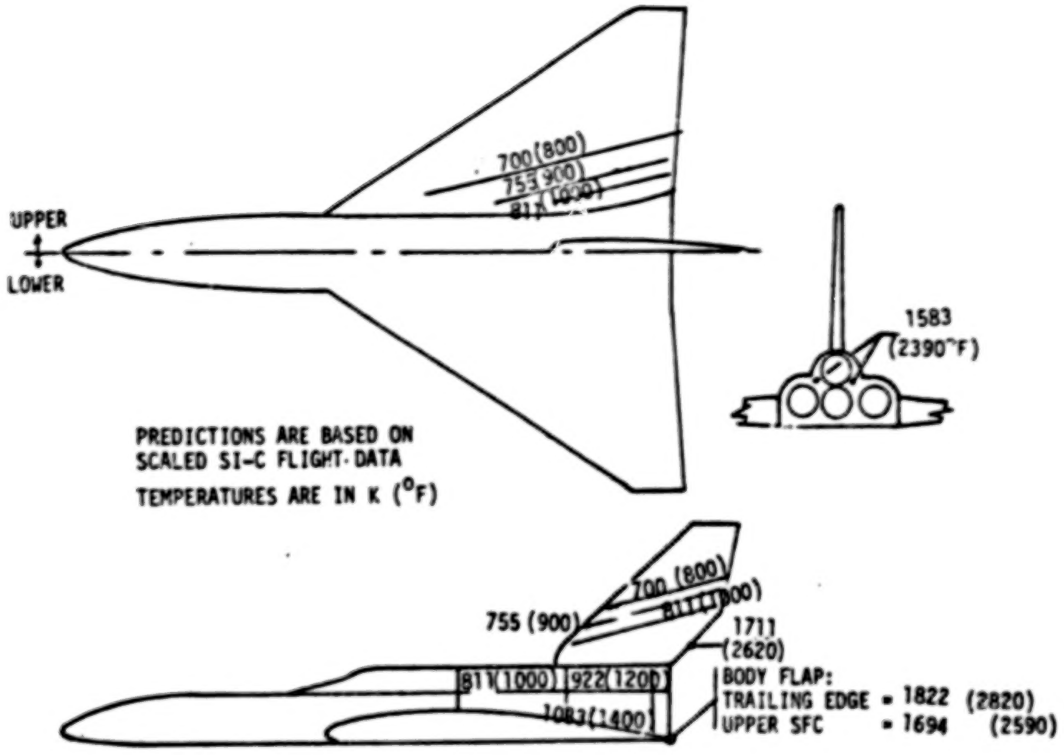

FIGURE 48 PROPULSION SYSTEM RADIATION TEMPERATURES

The weight penalties involved with this type of heating indicate that it may be more efficient to switch to LH_2 at lower altitudes and accept a smaller performance penalty.

Structural Temperature Distributions---For structural sizing, actual temperatures and temperature distributions are required including the effect of heat sinks and internal radiation exchange as shown in Figure 49 for a typical body cross section. The temperature distributions were obtained using the Boeing Engineering Thermal Analysis (BETA) program accounting for internal radiation, conduction and heat storage.

The body cross section, taken approximately 24.4 m (80 ft) aft of the nose consists of Rene'41 frames, face sheets and honeycomb core on the lower, and titanium frames, face sheets and honeycomb core on the upper half. The internal face sheet and the frame of the upper body half are gold coated in order to reduce upper surface temperatures affected by radiation from the lower part of the body. Both ascent and reentry regions are represented.

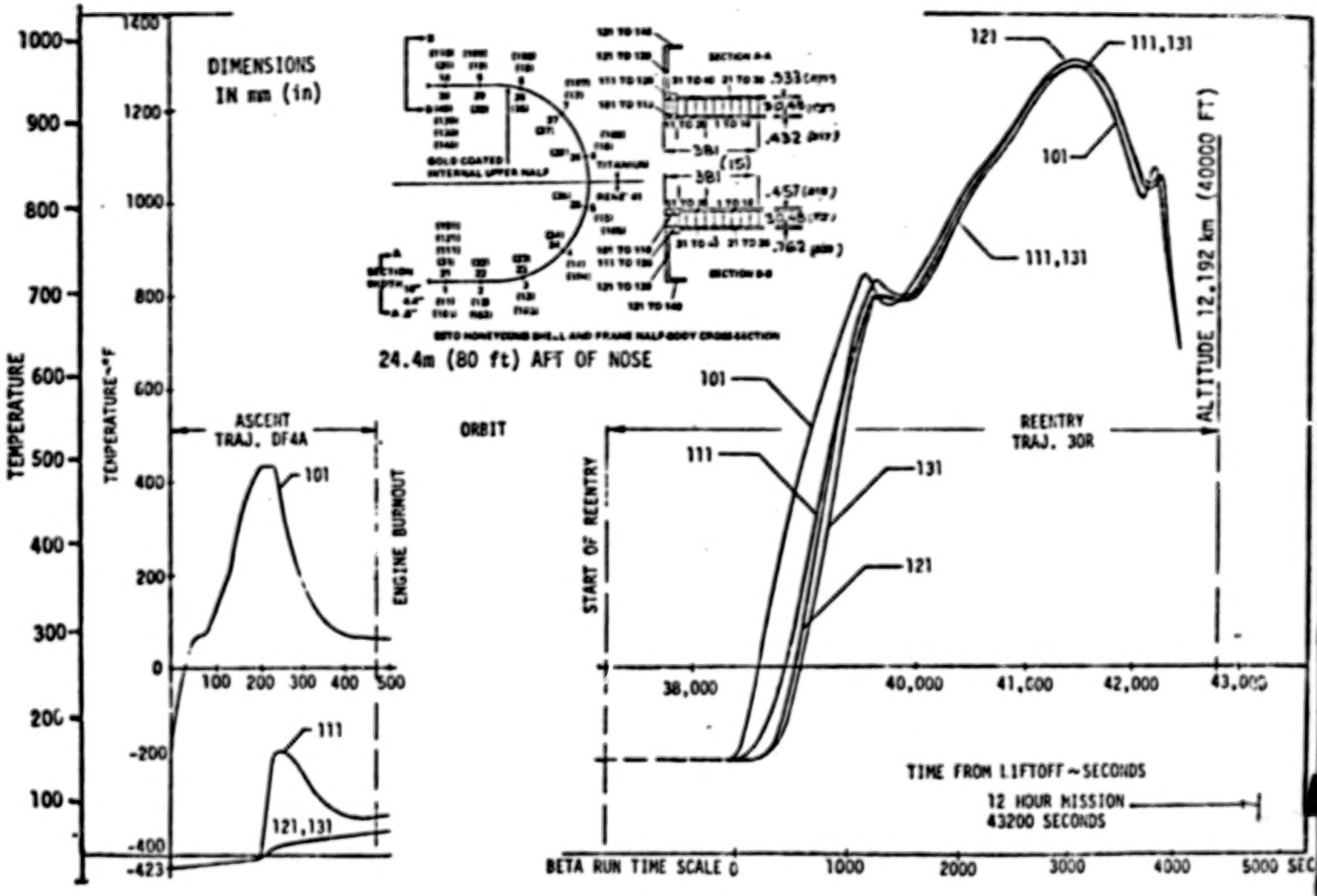

FIGURE 49 BODY, SHELL AND FRAME TEMPERATURE DISTRIBUTION

Weights

Structural Weight. The structural weights were developed using a combination of data from Reference 1 and detail unit weights resulting from structural sizing. Table 4 shows the detail weight buildup for the body. The body weight is 38,489 kg (84855 lb) not including growth.

ITEM	WEIGHT kg	LB
NOSE COMPARTMENT	746	(1,645)
FORWARD BODY	10,342	(22,800)
NOSE GEAR WELL	649	(1,430)
MID BODY	13,526	(29,820)
FORWARD RP TANKS & INSULATION	1,905	(4,200)
AFT BODY	1,992	(4,392)
AFT RP TANK & INSULATION	558	(1,230)
THRUST STRUCTURE	2,114	(4,660)
HEAT SHIELD	355	(782)
SIDE OF BODY REINFORCEMENT	485	(1,070)
PAYLOAD DOORS	2,098	(4,626)
SIDE OF BODY RIB	3,719	(8,200)
TOTAL BODY STRUCTURE	38,489	(84,855)

TABLE 4 BODY STRUCTURES WEIGHT SUMMARY

Table 5 summarizes weights of the airframe components.

The total weight, 82,259 kg + 8,210 kg growth (181,360 lb + 18,100 lb) represented a vehicle sized using unit ALRS 205 wing surface, spars and rib unit weights and neglecting the effects of the RP plume radiation on the base heat shield and heating from plume induced flow separation.

ITEM	WEIGHT kg	LB
BODY	38,489	(84,955)
CREW COMPARTMENT	2,440	(5,380)
VERTICAL TAIL	4,704	(10,370)
LAUNCH SUPPORT	925	(2,100)
LEADING EDGE	4,649	(10,250)
ELEVONS	4,989	(11,000)
MAIN GEAR WELL	2,431	(5,360)
WING PANELS, SPARS & RIBS	22,416	(49,420)
WING BULKHEADS	1,197	(2,640)
TOTAL STRUCTURE	82,270	(181,375)
GROWTH	8,227	(18,137)
ACTUAL WING ANALYSIS	4,327	(9,540)
RADIATION HEATING (PIFS & BASE)	4,536	(10,000)
TOTAL STRUCTURE	99,360	(219,052)

TABLE 5 VEHICLE STRUCTURES WEIGHT SUMMARY

Detail sizing of the wing resulted in a delta weight increase of 3901 kg (8,600 lb). This weight is consistent with the detail wing sizing presented in this report.

Plume heating resulted in weight increases of approximately 4536 kg (10,000 lb). The basis for these are the structural concepts presented for the base heat shield and the wing and body upper surfaces in the sections on plume heating.

The result of these items is a total structural weight of approximately 98,883 kg (218,000 lb) including growth.

Subsystems Weight. The subsystems weight data illustrated on Table 6 were developed utilizing the data from Task 4 of Reference [1]. In those cases where no significant change results as a consequence of either dual fuel or size change, the weights are as developed previously, e.g. personnel provisions.

ITEM	WEIGHT - lb	kg
FORWARD RCS	967	439
FORWARD LANDING GEAR	1,455	660
ECS	1,000	454
AVIONICS	3,168	1,437
ELECTRICAL POWER (FWD)	2,340	1,061
PERSONNEL PROVISIONS	877	398
PRESS SYSTEM	2,010	912
THERMAL CONTROL	2,085	946
AFT LANDING GEAR	8,200	3,719
PROPELLANT FEED & VENT	4,860	2,204
ELECTRICAL POWER (AFT)	1,964	891
APU	660	299
HYDRAULIC POWER	2,498	1,133
AFT RCS	1,345	610
OMS ENGINES	768	348
RCS APU OMS TANKAGE & PLUMBING	783	355
ENGINES (MAIN)	43,033	19,520
FLIGHT CONTROLS	2,400	1,089
	80,413	36,475

TABLE 6 SUBSYSTEMS WEIGHT SUMMARY

In those systems where only a partial impact is apparent, e.g. avionics, only that portion of the system impacted was incrementally increased. The systems which scaled with weight, e.g. landing gear, were proportionately increased as a function of the increased landing weight. The systems which were new or significantly changed, e.g. main engines and propellant feed and vent, were weighed based on the specific parametric factors applicable. The weights include growth allowance.

The total vehicle weights are summarized in Table 7. The structural and subsystem weights are first tabulated without the effect of the recycled wing analysis, PIFS and base heating, and center of gravity position control (See Figure 54). As may be seen, the effect of these items reduces the payload to 19710 kg (43,368 lb) (i.e. holding GLOW constant at 1377860 kg (3,031,300 lb). The 5772 kg (12,700 lb) weight saving is, as noted on Table 7, the result of utilizing the perturbed technology projections developed under Task IV of Ref. 1. Using an extrapolation procedure that would keep main ascent propulsion characteristics relative to GLOW constant (Ref. 1), it is estimated that GLOW would be increased to approximately 1,568,000 kg (3,450,000 lb) for a 29545 kg (65,000 lb) payload delivery capability.

	kg	(lb)			
STRUCTURE	90,498	(199,512)			
SUBSYSTEMS	36,475	(80,413)			
	126,973	(279,925)	121,217	(267,235)	[Δ = 5,756 kg (12,690 lb) ▷]
Δ DRY WEIGHT					
ACTUAL WING ANALYSIS			4,327	(9,540)	
PIFS AND BASE HEATING			4,536	(10,000)	
CENTER OF GRAVITY CONTROL			1,566	(3,453)	
PERSONNEL			263	(580)	
PAYLOAD			19,671	(43,368)	
FLUIDS					
FLIGHT PERFORMANCE RESERVES			2,729	(6,081)	
REACTION CONTROL PROPELLANT			1,469	(3,239)	
ORBIT MANEUVER PROPELLANT			6,816	(15,028)	
RESIDUALS UNUSABLE			6,044	(13,325)	
SUBSYSTEM FLUIDS			1,770	(3,904)	
VEHICLE INJECTED WEIGHT			170,508	(375,900)	
ASCENT PROPELLANT			1,204,489	(2,655,400)	
VEHICLE GROSS LIFT OFF WEIGHT			1,374,997	(3,031,300)	

▷ WEIGHT SAVING OBTAINED THROUGH USE OF PERTURBED TECHNOLOGY, REFERENCE 1

TABLE 7 VEHICLE WEIGHT SUMMARY DUAL FUEL SERIES BURN

Flight Performance

Ascent Trajectory. The HTO dual fuel vehicle is east launched from ETR with a GLOW of approximately 1,360,000 kg (3×10^6 lb). A digital computer program (Boeing) AS2530 was used to determine the trajectory characteristics as presented in Figure 50. These characteristics are near optimum for the imposed thermal constraints on the vehicle structure. The flight sequence of the selected trajectory is described as follows: With a horizontal takeoff from a sled ground accelerator of 182.9 m/s (600 fps), a pull-up is made to a flight path angle of 25.5 degrees (with angle of attack not exceeding 13 degrees and normal load factor of 1.25). This flight path is held until after passing the maximum dynamic pressure region 43.67 k Pa (912 psf), then gradually reduced at a rate of 0.08 degrees per second until the angle of attack increased to 17 degrees. At a relative velocity of 1703 m/s (5587 fps) the dual fuel engines

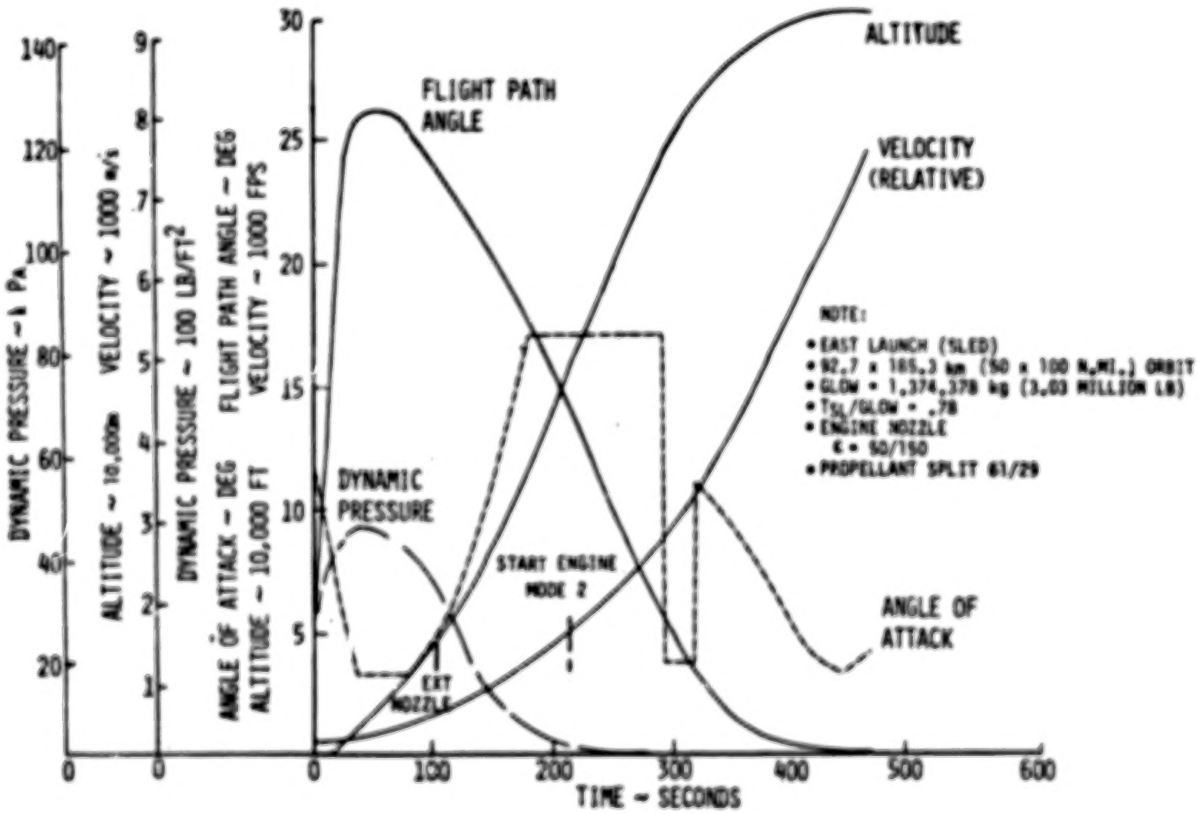
DYNAMIC PRESSURE - k Pa
ALTITUDE - 10,000m VELOCITY - 1000 m/s
DYNAMIC PRESSURE - 100 LB/FT²
ANGLE OF ATTACK - DEG ALTITUDE - 10,000 FT
FLIGHT PATH ANGLE - DEG VELOCITY - 1000 FPS
TIME - SECONDS
ALTITUDE
FLIGHT PATH ANGLE
VELOCITY (RELATIVE)
DYNAMIC PRESSURE
ANGLE OF ATTACK
START ENGINE MODE 2
EXT NOZZLE
NOTE:
• EAST LAUNCH (SLED)
• 92.7 x 185.3 km (50 x 100 N.MI.) ORBIT
• GLOW = 1,374,378 kg (3.03 MILLION LB)
• T/W/GLOW = .78
• ENGINE NOZZLE
ε = 50/150
• PROPELLANT SPLIT 61/29

FIGURE 50 SERIES BURN ASCENT TRAJECTORY

are phased over (Mode 1 to Mode 2) from RP-1 to LH_2 fuel (with a 3.5 second power off coast). The angle of attack of 17 degrees was held constant until the inertial velocity increased to 3,048 m/s (10,000 fps) where an iterative guidance mode was activated to steer the vehicle to the terminal insertion.

points (inertial velocity = 7,891 m/s (25,890 fps), altitude = 92.35 km (303,000 ft) and zero flight path angle). The 2-position nozzle was extended (ϵ = 50/150) at an altitude of 13.72 km (45,000 ft) to increase engine performance, and the engine was throttled to limit the tangential load to 3 g's.

Entry Trajectory. The descent trajectory (Figure 51) was initiated with a deorbit of 33.5 m/s (110 fps) from a 185.2 km (100 n.mi) circular orbit with an east entry and with 28.5° orbit inclination. An initial angle of attack of 50 degrees was maintained until the flight profile first leveled off (i.e. flight path angle = 0 degrees) followed by a decrease in angle of attack to 30

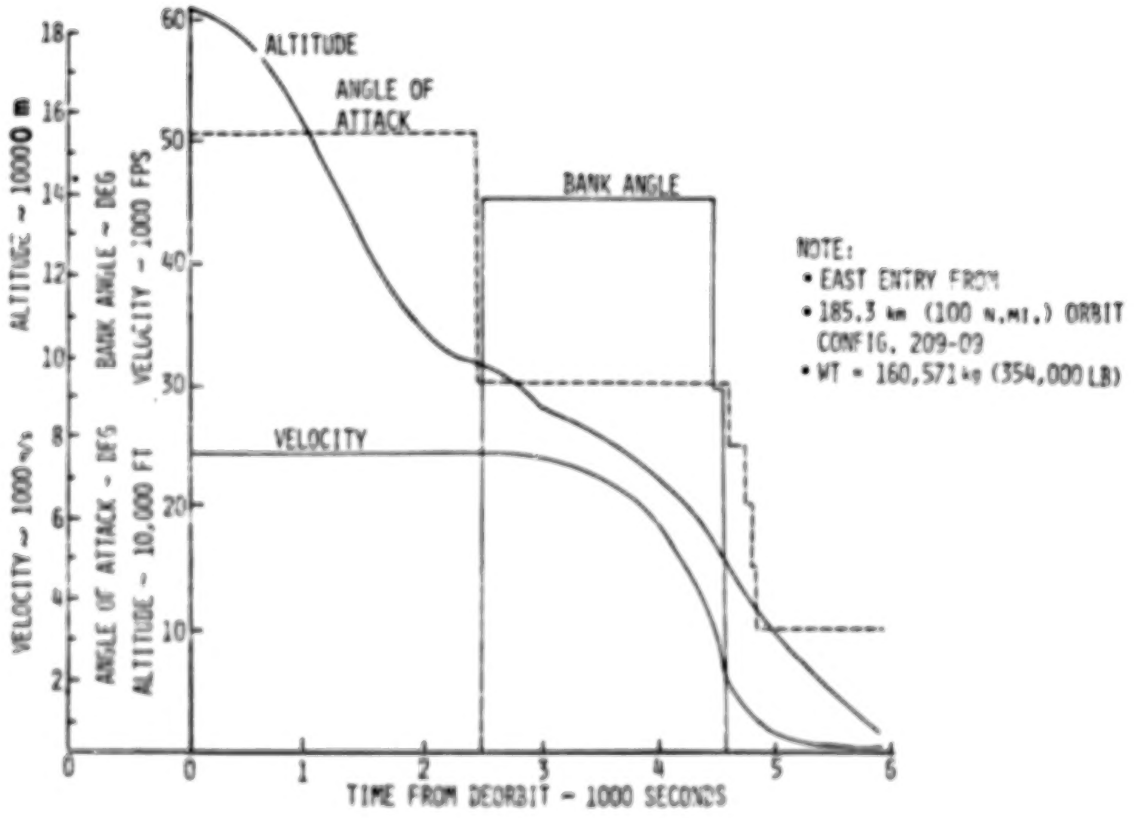

FIGURE 51 SERIES BURN ENTRY TRAJECTORY

degrees to provide a high cross range. Bank angle of 45 degrees was also initiated at this time. These control angles were held fixed until the velocity had decreased to about 1524 m/sec. (5,000 fps) at which point the bank was removed and a transition from 30 degrees to 10 degrees angle of attack was accomplished. It was estimated that aerodynamic directional control was restored at these flight conditions (RCS not required beyond this point). This trajectory achieved a cross-range slightly in excess of 2,222 km (1200 n.mi). The thermal analysis was based upon this entry trajectory. Entry wing loading (based upon reference area) is about 1293 Pa (27 psf) and at 30 degrees angle of attack equilibrium glide, W/SC_L, is 317 kg/m^2 (65 psf).

Aerodynamics

Aerodynamic lift, drag and angle of attack characteristics were estimated for the dual fuel baseline design vehicle and were used as input data for performance/trajectory analyses. Additional pitch moments were determined to satisfy basic stability and control requirements for ascent and entry flight profiles.

Vehicle Stability and Trim Limits. Vehicle aerodynamic stability and trim limits were estimated at both hypersonic and subsonic speeds to determine acceptable c.g. limits for the configuration as shown in Figure 52. These c.g. limits were between 0.716 and 0.74 of body length. These limtis permitted the elevons to be deflected between -30 to +5 legrees hypersonically. Additional preliminary checks were made on thrust vector control requirements, as shown in Figure 53, to assure a controllable vehicle. Figure 54 shows a c.g. configuration arrangement trade presented to indicate solutions to adjust the c.g. to meet these requirements.

Ascent Thrust Vector Control Requirements. Checks of thrust vector control requirements at takeoff and 50 percent burn were made to determine if these were within the engine gimbal limits of 3 degrees up and 6 degrees down. Figure 53 shows that at takeoff the static gimbal angle required is 0.3 degrees up and at 50 percent burn 2.17 degrees down.

C.G. Configuration Arrangement Trade. The most aft acceptable c.g. from the aerodynamic stability and trim analysis was 74 percent of body length, but the estimated c.g.'s for the vehicle were 74.4 and 75.5 percent payload in/out, respectively. Three options were briefly examined, as shown in Figure 54, including nose ballast, crew cab forward and aft body plug. The aft body plug resulted in the smallest inert weight penalty of 1566 kg (3453 lb).

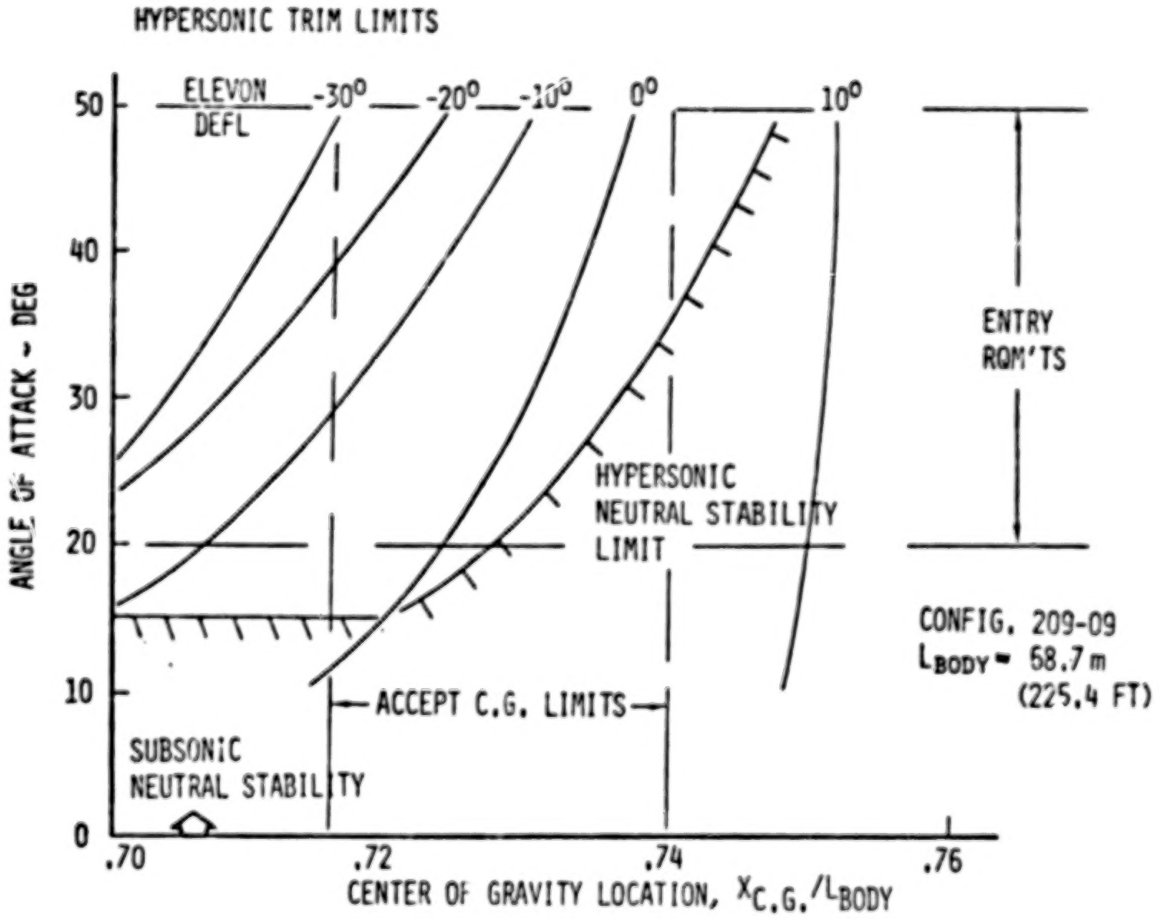

FIGURE 52 VEHICLE STABILITY AND TRIM LIMITS

NOTE: ASSUMES GIMBALLING OF ENGINES WITH NO ELEVON DEFLECTION

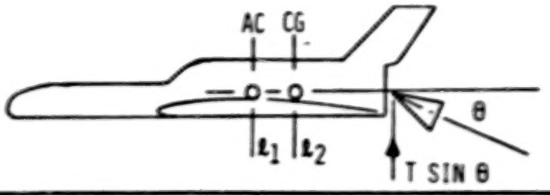

ITEM	TAKE-OFF	50% BURN
AERODYNAMIC CENTER (AC)	49.657 m (1,955 IN)	50.165 m (2,533 IN)
CENTER OF GRAVITY	49,632 m (1,954 IN)	50.749 m (1,998 IN)
ENGINE GIMBAL STATION	64,338 m (2,533 IN)	64.338 m (2,533 IN)
MAIN ENGINE THRUST	7.87 MN (1,770,000 LB)	11.74 MN (2,639,000 LB)
VEHICLE MASS	1,369,727 kg (3,019,748LB)	1,055,486 kg (2,326,962LB)
ℓ_1 (AC MOMENT ARM)	.0254 m (1 IN)	.5842 m (23 IN)
ℓ_2 (ENGINE MOMENT ARM)	14.707 m (579 IN)	13.589 m (535 IN)
REQUIRED FORCE $\left(\frac{\text{VEHICLE WT X } \ell_1}{\ell_2}\right)$	2,365 kg (5,215 LB) x 1.75	45,376 kg (100,038 LB) x 1.0
REQUIRED GIMBAL ARC SIN $\frac{\text{REQD FORCE}}{\text{TOTAL THRUST}}$	.30° UP	2.17° DOWN

FIGURE 53 ASCENT THRUST VECTOR CONTROL REQUIREMENTS

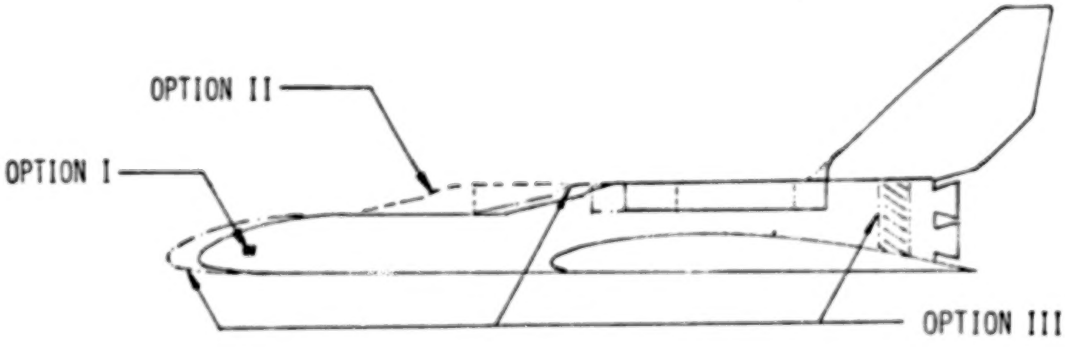

PROBLEM

MAXIMUM AFT C.G. PERMISSIBLE - 74% BODY LENGTH (STA 1892)

C.G. LOCATION PAYLOAD IN STA 1903 (74.4%)
PAYLOAD OUT STA 1933 (75.5%)

OPTIONS

I INSTALL BALLAST IN NOSE COMPARTMENT, STA 53, TO MOVE C.G. TO STA 1892

BALLAST REQUIRED PAYLOAD IN 921.7 kg (2032 LB)
PAYLOAD OUT 2778.2 kg (6125 LB)

II MOVE CREW CAB, PAYLOAD BAY, RP TANKS AND ASSOCIATED SUBSYSTEMS FORWARD TO BALANCE

TRAVEL REQUIRED 13.233 m (521 IN)

III INSTALL PLUG IN BODY FORWARD OF THRUST STRUCTURE AND MOVE COMPLETE BODY AND SUBSYSTEMS FORWARD TO BALANCE

LENGTH OF PLUG 2.794 m (110 IN)
WT OF PLUG 1566 kg (3453 LB)

FIGURE 54 C. G. CONFIGURATION ARRANGEMENT TRADE

Vehicle Weights Assessment

Numerous physical and operational constraints combined with various design options throughout the vehicle assessment effort tend to confuse the main issues of integrating a dual fuel propulsion system into an all-metallic, horizontal takeoff vehicle system. The following discussion attempts to simplify the basic reasons behind the inability of an all-metallic HTO vehicle to take advantage of the potential structures reduction of a dual fuel propelled vehicle.

Table 8 shows the propellant tankage volume and resulting weight comparison between ALRS 205 (all LO_2/LH_2 vehicle) and ALRS 209 (series burn dual fuel vehicle). Body tank volume is reduced approximately 32.5% due to the heavier but higher density RP-1 usage. However, as noted in the body weights, the dual fuel body weight, excluding the heat shield, thrust structure, crew compartment and gear wells, actually increases by 3.1%. The body structure volume/area

	SINGLE FUEL LO_2/LH_2 ALRS 205		DUAL MODE ALRS 209		% INCREASE DECREASE
VOLUME m^3 (ft^3)					
BODY					
LH_2	1,732	(61,178	936	(33,055)	32.5% ↓
RP			232	(8,185)	
WING					
LO_2	644	(22,748)	833	(29,406)	29.0% ↑
	2,377	(83,926)	2,000	(70,646)	16.0% ↓
WEIGHTS kg (lb)					
BODY NOT INCLUDING HT SHIELD, THRUST STRUCT P/L DOORS, CREW COMP. & GEARWELL	31,354	(69,124)	32,333	(71,282)	3.1% ↑
WING NOT INCLUDING ELEVONS, GEARWELL	21,654	(47,740)	35,181	(77,561)	62.0% ↑
	53,0008	(116,864)	67,514	(148,843)	27.0% ↑

TABLE 8 SINGLE VS. DUAL FUEL VOLUME/WEIGHT COMPARISONS

analysis detailed on Figure 55 shows the comparisons between an unconstrained body volume reduction and a reduction constrained by the thermal isolation of RP-1 tankage. The upper portion of the figure depicts a cylinder which represents the SSTO body of 3.66 meters (12 feet) diameter by 48.8 meters (160 feet) length. Its volume which includes the payload bay volume is shown. This cylindrical volume relates to an exposed area of 1200 meters^2 (12,911 feet^2) which has a more direct relationship to weight. Thus, the use of dual fuel

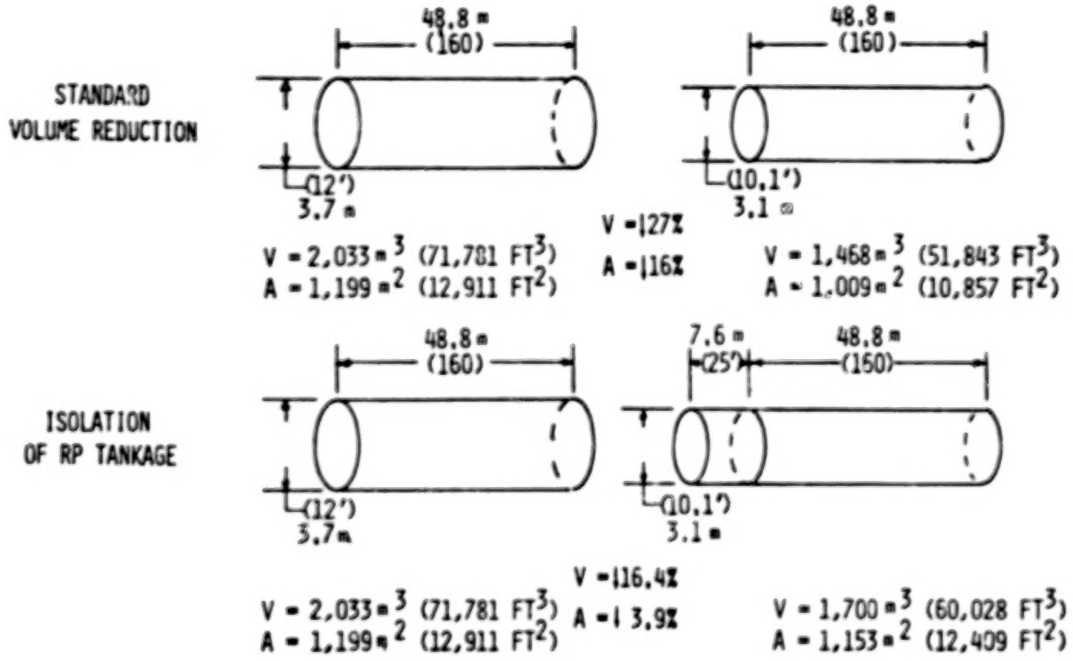

FIGURE 55 BODY STRUCTURE VOLUME/AREA ANALYSIS

body tankage including the constant payload bay volume, is reduced by 27% to a 3.08 meter (10.1 feet) diameter tank which relates to an exposed area of 1009 meters^2 (10,857 feet^2). Thus a 27% reduction in volume transcribes to a 16% reduction in area or in simple terms - weight.

However, the body volume/area cannot be reduced directly because the RP tankage must be thermally isolated (separate tankage) from the LH_2 and LO_2 moldline tankage. This is reflected in the comparison of tankage on the lower portion of Figure 55. The separate RP tankage is represented by a

7.62 meter (25 feet) extension to the 3.08 meter (10.1 ft) diameter tank. The true volume reduction is 16.4% which results in a wetted area reduction of 3.9%. Actual weight analysis shown on Table 7 indicates a 3.1% increase in body weight.

The wing volume, as shown on Table 8, increases 29% because of the increased oxygen requirement in the dual fueled vehicle design. Wing weights, not including the elevons and gear well, indicate a 62% increase. The rationale for this weight increase is illustrated in Figure 56. The upper portion of the figure shows the

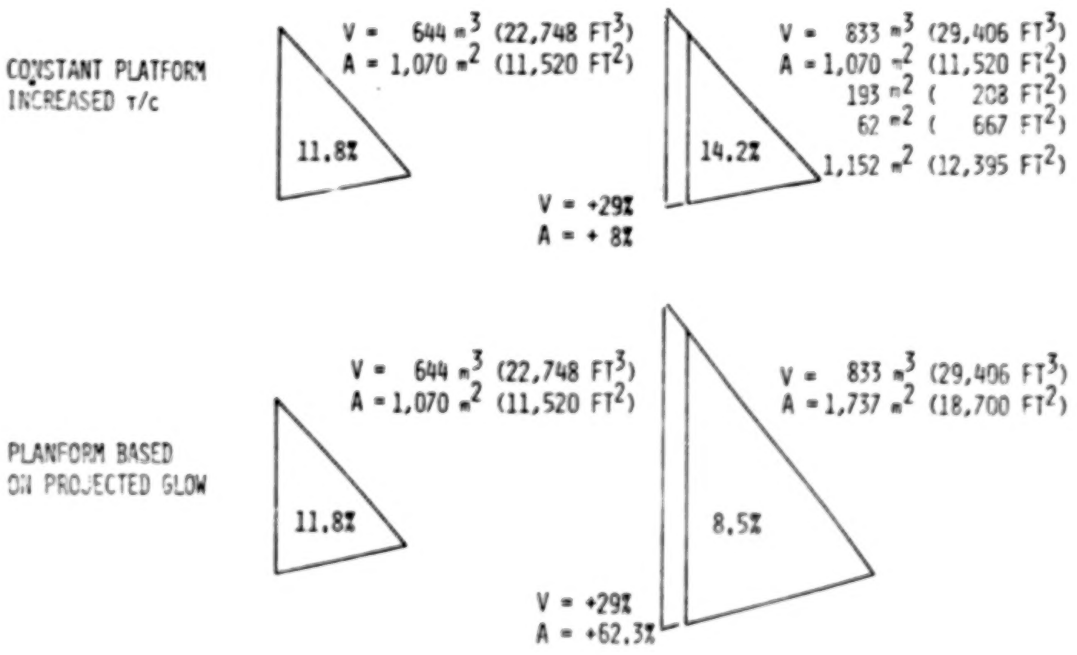

FIGURE 56 WING STRUCTURE VOLUME/AREA ANALYSIS

volume/area impact of a constant planform wing with increased thickness to chord ratio. The thickness ratio must increase from 11.8% to 14.2% to accommodate the additional oxygen which includes the fact that the body volume and width were decreased, and, as a result, the exposed area increased. The resultant area increase is 8% when assuming a constant planform wing. However, due to both takeoff and entry wing area requirements, the wing reference area for a horizontal takeoff all-metallic system increases nearly proportional to GLOW.

Thus, for the same volume increase the wing exposed area increases 62.3% which is in good agreement with the weights in the table. This results in a wing with a thickness ratio of 8.5%.

In summary, due to design constraints imposed on the dual fuel vehicle, the potential volumetric reductions do not give corresponding area or weight reductions. This analysis is very cursory in nature and is only intended to show the area/weight relationships in a very simplified form. It also does not include the effects of these changes on the vehicle body and wing loads.

TECHNOLOGY EVALUATION - STEP 4

The costs are shown on Figure 57 for the series burn design configuration under detailed study in comparison with an all LO_2/LH_2 vehicle. The figure shows

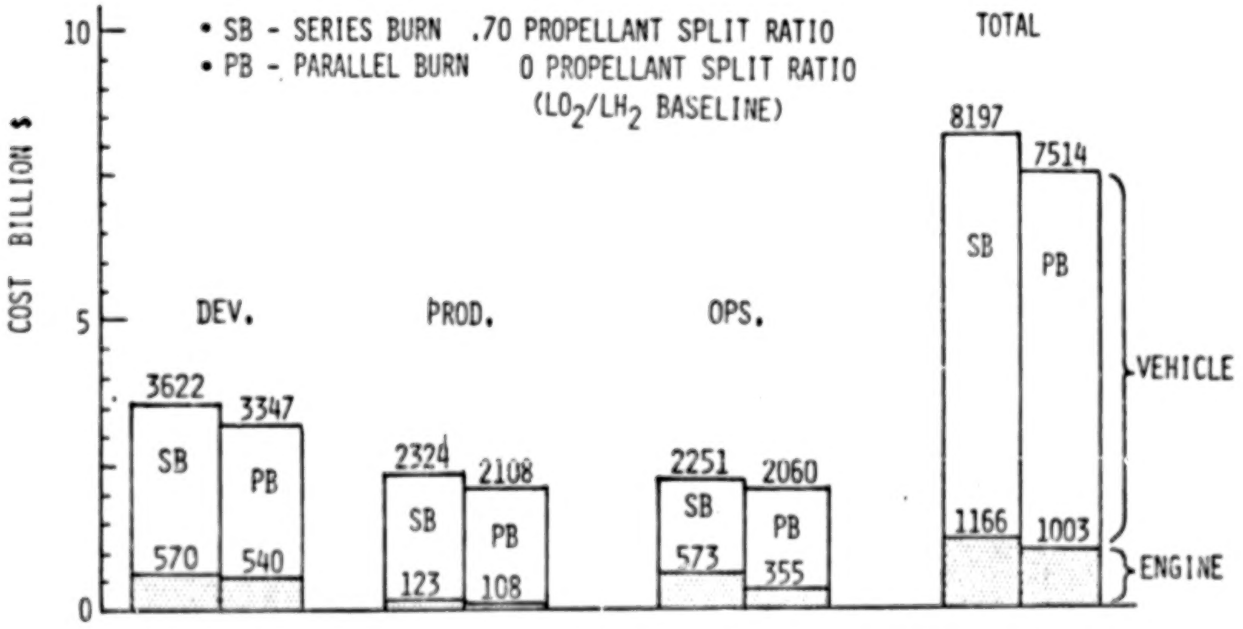

FIGURE 57 LIFE CYCLE COST COMPARISON DETAILS

the total program costs and also the development, production and operations cost phases making up the total. With the present cost estimating relationships, the all LO_2/LH_2 vehicle shows lower costs in each category. In other words, increases or decreases to the mission model or production cycle will not alter the overall conclusions. For this reason, the dual fuel configuration shows no program cost savings and, as a result, there are no associated technology programs to project or recommend based on figure of merit. Several technology developments would benefit this assessment but possible solutions cannot be projected at this time. These items are discussed in the conclusions and recommendations.

CONCLUSIONS AND RECOMMENDATIONS

This additional effort on studying the technology requirements associated with advanced earth orbital transportation systems reinforced the feelings that the potential advantages of an SSTO concept on a cost/performance basis warrants continued investigation and study.

Study Results

Dual fuel engines themselves, along with the high pressure LO_2 RP-1 engines appear to be the only major technology projections. Continual study and design effort in these areas should provide a technical capability to develop these engines at the costs projected in this study. The vehicle configuration differences between parallel and series burn propulsion concepts are very slight. The major areas of difference are associated with propulsion systems themselves. The effective I_{sp} and associated velocity losses, along with the actual engine weights, are the driver behind dual fuel concept differences, and so the rationale for selection of one or the other will have to be made based on other criteria. This could include other program propulsion system requirements such as shuttle growth/derivatives or heavy lift launch vehicles. Lift-off speed, entry planform loading and RP-1 tank thermal isolation are major constraints to all-metallic horizontal takeoff design. The combination of these constraints not only eliminates the potential weight savings due to the volumetric reduction in tank size but penalizes the vehicle in terms of wing loading and efficiency. Base radiation heating and plume induced flow separation will have some impact on

dual fuel aft body/wing design. The configurator must be aware of these problems so that the problems may be circumvented or penalties minimized regardless if the ultimate or best candidate is horizontal or vertical takeoff. The configuration factors associated with an extra fuel and its associated installation increase stability problems on the SSTO vehicle. The horizontal takeoff horizontal landing vehicle is more susceptible to this problem due to the balance requirements during ascent being nearly as critical as that for descent.

Conclusions

Dual fuel vehicle GLOW and performance trending curves have a significant impact on the life cycle costs. When optimizing parallel burn and series burn configurations for the minimum life cycle costs the parallel burn system is favored. However, technology advances to increase inert weight savings in terms of performance, subsystems or structure would tend to favor the series burn. In conclusion, dual fuel propulsion as constrained by the study requirements is not attractive for a fully reusable, all-metallic horizontal takeoff SSTO based on figure of merit.

Study Recommendations

RP-1 was selected as the "heavy" fuel for this study based on data available and study consistency. There are several fuels which would have a broader temperature limitation and thus be more adaptable to the hot structures type of tankage required on an all-metallic system. The ultimate potential for reducing refurbishment costs with this type of structure could warrant consideration of one of these fuels. Future effort on dual fuel propulsion should investigate configuration arrangements, insulation techniques and alternate material systems to eliminate or lessen the impact of base heating and plume induced flow separation resulting from a hydrocarbon engine.

Any comparison of a dual fuel concept with an all LO_2/LH_2 concept will be strongly influenced by the propulsion system cost assumption. In any case, a more detailed examination of propulsion system development and unit costs is required to add credibility to the most promising approach.

A recommendation was made during the previous study on all LO_2/LH_2 systems that control configured design options be investigated to alleviate stability problems which seem to plague rocket powered SSTO type vehicles. This recommendation is repeated as the dual fuel concept as studied does not improve vehicle stability.

REFERENCES

1. Hepler, A. K., and Bangsund, E. L.: Technology Requirements for Advanced Earth Orbital Transportation Systems. Volume 1: Summary Report. NASA CR-2879, 1978.

2. Lusher, W. P., and Mellish, J. A.: Advanced High Pressure Engine Study for Mixed-Mode Vehicle Applications, NASA CR-135141, 1977.

3. A Model for Estimating Total Program Cost of Aircraft, Spacecraft and Reusable Launch Vehicles. NASA-OART Working Paper MA-71-3, August 1971.

1. Report No.	2. Government Accession No.	3. Recipient's Catalog No.
NASA CR-3037		

4. Title and Subtitle	5. Report Date
Technology Requirements for Advanced Earth Orbital Transportation Systems Volume 3: Summary Report - Dual Mode Propulsion	July 1978
	6. Performing Organization Code

7. Author(s)	8. Performing Organization Report No.
A. K. Hepler and E. L. Bangsund	D180-19168-3
	10. Work Unit No.
9. Performing Organization Name and Address Boeing Aerospace Company P. O. Box 3999 Seattle, Washington 98124	11. Contract or Grant No. NAS1-13944 Mod. 1
	13. Type of Report and Period Covered Contractor Report
12. Sponsoring Agency Name and Address National Aeronautics and Space Administration Washington D.C. 20546	14. Sponsoring Agency Code

15. Supplementary Notes

Langley Technical Monitor: Charles H. Eldred
Volume 3 of Final Report

16. Abstract - The fundamental overall objective of the basic study reported in Volumes 1 and 2 was to identify those areas of technology associated with future earth-to-orbit transportation systems which are either critical to the development of such systems or which offer a significant cost and performance advantage as a result of their development. Additional objectives were to determine the most efficient operational mode for such systems and to define performance potential as a function of technology growth. The intent was to utilize vehicle system studies as a means of identifying critical and high yield technology areas upon which to base the planning for and the development of advanced technology programs. The primary objective of the additional task reported upon in this volume was to determine the impact of dual-mode propulsion on the cost-effective technology requirements for advanced earth-orbital transportation systems. Additional objectives were to determine the most efficient propulsion mode for these systems by the comparison of series burn and parallel burn dual mode concepts and to determine the advantages of the best dual mode concept relative to the LO_2/LH_2 concept of the basic study. Normal technology requirements applicable to horizontal take-off and landing Single-Stage-to-Orbit Systems utilizing dual mode rocket propulsion were projected to the 1985 time period in Step 1. These technology projections were then incorporated in a vehicle parametric design analysis for two different operational concepts of a dual mode propulsion system in Step 2. The resultant performance, weights and costs of each concept were then compared and a system concept selected. The selected propulsion concept was then evaluated to confirm the parametric trending/scaling of weights and to optimize the configuration based on a figure-of-merit. Based on study results, recommendations are provided in the two above mentioned categories of technology areas associated with future earth orbit transportation systems dual mode propulsion.

17. Key Words (Suggested by Author(s))	18. Distribution Statement
Single Stage to Orbit Vehicles Space Vehicles Hypersonic Flight Advanced Technology Dual Mode Propulsion	Unclassified - Unlimited Subject Category 16

19. Security Classif. (of this report)	20. Security Classif. (of this page)	21. No. of Pages	22. Price*
Unclassified	Unclassified	94	$6.00

*For sale by the National Technical Information Service, Springfield, Virginia 22161

NASA-Langley, 1978

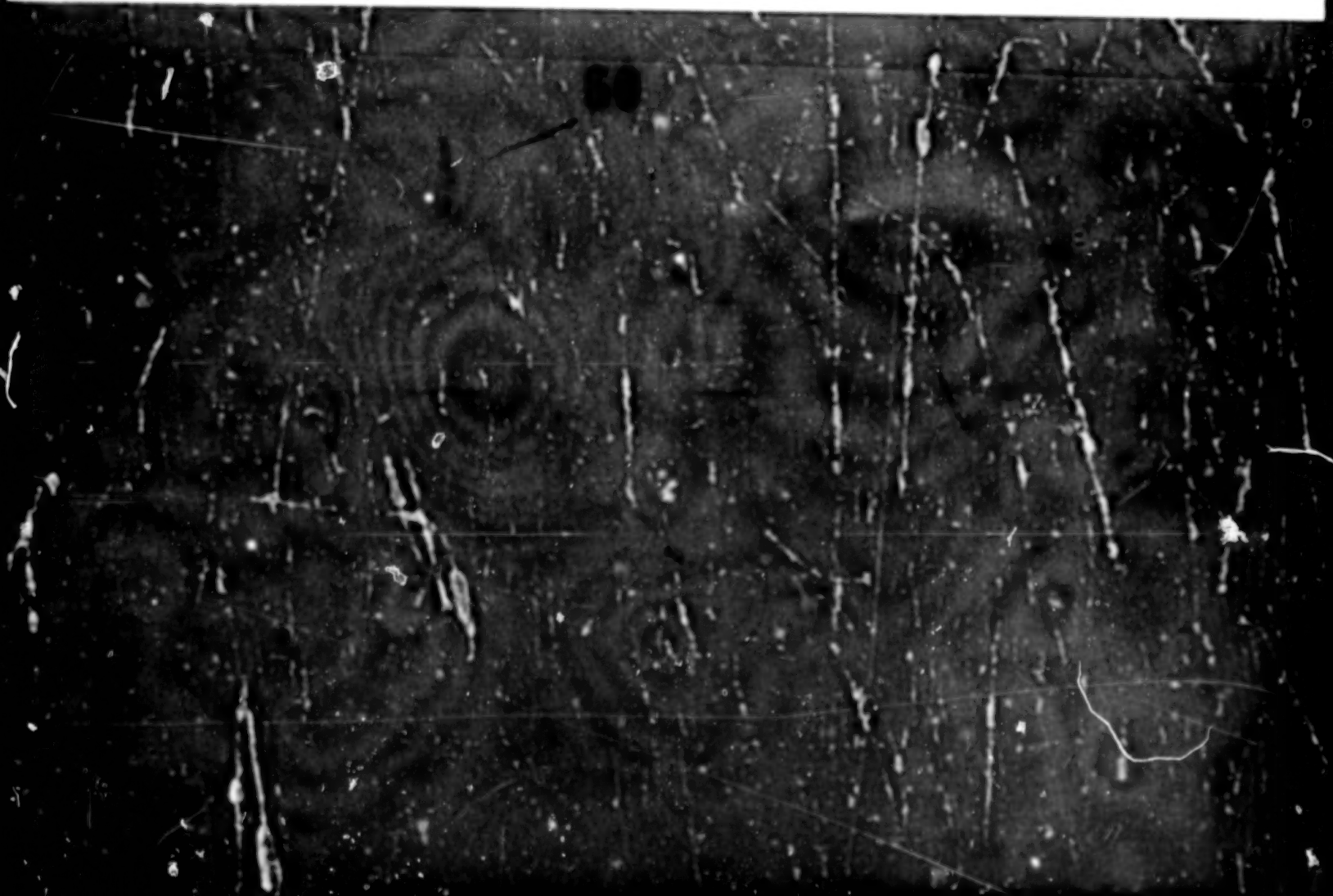
60